UiT
THE ARCTIC UNIVERSITY OF NORWAY

Faculty of Science and Technology

Department of Geology

Seismic Modeling of Free Gas Occurrences and Bottom Simulation Reflection (BSR) Beneath Hydrate-bearing Sediments

—

Daniel Adhanom Tesfamariam

Master thesis in marine geology and marine geophysics (Geo-3900)
January 2016

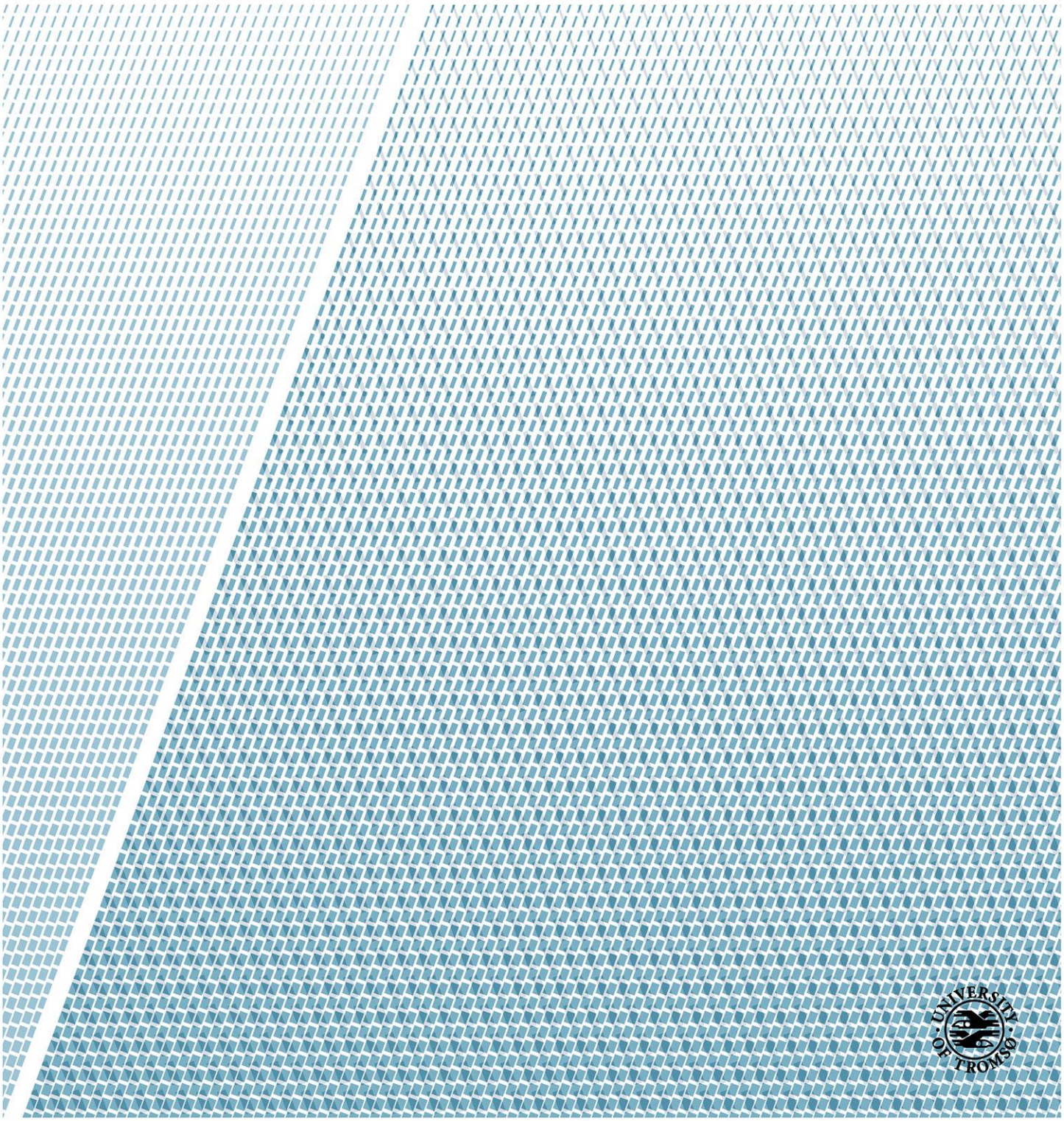

UNIVERSITY OF TROMSØ

Seismic Modeling of free gas occurrences and Bottom Simulation Reflection (BSR) beneath Hydrate-bearing sediments

Daniel Adhanom Tesfamariam

Master's thesis in Marine Geology and Marine geophysics (GEO-3900)

January 2016

Abstract

Gas hydrates are an ice-like crystalline substance that occurs in upper few hundreds of meters on continental margins worldwide where appropriate pressure and temperature conditions exist and there is an abundance of free gas available for their formation. Mostly, free gas migrates into the hydrate stability zone and forms hydrates at the base of this zone. Hydrate formation leads to a decrease in permeability, which in turn leads to the accumulation of free gas beneath hydrate-bearing sediments. Hence, a free gas zone exists associated with the presence of gas hydrates in overlying sediments.

This master thesis study uses seismic modeling to better understand the seismic response of the free gas that accumulates beneath hydrate-bearing sediments in marine sediments. To this end, I developed 12 different geological models ranging from very simple geometries to anticline structures. Within these models, I varied the distribution of free gas in the layers beneath the BSR. Sediment properties were taken from velocity profiles of the Storegga gas hydrate system and the density approximately estimated from a computed Gassmann diagram. Norsar 2D, Norsar 3D and Seisrox modeling programs were used to generate Pre-Stack Depth Migrated (PSDM) seismic images.

Higher frequencies (250Hz, 150 Hz, 100 Hz, 90 Hz, and 80 Hz), large incident angle and long horizontal sampling distances has resulted in the generation of BSR as termination of enhanced reflection. The termination of the enhanced reflections coincided with anticlinal and dipping BSR in this study. The presence of intercalation of gas free and hydrate bearing layers (both 5m in thickness) above the dipping BSR and gas free and gas bearing sediments below the dipping BSR (both 5m in thickness) led to the termination of enhanced reflection at the BGHSZ. Low frequency 40 Hz, near angle and small sampling distances resulted in proper BSR reflections for the geologic setting mentioned above. Lower frequency (40 Hz) and large sampling distances results in termination of enhanced reflection of the BSR.

Homogenous contact of gas hydrate bearing sediments and gas free sediments with lateral extent larger than Horizontal sampling in PSDM resulted in proper reflections at higher and lower frequencies.

A seismic section from high-resolution Hydratech 3D data was compared to the synthetic seismic model. The 2D seismic section matches with synthetic seismic model in one of the models that includes sediments free of gas extended in the HSZ and area below BGHSZ, intercalated with hydrates and free gas accumulating layers. The properties of the gas free sediments are more similar with the nearby gas hydrate bearing sediments. As it is known in geophysical interpretation different model can give similar result this study agreed with the previous study of the Hydratech 2D interpretation.

Contents

1 Introduction 1
1.1 Objective 1
1.2 Basic Theory 1
1.2.1 Seismic Reflection Principle 2
1.2.2 Seismic Wavelets 4
1.2.3 Resolution and Limitation of Seismic Reflection 5
1.2.4 Seismic Acquisition, 3D Seismic Surveys 8
1.2.5 AVO/AVA 8
1.2.6 Seismic Indication of Gases 10
1.2.7 Seismic Indication of Fluid 11
1.2.8 Gas Hydrates 12
1.2.9 Bottom Simulation Reflection 13
1.2.10 Ocean Bottom Cable (OBC) 18

2. Seismic Modeling 19
2.1 Geological Model 20
2.2 Rock Physics 21
2.2.1 Seismic wave velocities 22
2.2.2 Gassmann 23
2.2.3Rock physics of gas hydrates 23
2.3 SeisRoX 24
2.4 Resolution in Seisrox 32

3.Data and Methodology 34
3.1Data 34
3.2 Norsar modeling program 36
3.2.1 Reservoir model 1, model 2 and model 3 40
3.2.2 Reservoir model 4 44
3.2.3 Reservoir Model 5 and Model 6 45
3.2.4 Reservoir model 7, Model 8 and Model 9 49
3.2.5 Reservoir Model 10 51
3.2.6 Reservoir model 11 and Model 12 52
3.3 Norsar 3D modelling 54

3.4 Seisrox modelling program……55
3.4.1 Seisrox Model ……55
3.4.2 Background model……55
3.4.3 Seisrox Surveys……55
3.4.4 Survey parameters…… 55
3.4.5 Wavelet……56
3.4.6 PSDM target……58

4.Result……63
4.1 Change in contact angle model, model2 and model 3……65
4.2 Change in sampling ……67
4.3 Change in frequency…… 72
4.4 Change in occurrences of BSR……82
4.5 Change in incidence angle……97

5.Discussion…… 103
5.1 Change in controlled parameter…… 103
5.1.1 Change in sampling ……103
5.1.2 Change in frequency……104
5.1.3 Change in incident angle…… 108
5.2 uncontrolled parameters……111
5.2.1 Model 9A, 9B and 9C is 30m thick intercalation of porous sediment and less porous sediment……113
5.2.3 BSR in mid Norwegian margin…… ……117

6. Conclusion……125

References

Appendix

Acknowledgement

I wish to thank first and foremost my advisers A.Prof. Stefan Buenz and researcher Andria Plaza without their close supervision this study would have not been completed.

Moreover, I would like to say thanks kai Mortensen, for his guidance and providing necessary information from the day of my arrival at the University of Tromsø up to I completed my study.

I would also like to give thanks to my friends especially Esaw Habtemichael for his endless encouragement and his friendly guidance starting from the time of my application to the University until the time of completion of this research.

It also gives me great pleasure to give my heartfelt appreciation to my friends Kisseri Drar , Dr. Biniam Asmerom ,Yohannes Tesfay, and my fellow master's students Johannes Johannesson and Håkon Karlsen for helping me in editing my thesis.

I owe my deepest gratitude to my friends and relatives who were calling and encouraging me, Isaack Habtemichael, Kibrom Mebrhatom, Michael Welderufael, Biniam Habtemichael, Siefu Haile and my cousins Dawit Birhane, Debretsion Abrham and Azeb Weldegeberiel with all her family.

I would like to say thanks my Norwegian family Ragnar Evenstad and his family who were always calling and made me feel at home, during my stay at the University of Tromsø.

Finally yet importantly, I would like to say thanks my family who were on my side all along my life journey my father Adhanom Tesfamariam and my mother Letemichael Beyene, who have devoted all they had to make me a winner.

Daniel Adhanom

Tromsø January 2016

1 Introduction

1.1 Objective

The major aim of this study is to better understand the seismic response from the free-gas zone beneath hydrate-bearing sediments. In order to identify the acoustic characteristics of bottom-simulating reflections (BSR), I have developed several geological models with variations in the occurrence of gas hydrates and free gas. Since it is well established that the BSR is a result from the presence of gas, the focus of the modelling work is on the free gas distributions beneath the BSR.

1. BSRs are the utmost widely used indicator for the presences of gas hydrate accumulations in the subsurface. (Shipley et al., 1979; Yamano et al., 1982).

BSR forms at a depth roughly estimated to be the bottom of methane hydrate stability zone (Kvenvolden and Barnard, 1983; Kvenvolden et al., 1993). BSRs are usually supposed to spot an interface in between high velocity gas hydrate bearing and underlying, uncemented gas hydrate-free sediments with lesser seismic wave velocity (Stoll and Bryan, 1997; Hyndman and Spence, 1992) or sediments of low velocity having free gas (Dillon and Paull, 1983; Miller et al., 1991).

The formation of gas hydrates depend on pressure and temperature, and as a result BSR is a reflection that follows the sea floor at a depth approximately with iso temperature and equal pressure (Sloan, 1998,Dillon et al., 1994) thereby crosscutting stratigraphic horizons which are not parallel with the sea floor (Kvenvolden ,1993). Due to the strong negative seismic impedance contrast, the BSR shows heightened seismic amplitudes and phase reversal which is opposite to the seafloor reflection (Jagannathan et al., 1983).

On marine reflection seismic data the BSR can show as a proper, coherent reflection with enhanced amplitudes However, some seismic data, mostly that with larger and higher frequency bandwidth show the BSR as the termination of enhanced reflection (Vanneste et al. 2001).

To understand the occurrences of free gas associated with a proper BSR or the termination of enhanced reflections at BGHSZ, several geological models have been developed. The models are based on velocity data from OBS JM516 velocity profiles (Bünz et al., 2005) and the density approximately estimated from the computed Gassmann diagram (Andreassen, 1997). The different models vary in the dip of the gas hydrates and free gas bearing sediment contacts (BSR), different layer thicknesses, and the continuity and discontinuity of the gas reservoir. Synthetic simulation of pre- stack depth migration (PSDM) has been generated for different settings of the target using incident angles, 10°, 20°, 30°, 40°, 45°, 50° and 60° and using wavelets from 10Hz-100Hz, 150 Hz and 250 Hz.

1.2 Basic Theory

1.2.1 Seismic Reflection Principle

Seismic reflections originate from interfaces that have sufficient density-velocity contrasts. Each seismic layer in the subsurface has particular acoustic impedance. The acoustic properties of a rock are defined as its acoustic impedance (z), the product of density (ρ), and velocity (V) (Andreassen, 2009).

$$Z = \rho V \qquad \textit{Eqn. 1.1}$$

Where (ρ) Greek alphabet RHO is density and

(V) Velocity

Velocity is more significant than density concerning acoustic impedance in the case of pore fluid content; gas in sand results to much lower velocity than density of the rock in contrast to gas free sand, (Andreassen, 2009). In the case of a seismic wave spreading through the earth, which comes across an interface between two materials with different acoustic impedances, some of the wave energy will reflect off the interface and some will refract through the interface (Veeken, 2007). The interface between layers is generally associated to sedimentary bedding planes, unconformities and/or pore fill characteristics (Veeken, 2007). The depth of the reflection can be calculated mathematically by eqn. 1.2.

$$\text{Depth} = \tfrac{1}{2}\,(\text{twt})*(V) \qquad \textit{Eqn. 1.2}$$

Where (twt) is two way travel time and

(V) Interval velocity

The seismic reflection method consists of sources of producing seismic waves and methods of recording the time taken from the sources to the reflector and then to the receivers (geophone or hydrophone) (Sheriff, Geldart and L.P., 1995). (Figure 1.1) illustrates the principle of the seismic reflection method.

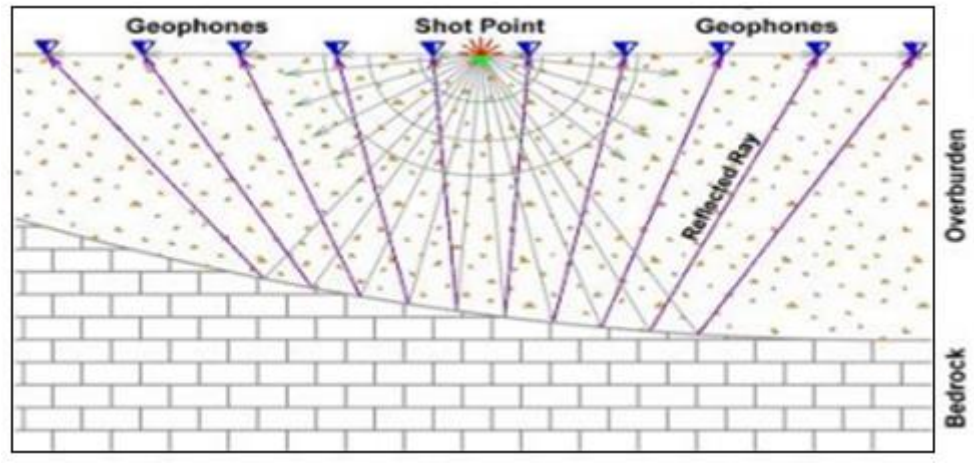

Figure 1.1 *Shows seismic energy shot and reflection recording setting.*

In anisotropic media, wherever wave fronts are not necessarily perpendicular to ray paths, Snell's law shows the angles measured between an interface and the wave fronts, by means of phase velocities (Sheriff, 2002). The phase velocity is a directional velocity. The seismic reaction of a reflected wave front is dependent on the amount Rho-Vee deviations over the interface. It is stated in terms of velocity and density of a media located on opposite sides of the interface. It can be defined in terms of a reflection coefficient (2D sense) and reflectivity R (Full 3D sense for the wave front). It is expressed by the following formula :(Veeken, 2007).

$$R = \frac{\rho 2v2 - \rho 1v1}{\rho 2v2 + \rho 1v1} \qquad \textit{Eqn. 1.3}$$

Some of the energy does not reflected back to the surface; a certain amount is transmitted to deeper levels, proportional to expressions of the following formula:

R Trans= 1-R *Eqn. 1.4*

The transmitted energy is crucial for the detection of the deeper interfaces (Veeken, 2007). The illustration of the reflected and transmitted rays is shown in (Figure 1.2).

Snell's law of reflection explains that the angle of incident is equal to the angle of reflection and the angle of transmission linked to the incident angle by velocity ratio.

A conversion from P to S or vice versa can also follow but still the angle is determined by velocity ratio (Veeken, 2007).

$$\text{SNELL's LAW: } \frac{\sin\theta_{inc}}{V1} = \frac{\sin\theta_{trans}}{V2} = \frac{\sin\theta_{ref}}{V1} \qquad \textit{Eqn. 1.5}$$

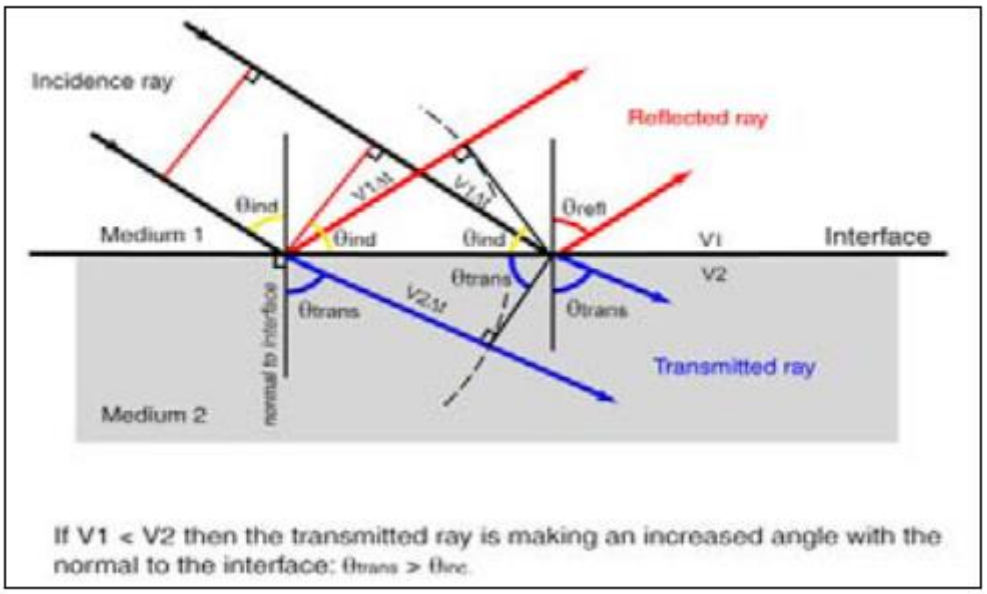

Figure 1.2 *Shows Basic ray path geometry, the reflected and transmitted plane wave fronts. From (Veeken, 2007).*

1.2.2 Seismic Wavelets

Seismic wavelets are generally defined by the polarity they appeared. The frequently used recording and display conventions are illustrated in (figure 1.3); the figure below shows the normal and reverse polarity displays for minimum and zero phase pulses both using the Convention of Badley 1985, and the SEG (Society of Exploration Geophysicists) Standard of Sheriff (2006) from (Andreassen, 2009).

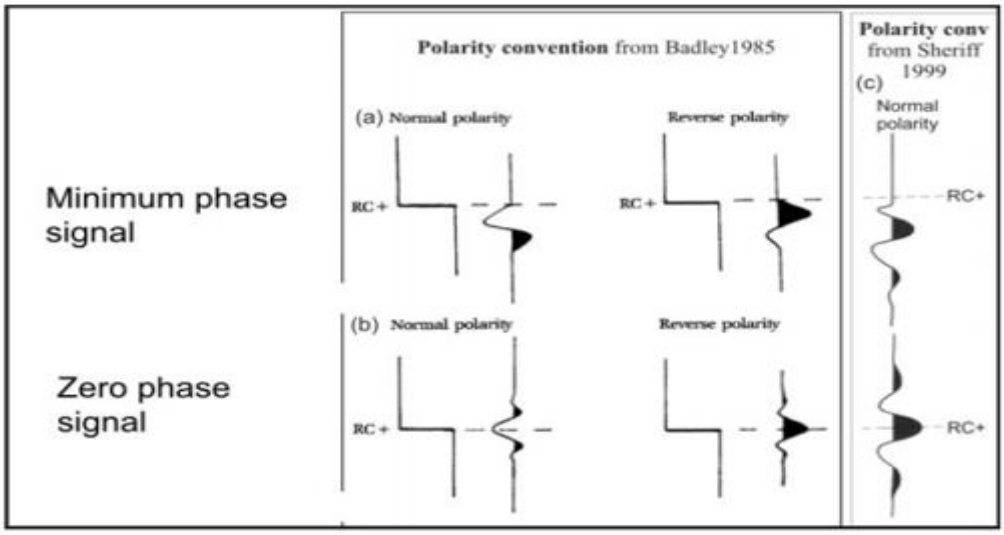

Figure 1.3 *Shows Polarity Convention from Badley 1985(Andreassen, 2009).*

1.2.3 Resolution and Limitation of Seismic Reflection

Seismic Resolution: In a typical sequence of sedimentary rocks, all acoustic impedance contrasts (Seismic reflectors) have the potential to generate seismic reflections. However, whether or not these variations are significant enough for their reflections to be well known depend upon the sensitivity of the seismic acquisition and processing system. (Andreassen 2009).

Seismic resolution is the crucial for taking out of stratigraphic details from seismic data. Seismic resolutions consist of two aspects: the vertical and horizontal resolutions. (Chopra et al., 2006).

As we go down deep, the frequency of the sound signal will reduce while the velocity and wavelength will go higher and higher; this reveals that with increasing depth the seismic resolution will be poorer. High frequencies reflect from not much deep depths and have a higher resolution, lower frequencies can penetrate to a deeper depth, but it has a lower resolution (Andreassen, 2009)

Vertical resolution: The vertical resolution denotes to the capability to distinguish two close seismic events corresponding to different depth levels (Chopra et al., 2006). Vertical resolution is an extent of how large an object needs to be in order to be seen during seismic imaging. The vertical resolution is resulting from the length of a sound wave and the layers can be distinguished when their thickness is over ¼ wavelength.

Layer can be potentially detected down 1/32 wavelength. When we talk about to vertical resolution, it is normally the ¼ wavelength (Rafaelsen, 2002).

$$\lambda = v/f \qquad \textit{Eqn. 1.6}$$

Vertical resolution is calculated = $\lambda /4$ *Eqn. 1.7*

Horizontal resolution: Horizontal resolution is concerned with the ability to differentiate and make out two laterally displaced features as two dissimilar adjacent events (Chopra et al., 2006).

Horizontal resolutions are resulting from the Fresnel-zone, the portion of the reflector enclosed by a seismic signal at a certain depth. On a buried horizon, all features with lateral extent exceeding the Fresnel zone will be visible.

Migration of the seismic data emphases the energy spread in the Fresnel zone, re-arranges reflections out-of-place due to dips, and removes reflection patterns from points and edges. This improves the horizontal resolution to about ¼-wave length. (Brown, 1999). This is illustrated in (Figure 1.4).

$$\lambda = v/f \qquad \textit{Eqn. 1.8}$$

Horizontal resolution= $V/2\sqrt{(t/f)}$ *Eqn. 1.9*

Where V= velocity, f= frequency and two way travel time

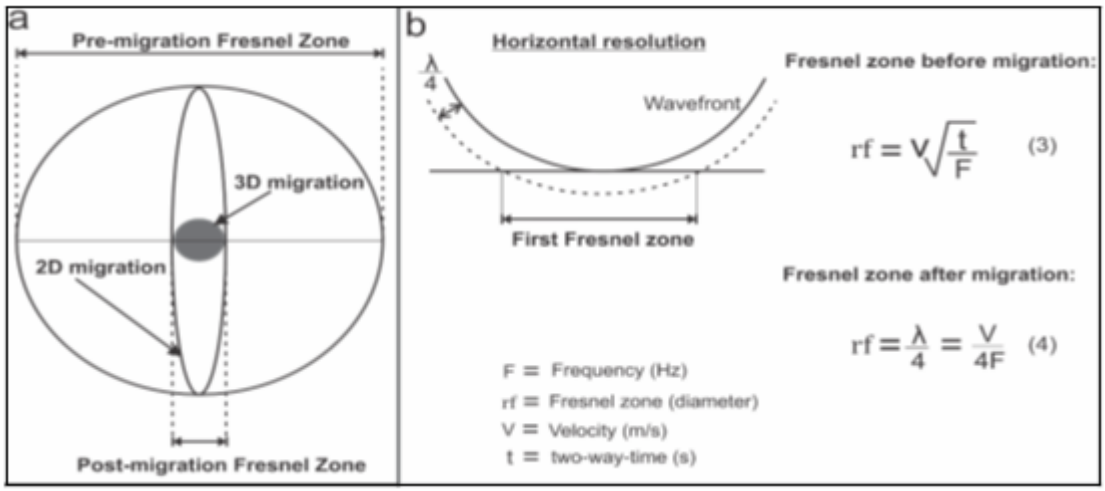

Figure 1.4 *shows resolutions and migration* ***a,*** *the migration in 2D and 3D, b, the first Fresnel zone; the first energy signal to reach the receiver from the plane reflector is the first tangent to the wave front. The area of the reflector that produces the reflection is limited by the area of that wave front, the 1/4 wavelength later makes with the reflector,*

the equations represent the magnitude of the Fresnel zone before and after migration, respectively from (Bjørnøy, 2015).

Limitation of seismic Reflection

Interference: Interference is the core problem of the seismic reflection method. Interferences occur among closely located reflectors because the seismic pulse is longer than the separation. The length of the seismic pulse (in milliseconds) governs interferences and the spacing of acoustic impedance contrast in time; which is a function of the interval velocity. (Figure 1.5 and 1.6) illustrate layers at sharp contact having maximum interferences at λ/4 of seismic reflection and no interferences at λ/2. (Andreassen, 2009).

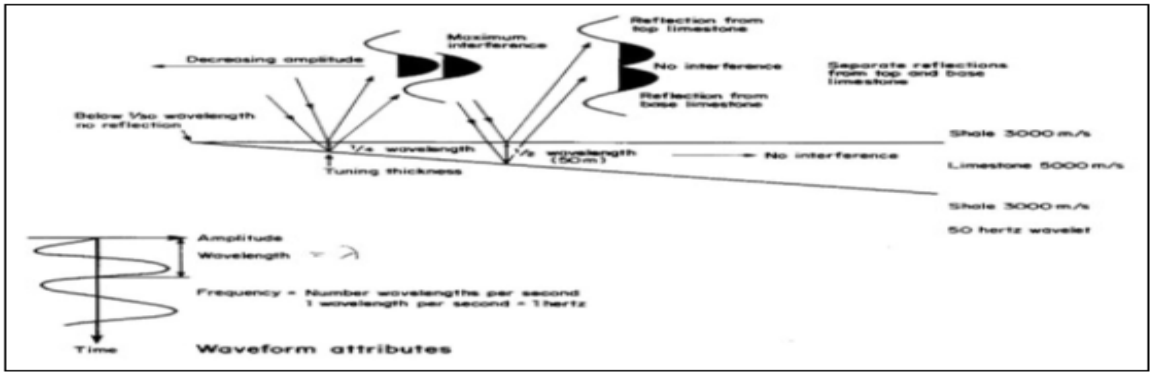

Figure 1.5 *Shows interference effects associated with high acoustic-impedance wedge encased in lower Acoustic impedance shale (Andreassen, 2009).*

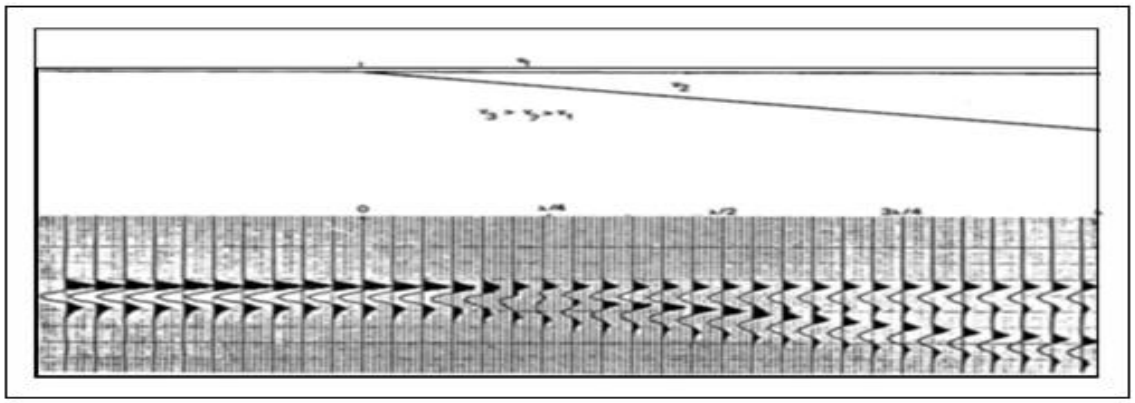

Figure 1.6-*Shows Reflection from a wedge of acoustic impedance intermediate in magnitude between that of the over and underlying units. The thickness of the wedge is indicated as a fraction of the dominant wavelength a Model b. Seismic response modified from (Badley 1985).*

1.2.4 Seismic Acquisition, 3D Seismic Surveys

3D surveys are very important method used to produce a seismic image. Seismic images, is the necessary tools for seismic stratighraphers along with Surface geology and Well data. The seismic images can be produced from either 2D or 3D Seismic Surveys loaded on a workstation. The difference between 3D and 2D surveys are the positioning between seismic lines. 2D surveys are frequently spaced 2.5 km apart and will follow individual direction whilst 3D surveys are preceded with well-ordered line spacing that is usually 25 or 12.5 meters apart (Veeken, 2007). The illustration of marine acquisitions is in (Figure 1.7).

The 3D seismic sampling in combination with innovative 3D seismic migration algorithms such as 3D dip move out and 3D migration gives accurate spatial information of reflections, thus collapsing the Fresnel Area in 3D. This allows for more realistic imaging of complex geological structures (Veeken, 2007). Lateral resolution cannot be lesser than the bin spacing (12.5-15m) of the 3D data set, while it may be more applicable to take in account the limit between the bin spacing and the principal wavelength (Cartwright and Huuse, 2005).

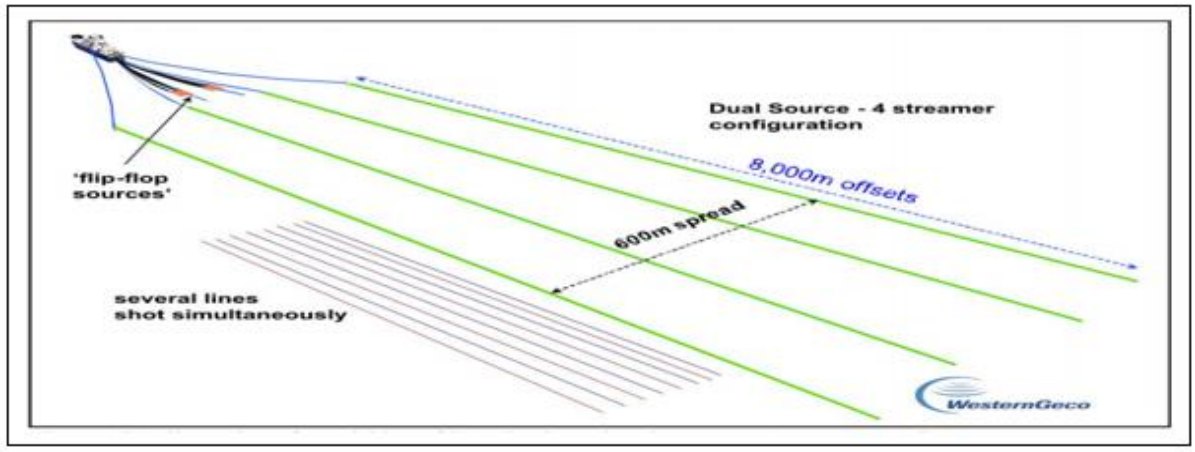

Figure 1.7 *shows acquisition of 3D seismic survey from westernGeco.*

1.2.5 AVO/AVA

In reflection seismology, amplitude versus offset (AVO) denotes to amplitude deviation with a distance between the sources and the receivers. AVO can be known as amplitude versus angle (AVA) for the reason that the change in offset is done to change the incident angle. AVO is generally used method (Schulumberger oil field glossary). It can be used

when we only know the change in P velocity; by means of a basic version of the Zoeppritz equations (1919); Aki and Richards (1980), it will allow us to calculate the reflection coeffient for P-to- P reflectivity with non-zero incident angle (θ) (Mavko et al., 1998).

$$Rpp(\theta)=\frac{1}{2}\left(\frac{\Delta Vp}{Vp}+\frac{\Delta\rho}{\rho}\right)+\left[\frac{1}{2}\left(\frac{\Delta Vp}{Vp}-2\left(\frac{\Delta Vs^2}{Vp^2}\left(+\frac{\Delta\rho}{\rho}+2\frac{\Delta Vs}{Vs}\right)\right)\right]sin^2\theta+\frac{1}{2}\frac{\Delta Vp}{Vp}[tan^2\theta-sin^2\theta]\right.$$

Eqn. 1.10

Where $\Delta\rho=\rho2-\rho1$ $\rho=\rho2+\rho1/2$

$\Delta Vp=Vp2-Vp1$ $Vp=Vp2+Vp1/2$

$\Delta Vs=Vs2-Vs2$ $Vs=Vs2+VS1$

Migration: Seismic migration is the process by which seismic events are geometrically repositioned to either a depth or time to the location where the reflection happened in the subsurface; (Figure 1.8) illustrates migration of reflection.

This is very vital to overcoming the limitation of geophysics with complex geology such as faulting, folding and salt bodies. Migration moves dipping reflectors to their correct subsurface positions and collapse diffractions (Yilmaz Ö, 2001).

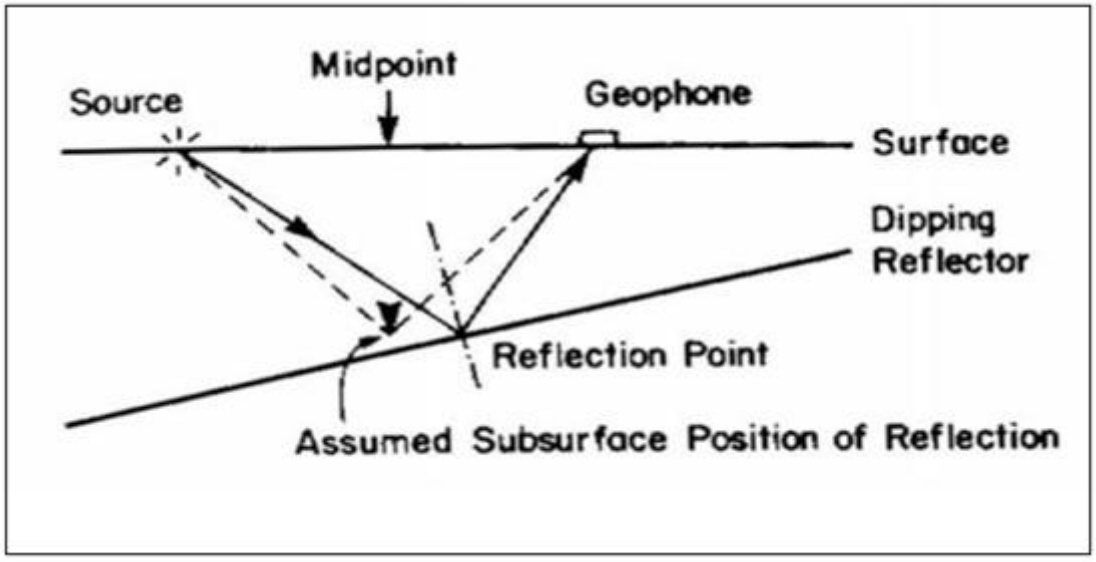

Figure 1.8 *shows the principle of migration of a reflection in a dipping layer, From (Andreassen 2009).*

Depth migration uses a velocity model of the earth, which is iteratively updated by conversions back into the time of the depth migration results and comparing the two seismic sections. One of the techniques is PSDM or prestack depth migration. The velocity allows in PSDM updates the CRP gather common reflection points (Veeken 2007).

Pre-stack depth migration was mentioned as a critical sucess factor in the exploration and appraisal of many deep-marine reservoirs because the imaging of reservoir architecture is ver important, and resolved some of the problems in the allocation of the field extent for multi storied channels that form stratigraphic traps (weimer and Slatt 2004).

1.2.6 Seismic Indication of Gases

The presences of gas in sediment is a reason for dramatic reduction of the P-velocity (Vp), this is illustrated in (Figure 1.10). The way in which a reservoir look like in seismic data is influenced by the acoustic impedance of the gas-filled portion of the reservoir, the water filled reservoir portion, the cap rock, and the thickness of the gas-filled interval.

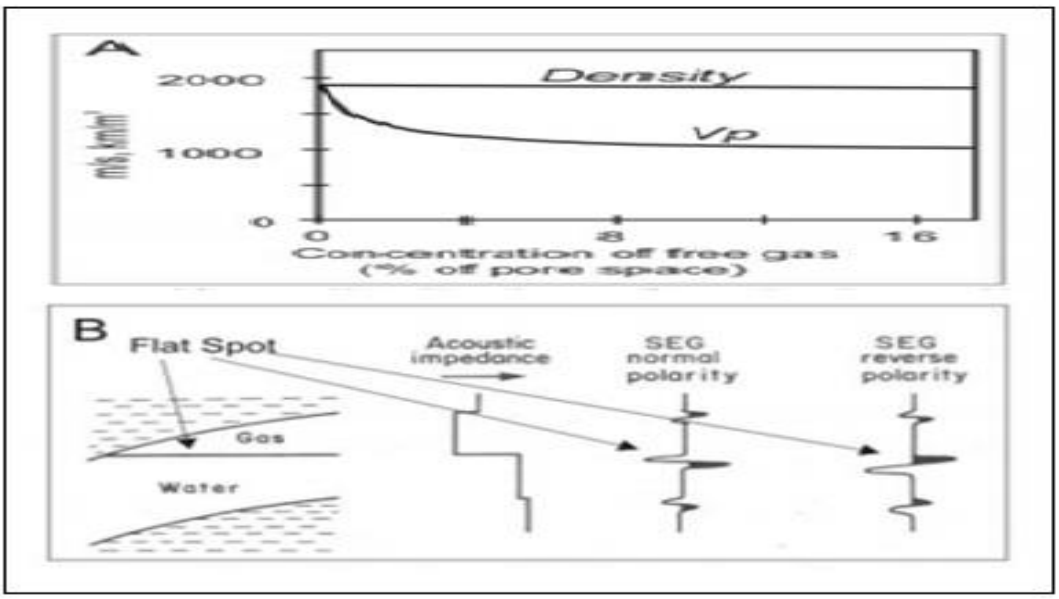

Figure 1.9 *A, Velocity and bulk density as a function of the gas saturation. The curve is calculated for sediments with porosity of 0.4 and Vp of 1900 m/s using equations from Gregory (1977) and supposing uniform spreading of a gas in the sediments. B.The effect of gas on acoustic impedance and seismic response. From (Andreassen 2009).*

The common signs of gasses presence are velocity effects is illustrated in Figure 1.9, polarity reversal, amplitude anomalies, flat spots and others (Andreassen 2009); these are illustrated in (1.10).

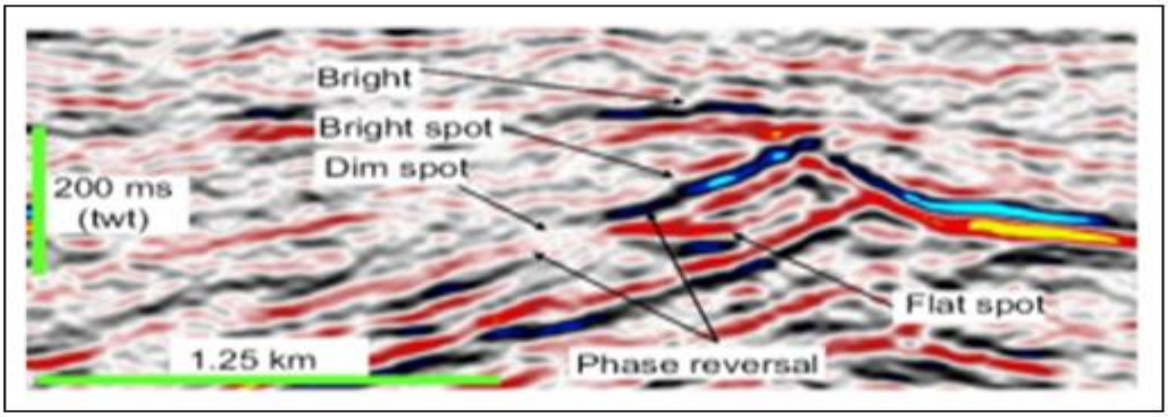

Figure 1.10 *shows the common seismic indicator of gas. From (Andreassen 2009).*

1.2.7 Seismic Indication of Fluid

Some of the seismic indications for fluid flows are as follows: Pockmarks, Gas chimneys, carbonate build-ups (mounds), mud volcano and diapers (Heggland, 2002) and BSR is direct indicator of hydrocarbon (Le. A et al., 2014). The occurrences of fluid flow are illustrated in (Figure 1.11). Since the late 80's, 3D seismic data has been used to find shallow gas accumulations (Heggland et al., 1996). Azimuth and dip are significant parameters, which can help to detect the geometry of gas chimneys as alternative to RMS amplitudes (Heggland, 2002). Some of the fluid venting sites worldwide observed to be related with the dynamics of gas hydrate systems (Judd and Hovland, 1988).

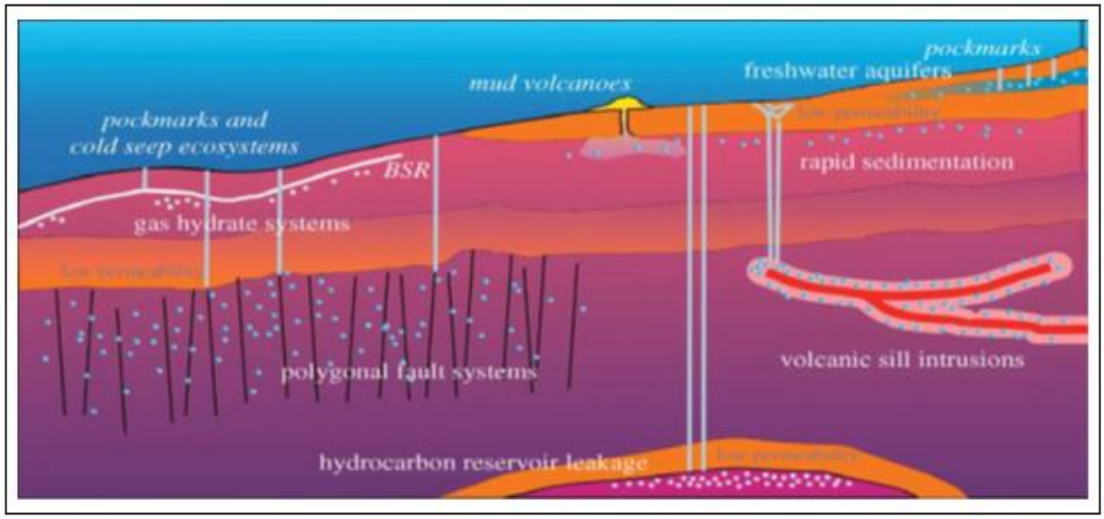

Figure 1.11 *showing focused fluid flow systems between deep and shallow systems in passive continental margins from (Berndt, 2005).*

1.2.8 Gas Hydrates

Gas hydrates are ice-like naturally occurring crystalline compounds organized in a framework of water molecules held in a cage-like structure (clathrate) that encompasses gas molecules of low-molecular weight, preferably methane (Sloan, 1998). With a adequate supply of gas and water, they form naturally and substitute pore fluids in sediments within a limited pressure and temperature region, known as the gas hydrate stability zone (GHSZ) (Hyndman and Davies, 1992).

The total amount of naturally occurring methane gas hydrates on a global scale likely exceeds 10^{19} g methane carbon. (Kvenvolden, 1993). Gas hydrates in sediments may exist as cement in the pore space, as a layer structure, or as a nodule of pure hydrate or scattered within the pore space (Chand and Minshull, 2003). Gas hydrates are very important in three aspects: economically as fossil fuel resource; methane as well as hydrogen. They have a role as submarine geohazards, by participating in the destabilization of gas hydrates below the seafloor, which leads to sub marine slump or slides. Finally, their effect on global climate change, through the release of methane a ''green house'' gas that increases global warming and is a factor of global climate change (Kvenvolden, 1993).

Two structures of gas hydrate are known in nature, I and II. Structure I is most common; the cage is set in body-centered packing and they are large enough to include methane,

ethane, and other gas molucules of similar diameter such as corbondioxide and hydrogensulfide. In the second structure II diamond packing is present, resulting in some cases big enough to take in larger molecules such as propane and isobutane (Sloan, 1990). In a fully saturated struture I, 1m^3 of methane hydrate can comprise up to 164 m^3 methane gas (Kvenvolden, 1993).

Gas hydrate occurrences are limited to two global regions: polar and deep oceanic. (Figure 1.12) shows the worldwide distribution of gas hydrates. In Polar Regions, gas hydrates are usually related with permafrost, both onshore in continental sediment and offshore in sediment of continental shelves. In deep oceanic regions, gas hydrates exist in outer continental margins in the sediment of slopes and rises where cold bottom water is present (Kvenvolden, 1993).

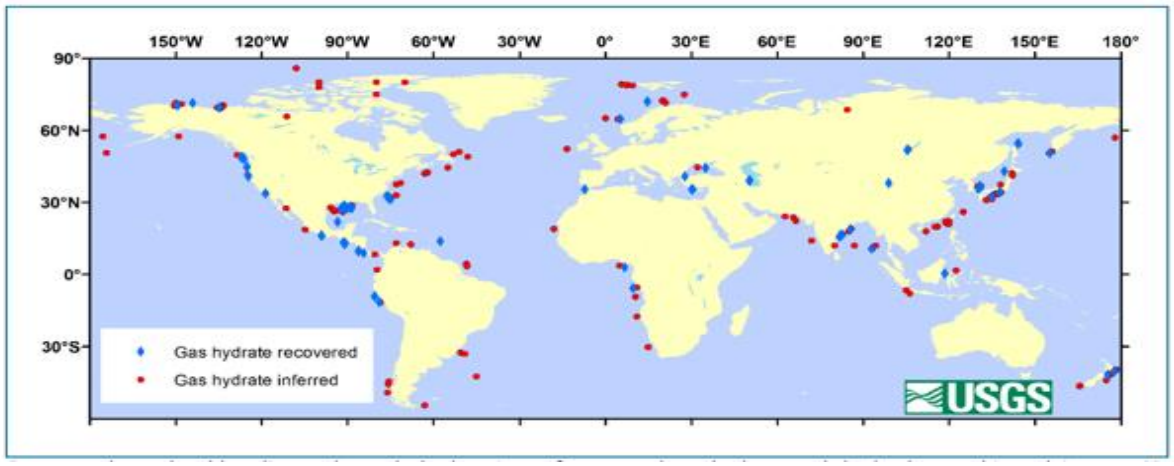

Figure 1.12 *shows the geographic location of gas hydrate occurrence from USGS.*

1.2.9 Bottom Simulation Reflection

Gas hydrate (BSR)

Gas hydrate occurrences are marked based principally on the presence of marine seismic reflection of an anomalous bottom simulating reflection profile. The nature of gas hydrate BSR can be observed in many ways, to mention some of them as follows:

2. Presences of anomalously strong reflection, BSR marks the interface between higher sonic velocities; hydrate cemented sediment above and lower sonic velocity or uncemented sediment below. Presence of bottom-simulating reflectors (**BSR**) in seismic data are taken to mean as marking the base of the hydrate stability zone (Shipley et al., 1979; Yamano et al., 1982).

3. The reflections match with depth predicted from phase diagrams (Figure1.13), it follows the sea floor topography; crosscutting primary strata which are not parallel with sea floor (BSR). The depth of the BSR and temperatures of the bottom water have been used to estimate geothermal gradients and heat flow in ocean sediment (Kvenvolden, 1993).

4. Seismic reflections from the base of the hydrate gasses are generally characterized by reversal polarity reflections opposite to those from sea floor (Figure 1.14). Current studies show BSR is more likely to be generated at the top of the free-gas zone and the bottom of the gas hydrates stabilty zone (GHSZ)(Bangs et al.,1993, Holbrook et al 1996, wood and Ruppel,2000).

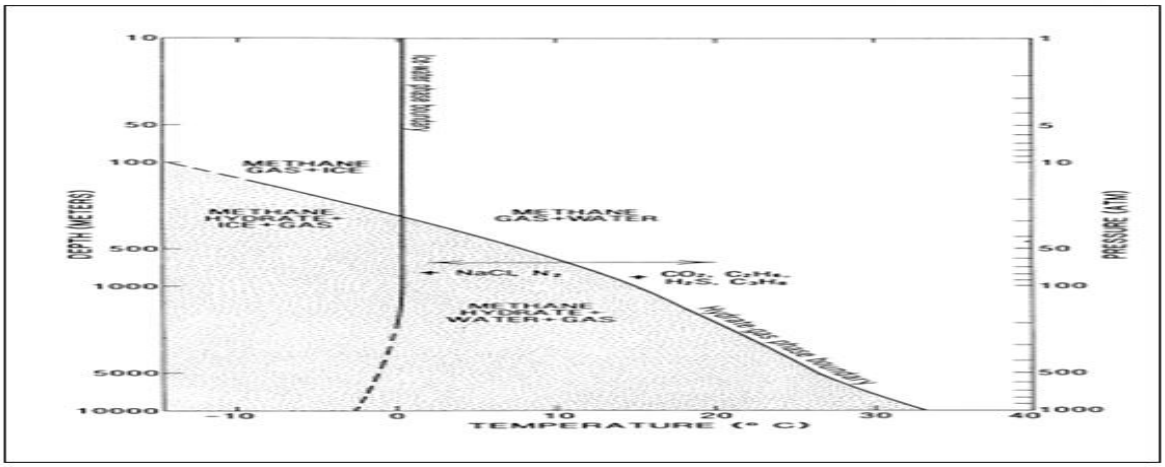

Figure 1.13 *Phase diagram showing the boundary between free methane gas (no pattern) and methane hydrate (pattern) for pure water and pure methane systems. The addition of NaCl to water shifts the boundary to the right and thus increases the area of the hydrate stability field. The depth scale assumes lithostatic and hydrostatic pressure gradients of 10.1kPa/m modified from (Katz et al., 1959).*

5. Amplitude blanking above the BHSZ

Amplitude blanking over the GHSZ shows a lessening of reflection, which is regularly observed in several gas hydrate studies (Vanneste et al., 2001). The presence of hydrates between porous spaces in sediment lower the acoustic contrast impedances between individual strata. It was argued to use amplitude blanking to estimate the hydrate accumulation above BSR (Lee et al., 1993). However, hydrate presences cannot be directly related to amplitude blanking (Vanneste et, al., 2001).

6. Enhanced reflection is a usually detected feature below and above the GHSZ. The BGHZ commonly shows the presence of enhanced reflection amplitude reflections (Andreassen 1995; Tayler et al 2000 Wood and Ruppels 2000).

Enhanced reflection is caused due to changes in acoustic impedances because of lithology and property variation across interfaces. Under normal conditions as velocity and density increases, it creates positive reflections. In the case of free gas presence below the interfaces the bright spot will be produced from a small amount of gas, a free gas level of <1% can also generate a strong decrease in p-Velocity which affects the acoustic impedances (Domenico,1974, Sheriff and Geldart 1995). Figure 1.15 is an example of proper BSR and termination of enhanced reflection at BSR.

BSR amplitude in relation to offset or angle of incidence determined by the properties of the reflecting interfaces. That is the difference in elastic properties between the two media divided by interface.

Increasing negative reflection amplitudes with increasing offset points towards a particular portion of pore spaces just below the reflector with free gases (Sheriff and Gedart 1995; Ecker et al.1998; *Yuan et al., 1999).*

7. Physical and chemichal prporties of gas hydrate

Studies suggest that gas hydrates can be spread heterogeneously in sequences of sediment according to textureal and mineralogical properties for the reason of capilarity and osmosis (Clennel et al., 1999). Interstial hydrates are favoured in coarse sediments, though it may be more dominant at great depth.

In the fine-grained sediments, the hydrate phase may be destabilized thermodynamically, and perhaps inhibited from nucleating until the normal temperature is significantly cooler than the bulk equilibrium value, probably by as much as 0.5 to 3°C. This is sufficient to shift the BSR upwards by several tens of meters, relative to estimates based in the bulk stability equilibrium curves, and will rise the depth of the first hydrate appearances by a similar amount. This estimation is based on published experimental data (Henry et al., the issue).

Several studies speculate that in the case, influx of methane is greater, water depletion and strong capillary force may stabilize isolated pockets of free gas above the HSZ. This may observed by the occurrences of anomalously low seismic velocity within the hydrate stability zone at Continental margins (Fontana and Mussumeci, 1994; Rowe et al., 1995).

The effect of the surfaces activities in clay and the fine pore space is in deep sea sediment is not fully understood.(Hyndman et al.,1992). The prences of BSR may show the presence of gas hydrate but the absences of BSR doesn't imply absences of gas hydrate (Rajuput et al., 2012). The strength of BSR reflection is governed by the amout of free gas below it (Andreassen et al., 2000a, Andreassen et al., 2000 b, Andreassen et al., 2003 ,chand and minshull 2003).

To understand the gas hydrate sytem is a major challenge including gas sources, gas migration pathway , reservoier emplacement and seal (collett et al., 2009).

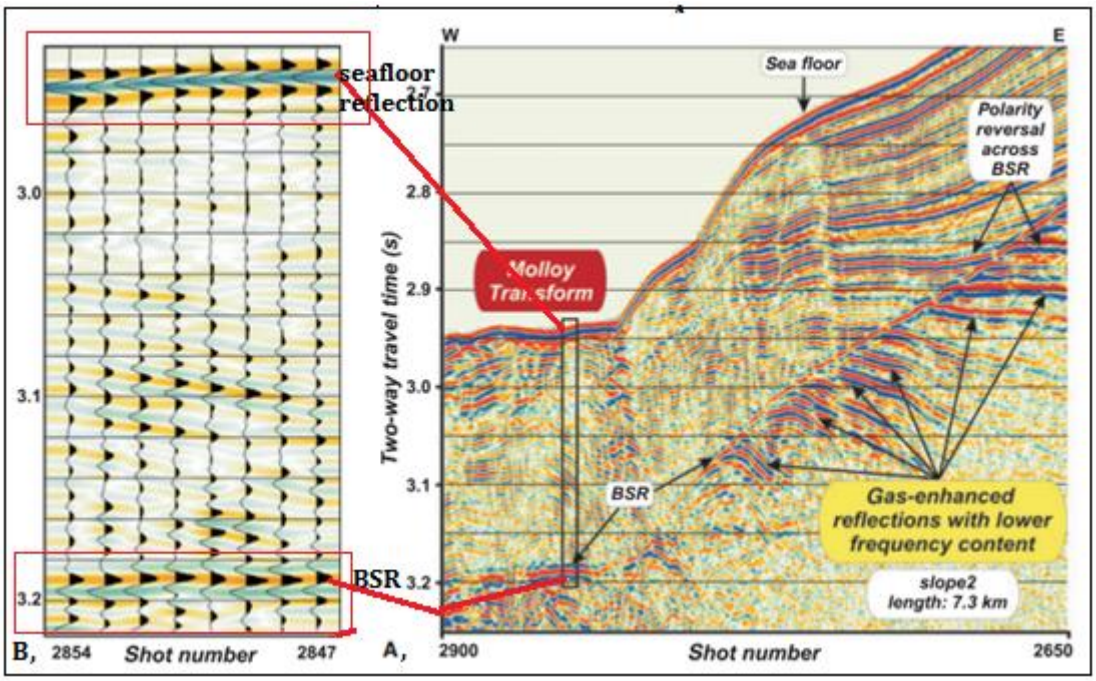

Figure 1.14 *shows seismic section from western margin of Svalbard modified A, seismic section showing proper BSR reflection and termination of enhanced reflections at BGHSZ and B, wiggle trace of BSR form the proper BSR reflection, which is opposite to seafloor reflection taken from the area with black box from (Vanneste et al., 2005).*

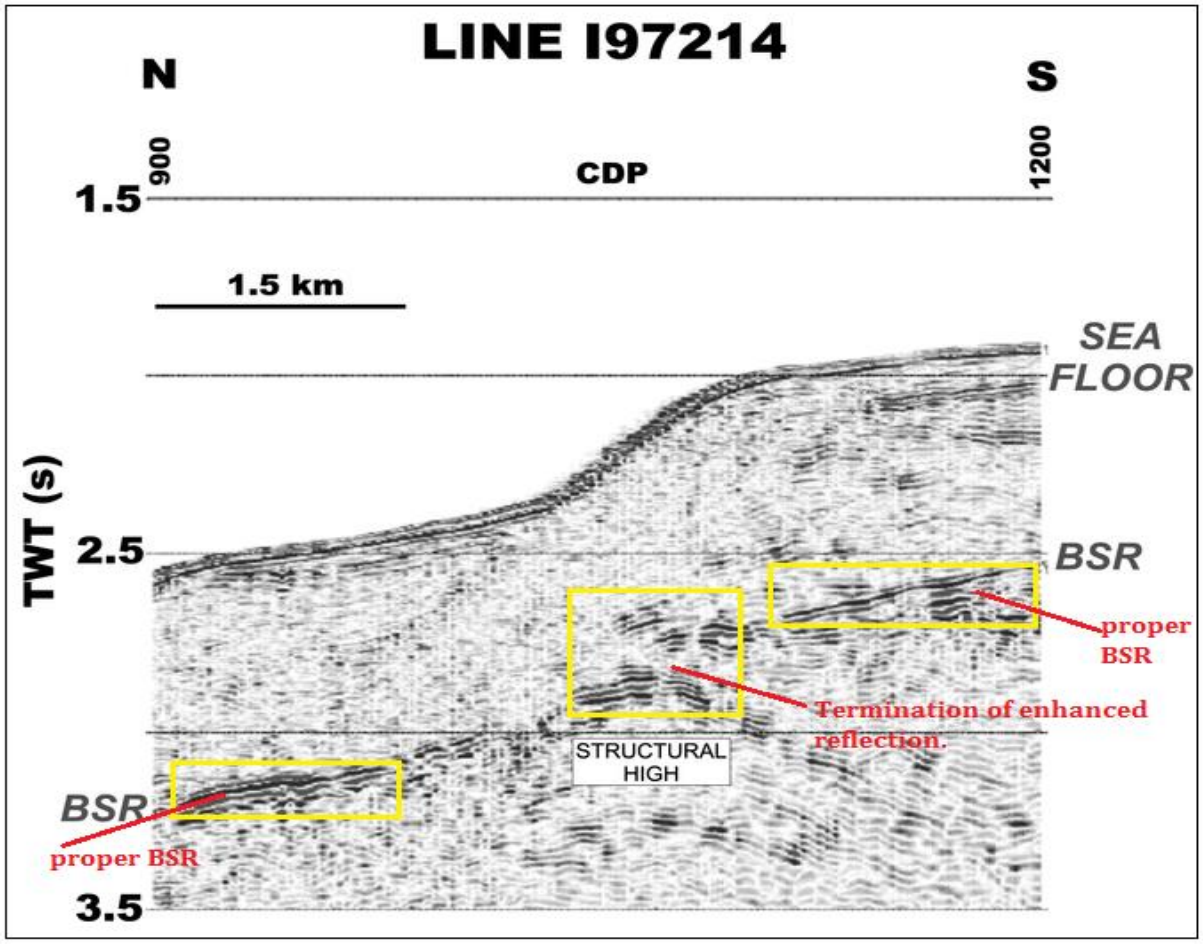

Figure 1.15 *showing BSR with proper reflections that follows the gentling dipping sea floor and termination of enhanced reflection parallel to the steeply dipping sea floor from south Shetland margin modified from (E. Lodolo et al., 2001).*

1.2.10 Ocean Bottom Cable (OBC)

The ocean bottom cables seismic activity is special occurrence, which comprises the laying of the receiver lines on the ocean floor, the multicomponent sensors of the receiver being consisted of a coupling of hydrophone and three geophones (Cafarelli, 1995). Figure 1.16 shows a typical ocean bottom cable.

A typical ocean bottom cable crew has four to six vessels, with minimum alignment being provided by a source boat, recording boat and at least one cable boat. The recording boat may be anchored along the line, or dynamically positioned; the source boat tows only the air gun (Ugbor, 2007).

An ocean bottom seismometer is designed to record man-made or natural motions under oceans and lakes. (Romanowicz et al., 1998).

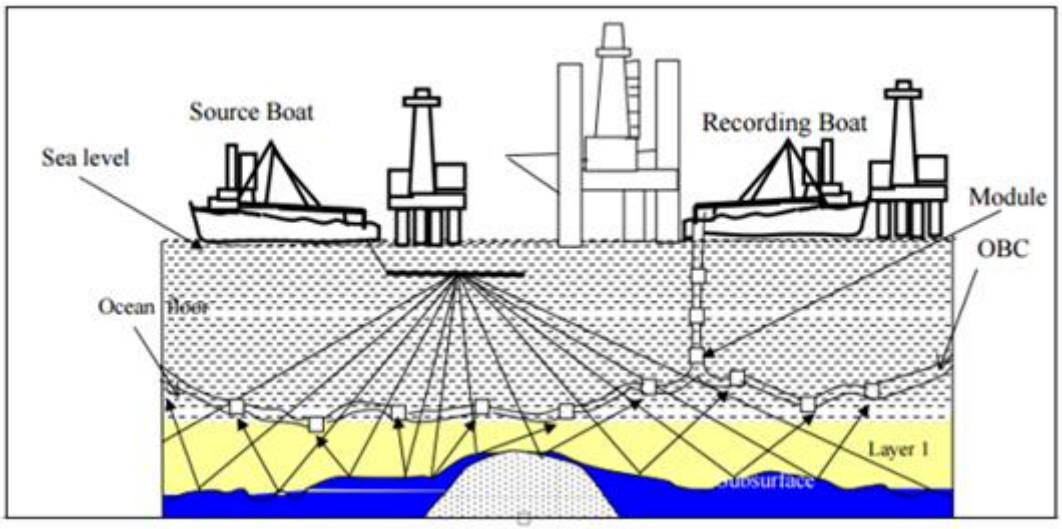

Figure 1.16 *Shows ocean bottom cable set up modified from (Ugbor, 2007).*

2. Seismic Modeling

Seismic modeling and synthetic seismograms are the result of forward modelling of the seismic response of an input Earth model; which is well defined in terms of 1D, 2D or 3D deviations in physical properties. This is used to correlate between changes in rock properties for borehole and seismic reflection data at a seismic location. It can be helpful to test an interpretation model for 2D and 3D seismic data, or to model the response of the expected geology as an aid to plan a seismic reflection survey (Makris et al., 1999). The 1D synthetics are performed in order to relate geological data from boreholes which are taken at lower sampling intervals, smaller than the vertical seismic resolution. The density and velocity from log data are averaged (blocked log) (Goldberg, et al., 1978). This is used to calculate the differences in acoustic impedance down the borehole using Zeoppritz equations (OBartels et al., 2007). The acoustic impedance log is combined with velocity to generate a reflection coefficient series in time. This is convolved with seismic wavelets to produce synthetic seismic images. The input seismic wavelet is chosen as close as possible as the original seismic acquisition. The 2D synthetics use the same approach as in 1D, where in the 2D synthetic seismic images can be used to study the seismic response of a 2D geological cross-section. For example, this can be implemented as thin beds or different responses of various fluids, gas oil or brine in a potential sand reservoir (Hodgetts and Howell, 2000). By further expanding the model

to a 3D geologic model, we can generate a 3D synthetic seismic image (Gawith and Gutteridge, 1996).

2.1 Geological Model

Geologic modelling is the applied science of generating computer-aided image of parts of the Earth based on geophysical and geological observations made on and under the Earth's surface. Geological models are the numerical equivalents of a three-dimensional geological map together with physical quantities (Mallet, 2008). Figure 2.1 and figure 2.2 show geological models and their seismic responses.

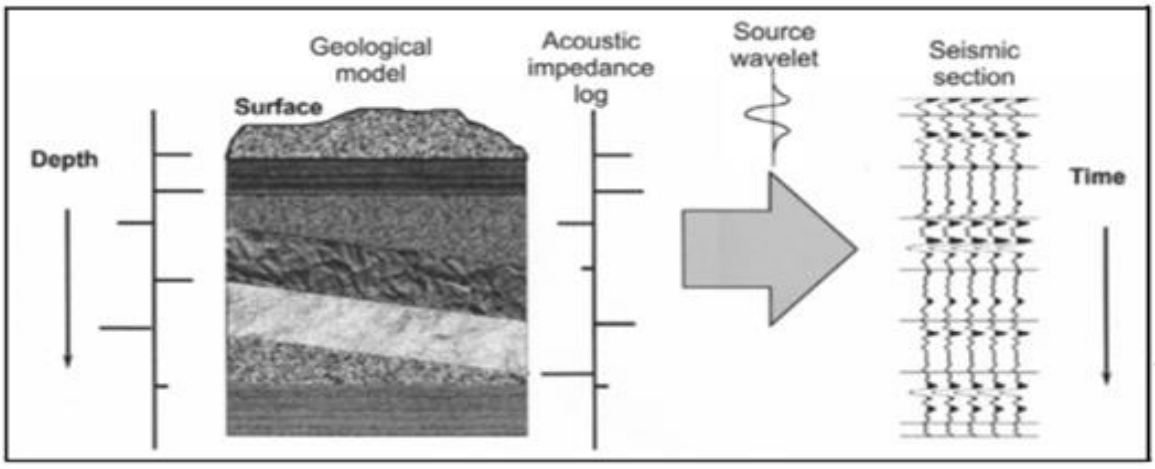

Figure 2.1 *Showing 2D geological model in depth, the sources wavelet and illustration of the possible seismic result from (Andreassen 2009).*

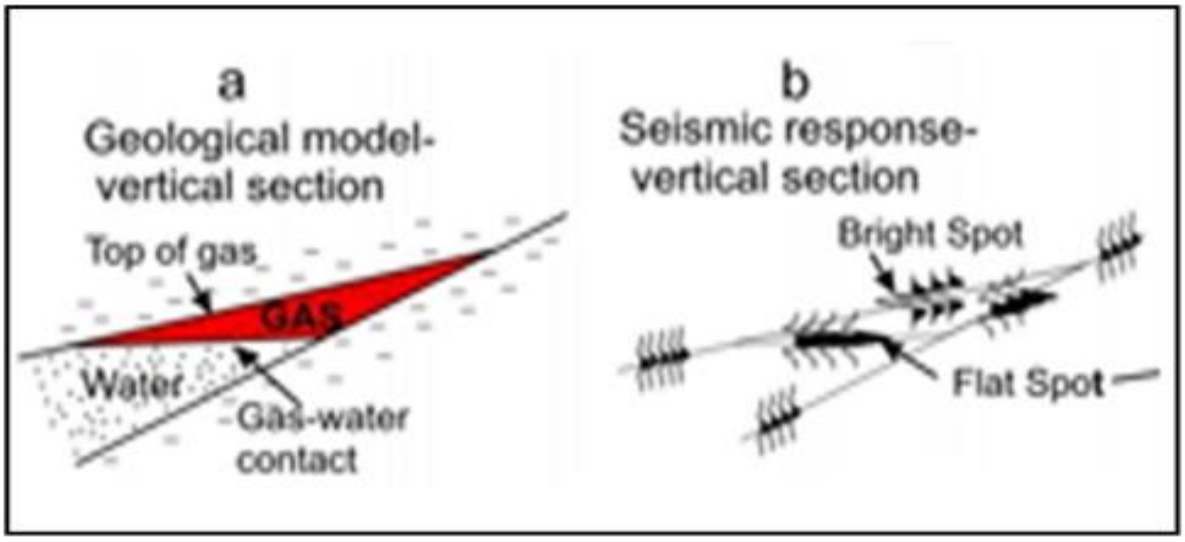

Figure 2.2 *Shows Bright spot and flat spot as the indicator of hydrocarbon in a reservoir, A, geological model and B, seismic response from (Løseth et al, 2008).*

2.2 Rock Physics

The rock physics theory clarifies the relationship between geological properties and the important elastic and seismic properties of a rock. Many sedimentary rocks are a combination of different mineral grains and fluids structured in different ways. Some of the essential properties are lithology, porosity and the presence of fluids, (Figure 2.3) illustrates the co-occurrence of fluid presence and the solid matrix in rocks from (Norsar 2011).

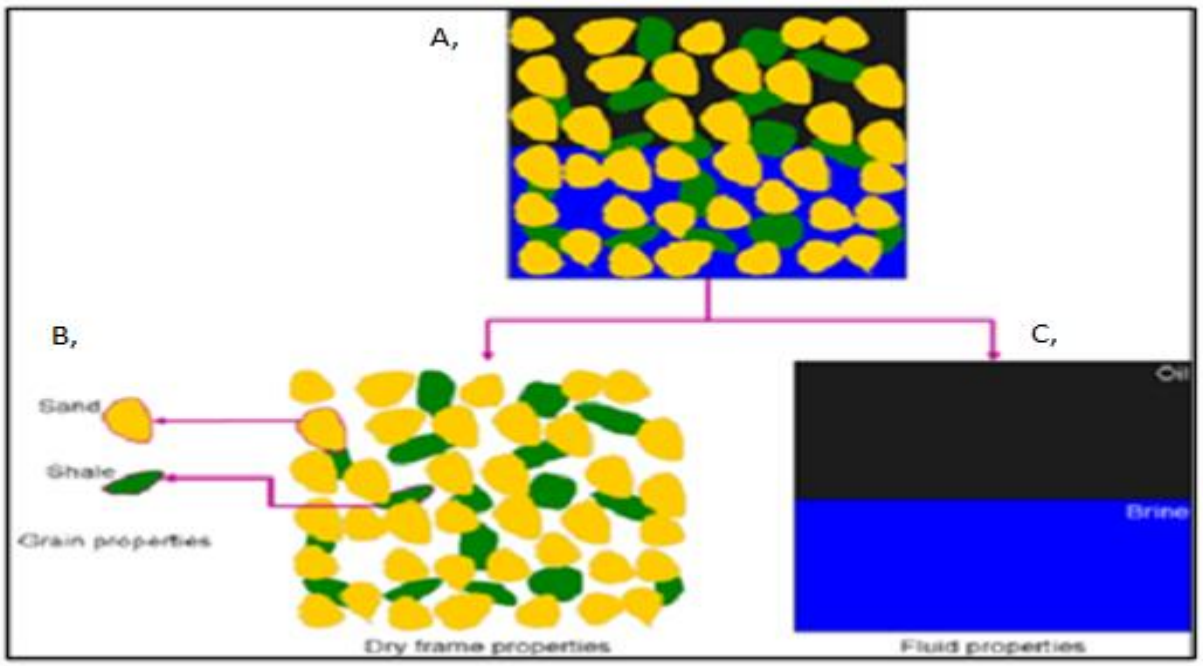

Figure 2.3 *Showing A, rock with two different solid grains and two different fluid filled within the porous space. B, grains of sand and shale and C, Brine and Oil modified from (Norsar 2011).*

Many theoretical models have been presented within scientific literature but none are more common than the Gassmann model. It has the major advantage that consists only a limited number of parameters, which can be estimated directly from the laboratory and well log observations. The Gassmann model is the chosen rock physics model applied in current SeisRoX (Norsar, 2011).

2.2.1 Seismic wave velocities

A result of the mechanical analysis that demonstrates the existence of P- and S-waves are equations, which give velocities in terms of the density ρ and elastic coefficient of a material. The velocities of P- and S-wave are:

$$Vp= \sqrt{K+4/3G/\rho} = \sqrt{E/\rho\ 1-\mu/\ (1-2\mu)(1+\mu)} \qquad \textit{Eqn. 2.1}$$

$$VS=\sqrt{G/\ \rho} = \sqrt{E/\ \rho 1/2(1+\mu)} \qquad \textit{Eqn. 2.2}$$

$$Vp/Vs= \sqrt{1-\mu/1/2-\mu} \qquad \textit{Eqn. 2.3}$$

Where K, bulk modulus, G rigidity modulus, μ the Poisson's ratio, Vp velocity of p-wave, Vs velocity S-waves, ρ density and E young'.

Because G is equal to Zero for liquids, the velocity of S-waves in liquids goes to zero. In other words, shear waves cannot be propagated through liquids. (Burger, Sheehan and Jones, 2006).

2.2.2 Gassmann

Gassmann's formulation is comprised of simple input parameters and typically can be assumed or measured from logs, as such it is important for geophysical techniques such as time lapse reservoir monitoring and direct hydrocarbon indicators (DHI) such as amplitude and the bright spot, and finally amplitude Vs offset (AVO).

The Gassmann equation provides a simple model to estimate influence of fluid saturation on bulk modules. The equation below is the useful form for the Gassmann relations, which shows the physical meanings:

$$K_s = k_d + \Delta k_d \qquad \textit{Eqn. 2.4}$$

$$\Delta k_d = \frac{ko(1-kd/ko))^2}{1-\phi-\frac{kd}{ko}+\frac{\phi ko}{kf}} \qquad \textit{Eqn. 2.5}$$

$$\text{And } \mu_s = \mu_d$$

Where K_o, k_f, k_d and k_s are the bulk moduli of the mineral, fluid, dry rock, and saturated rock frame, respectively

ϕ is porosity

μ_s and μ_d are the saturation and dry rock shear moduli.

Δk_d is an increment of bulk modulus produced by fluid saturation. These equations show that fluids in pores will affect bulk modules but not shear modulus. A shear module is independent of fluid saturation and it is a direct result of the assumptions used to derive Gassmann's equation (Berryman, 1999).

2.2.3Rock physics of gas hydrates

Gas hydrate system important elastic properties are govern by the elastic properties of the host sediment, how densely concentrated is the hydrate, how gas hydrate are spreading all over the host sediment and the elastic properties of pure gas hydrate.

According to the concentration of gas hydrate the four model in the Figure 2.4 below are made from (Sava and Hardage, 2009). The first model are uniformly dissemination of

gas hydrate throughout the host sediment it is denoted by model 1 on the Figure 2.4. The second model 2 denoted by model two hydrate fill only porous space. Model 3 thin anisotropic layer with pure layer of gas hydrate layer, with fluid saturated sediment and the last model 4 thin layer with disseminated gas hydrate in some of layers about 99%.

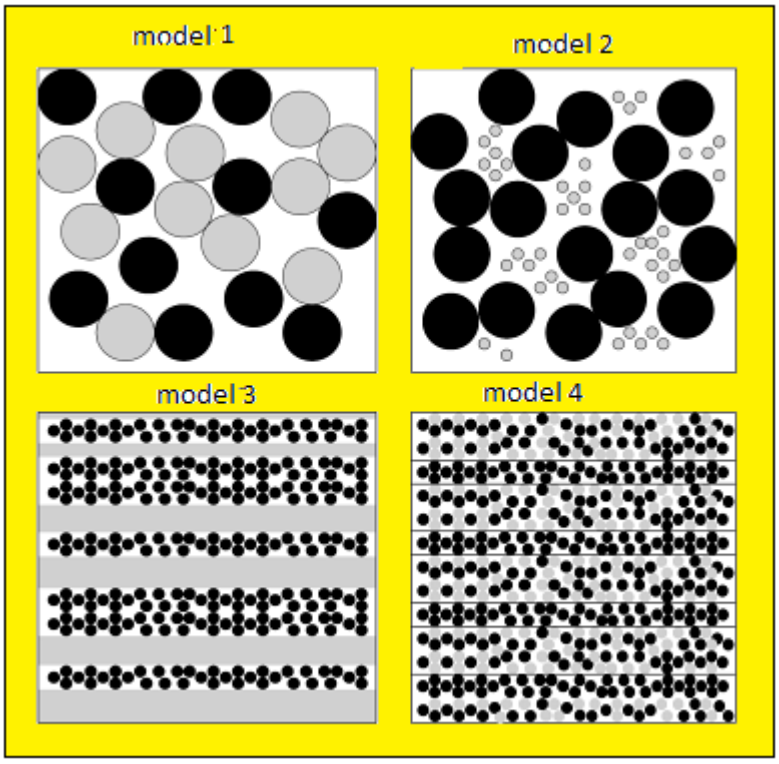

Figure 2.4 *Showing four model of gas hydrate distribution in the host sediment black color are the matrix of the rock the light gray are hydrates. Modified from (Sava and Hardage, 2009).*

2.3 SeisRoX

SeisRox is a useful seismic modeling tool, which make the calculation of the seismic response of geological reservoir models, while at the same time, simulates the influence of complex overburden and sources receiver illumination effects.

The key elements of SeisRox are multi domain model, background model, SimPLl (simulated pre-stack local imaging). (SeisRox 2.2 manual).

Multi domain model

Multi domain model denotes to the geometrical structure and rock physics properties of the model and are categorized into three different domains: the geological, the elastic

and the reflectivity domain. The model can bring in from e.g. an Eclipse file, made from Norsar 3D Model or interactively in the model editor.

Background model

Background model reflects for the seismic wave transmission effects down to and up from the reflectors, together with survey geometry, source and overburden.

SimPLI (simulated prestack Local Imaging)

SimPLI (simulated prestack Local Imaging) this aids us to take the reflection properties of the multi domain model. SimPLI combined the reflection properties with illumination and resolution information; which are produced for a given background model and survey. SimPLI rapidly simulate the synthetic prestack depth migrated (PSDM) seismic response from a give target of the model. SimPLI as a PSDM simulator is major step advancing compared to the standard seismic simulator used in the oil industry; that is the 1D-convolution methods. The 1D convolution method extract the reflectivity along the vertical lines before convolving with time-pulse. In this method, there is no 2D or 3D effects consideration. That is illumination and lateral resolution effects In this 1D convolution method only, simulate post stack time-migrated sections. (SeisRoX 2.2 manual).

SimPLI is also a simulator that works as a convolution between reflectivity and pulse. However, the reflectivity is given as a 2D/3D grid and the convolution is done in the prestack depth domain with a 3D spatial pulse corresponding to a point-spread Function (PSF). The main elements of SeisRox are illustrated in (Figure 2.5). from (SeisRoX 2.2 manual).

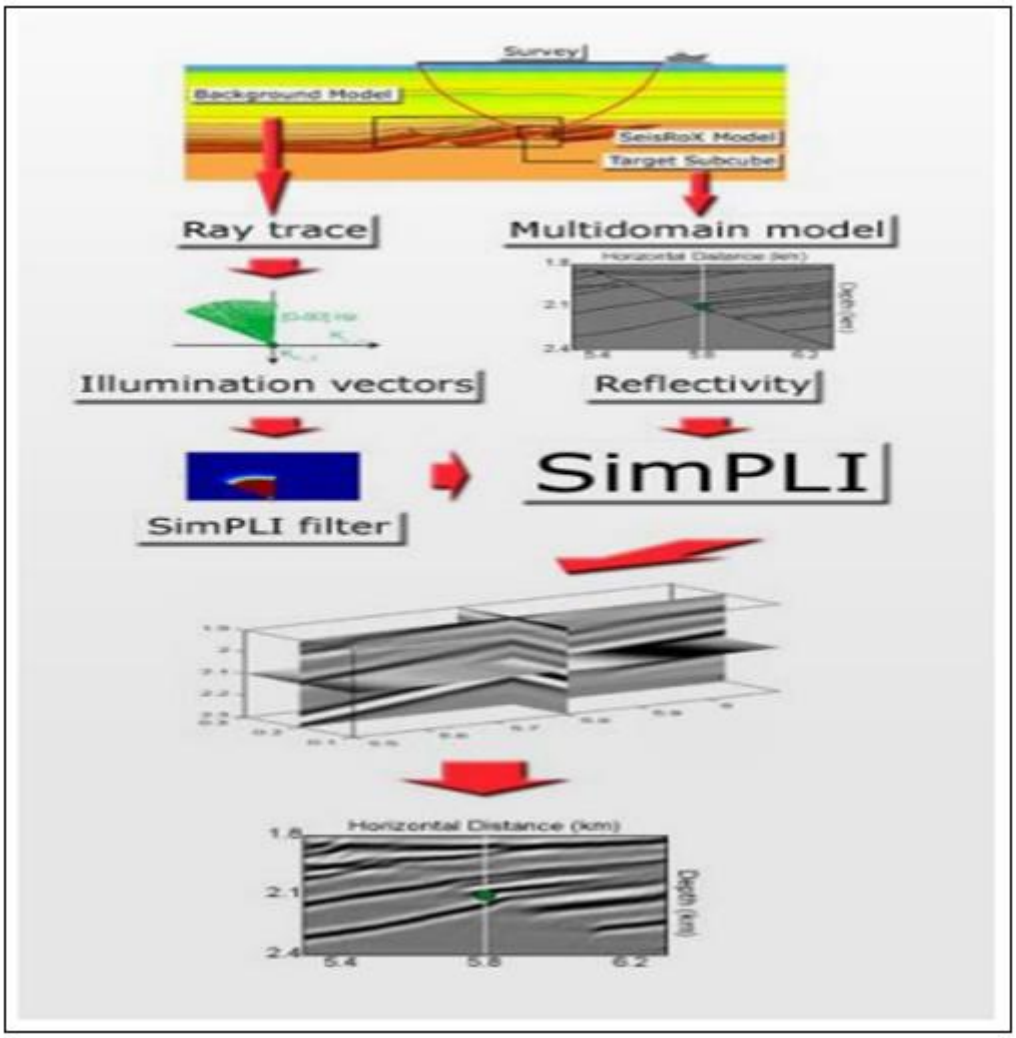

Figure 2.5 *Shows the main elements of SeisRoX. From (Norsar 2011).*

Workflow

Workflow in SeisRoX consists of the different steps and alternatives in the modelling process. Workflow explains a setup of objects and run parameters for a specified modelling process.

Data in SeisRoX, catalog of various data elements appears in data folders in the object tree. The data folder contains the various simple and complex elements that are input to a seisrox modelling process.

SeisRoX multi domain model

The SeisRox model is the essential of the SeisRoX system. It is a numerical model of a part of the sub-surface consisting various physical attributes or properties

characterizing the medium contained in the model. The SeisRoX model is designed to produce a seismic response; hence, an essential feature of the model give view of a seismic reflector in a proper way. As it is known from wave theory, a seismic reflector is exist at a place in space where the elastic parameters change abruptly over a fraction of the seismic wavelength. (SeisRoX 2.2 manual).

The basic element of SeisRoX model can be two types: a SeisRoX horizon (explicit reflector representation) and a SeisRoX volume (implicit reflector representation). In the horizon, representation all properties tied to explicitly defined surfaces (horizons) in space, where all properties are in the volume representation defined throughout a given volume.

In both representation the properties are described in a given node/cell structure. Nodes arranged in surface mesh describing the horizon space describe a seisrox horizon.

Nodes arranged in a volume mesh describe SeisRoX volume. Primarily the volume mesh is often well defined as a regular 3D grid (cube). However, the geometry of the 3D grid may later be distorted, e,g. due to time-depth conversions. However, the grid topology will always be regular and will not be changed in the model representation. (SeisRox 2.2 manual).

SeisRoX horizons/ Volumes-Geometry

A SeisRox horizon or a SeisRoX volume, as a minimum, must always include of node mesh with spatial coordinates (x, y, z) or (x, y, T) in the domain given to the nodes. That means that the SeisRox horizon and volume can always be displayed in the 3D view. (SeisRoX 2.2 manual).

SeisRoX horizon- Rock properties

The SeisRoX horizon should be considered as an interface between two physical (geological) media, which we shall, termed rocks. The horizon will have two sides, usually the above side and the below side. The rock on the above side and the rock below side can generally have different physical properties, termed rock properties. A rock property is given by numerical values assigned to the nodes or to the cell defined by the nodes, one value for each side. (SeisRoX 2.2 manual).

SeisRoX horizon- Reflector (horizon) properties

Whereas the rock properties assigned to the horizon nodes characterize the rock above and below the horizon, one can also define so called reflectors properties characterizing the reflector (horizon) itself.

A reflector property is defined on the horizon rather than the above or below. An example is the seismic reflection coefficient, characterizing the contrast (difference) between rock properties on the above and below side.

SeisRoX –volume- rock properties

The SeisRoX volume is used for describing the variation of the rock properties in space occupied by the volume grid. The properties are considered as continuously varying spatial functions between the nodes, that is, a property value in the volume is calculated by trilinear interpolation using the 8 nodes in the corresponding cell. As opposed to the horizons, the reflectors in the volume is not explicitly given, however, the reflection properties(e.g the reflection coefficient) can be estimated in each node from the variation (derivatives) in the elastic properties (implicit reflector representation).

SeisRoX property domains

SeisRoX properties (rock properties and reflector properties) can be sub divided in to categories of domains:

The geological domain: rock properties like porosity, sand/ shale fraction, oil/water saturation etc, explains the rock geologically.

The elastic domain: Rock properties like elastic moduli, seismic impedance, seismic velocity, density, etc, shows the elastic properties on scale related to the seismic wavelength.

The reflectivity domain: reflection properties like reflection coefficient, AVO/AVA attributes etc tell as the horizon and volume's behavior with reflection of seismic waves.
The free (user defined) domain: here the user can define her/his own properties/ attributes, which can be displayed in the 3D viewer.

SeisRoX model

SeisRoX model can contain one or several of SeisRoX model element that is a number of SeisRoX horizons and / or SeisRoX volumes.

SeisRoX model variants

A SeisRoX model can optionally contain one or several model variants (often termed only variant). All variants in a SeisRoX model share the same model structure that is the same number of horizons / volumes and nodes with the same topology, and the same list of properties. However, the exact positions of each node may vary, and the values of the properties in each node or cell may vary between the different variants (SeisRoX 2.2 manual).

SeisRoX recommends small PSDM target, not to use several km by several km target. The whole process use 3D FFT so large cube means high computation cost. The inline width up 1-2 km and the thickness is what you need to cover the target. The cross line few hundreds meter. The recommended sampling are 10m laterally and 5m vertically .If the structure require small sampling specially in vertical it can be chosen small sampling only in Z. This will give good reflectivity and avoid aliasing of the structure (SeisRoX 2.2 manual).

The user choose the location by defining the cube size (x, y. z) and the sampling. Based on that, The SimpLl filters will be automatically adapted in the scattering wavenumber domain (Kx, Ky, Kz) to fulfill FFT requirements (SeisRoX 2.2 manual) it is shown in Figure 2.6 the red box is the selected target.

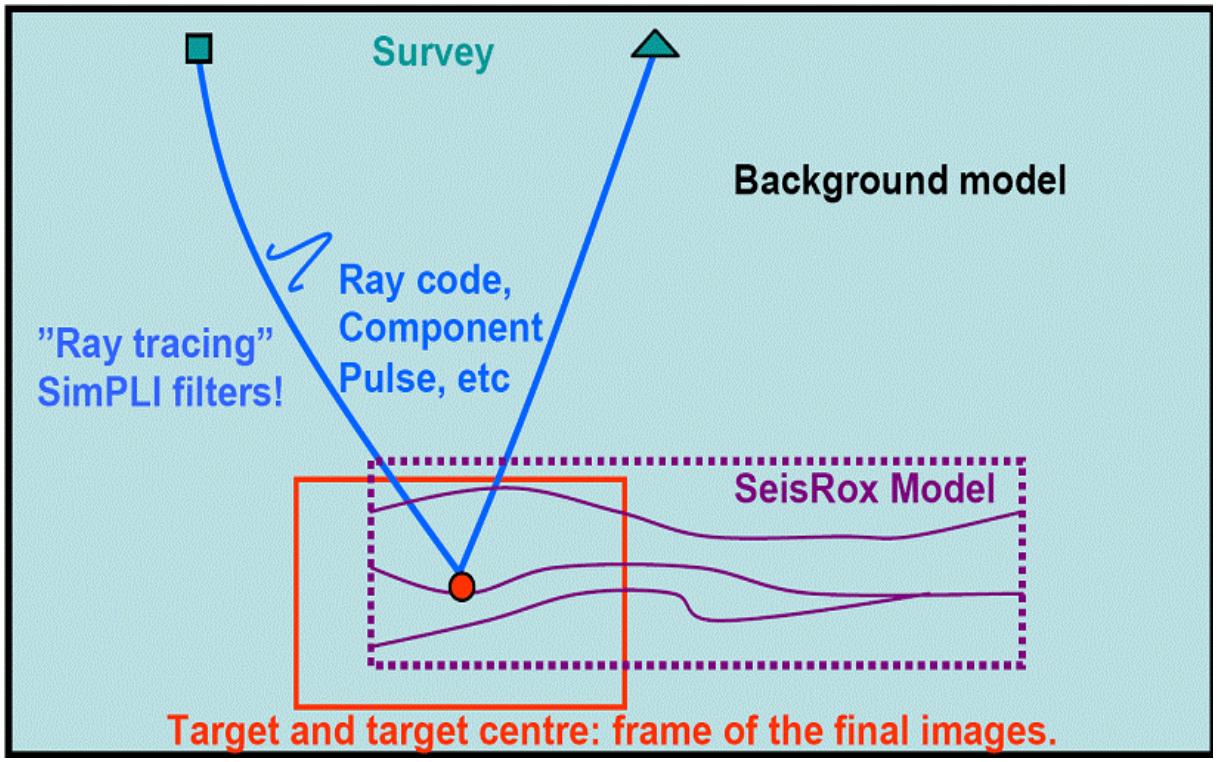

Figure 2.6 *Shows example of a point of reflection scattering include with background and seisrox model (target model), associated with survey (sources and receiver and given pulse From (Norsar 2011).*

Illumination vector

Illumination vector are automatically calculated at the center of the target when all workflow parameter are setted up. Figure 2.6 show the target and target center and Figure 2.7 illustrates how the illumination vectors Ksr are calculated as Kr- Ks.

Ksr = Kr-Ks

Where Kr is the scattered vector and Ks is the incident vector.

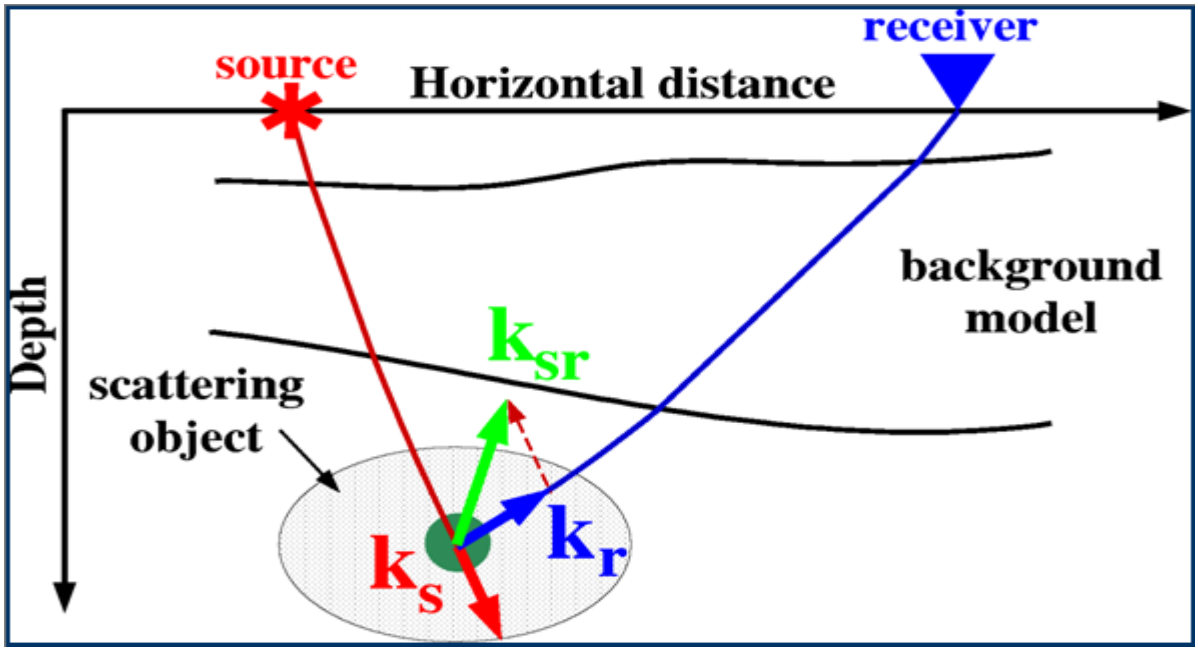

Figure 2.7 *Shows the illumination vectors at the center of the target. From (Norsar 2011).*

The illumination vector in SeisRoX calculated in the background model for a given shot / receiver couple and ray types, this tells us if there is reflector perpendicular to that vector approximately the calculation point, this reflector will indeed be illuminated in real acquisition. To visualize the illumination information contained the illumination vectors in seisrox we use the Schmidt diagram (Sheriff, 2002) which are polar plots where the angle indicates dip direction Azimuth and the distance from the origin of the plot indicates dip angle.(Sheriff 2002 the angle that a reflector makes with the horizontal; a horizontal reflector correspond to zero degree dip. Shown in Figure 2.8.

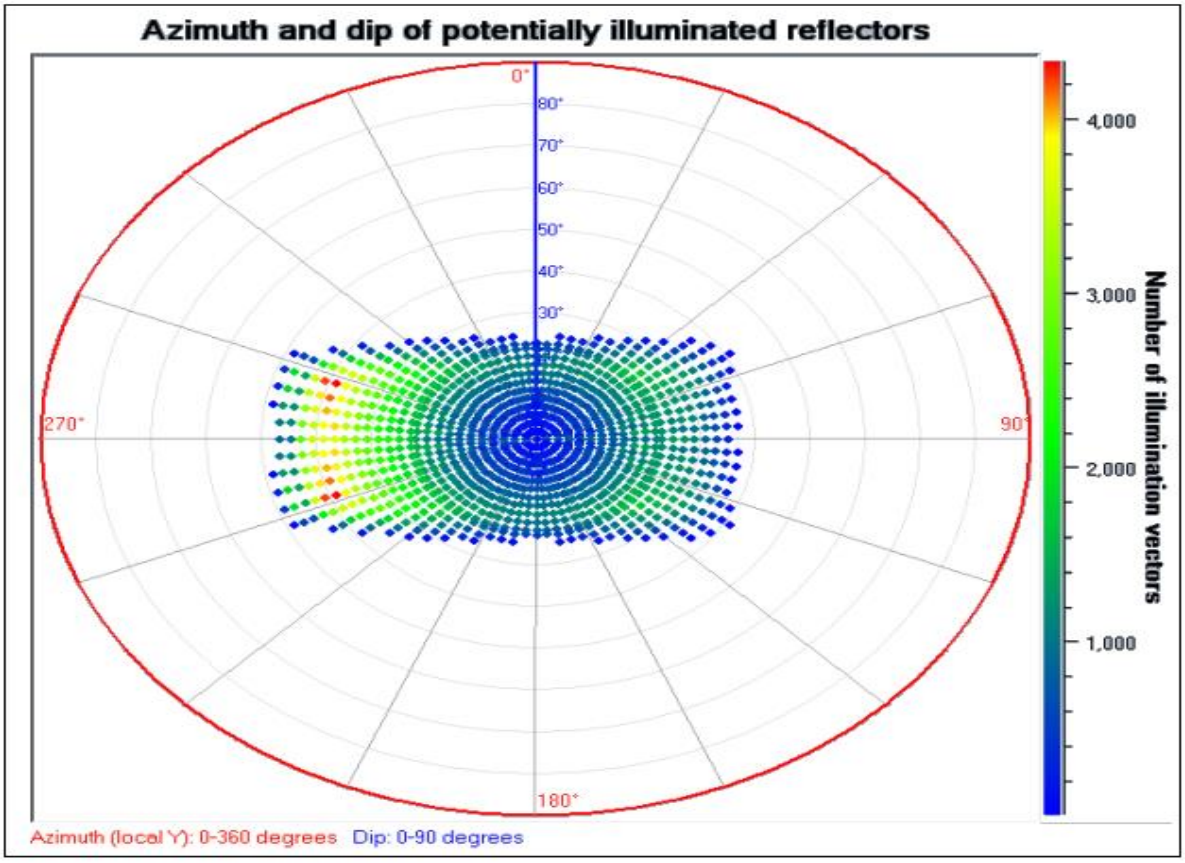

Figure 2.8 *Shows the Schmidt diagram with azimuth and dip of illuminated reflector colored scale bar for number of illuminated vector at the given area. Modified from (Norsar manual 2011).*

2.4 Resolutions in SeisRoX

Scattering wave number and psf , After all K_{SR} are calculated at an image point for selected SR pair, numerical approximation will make the local superposition of the scattering isochrones by mapping all K_{SR} in the wave number domain for certain frequency band wavelet then applied a Fourier transformation to get corresponding depth images.

The psf considers image points at a selected SR pair background velocity of model. PSF images characterized by HR high resolution and LR low resolution, the high R corresponds vertical resolution and the low R horizontal resolution it is shown in Figure 2.9 (Lecomte, I 2008).

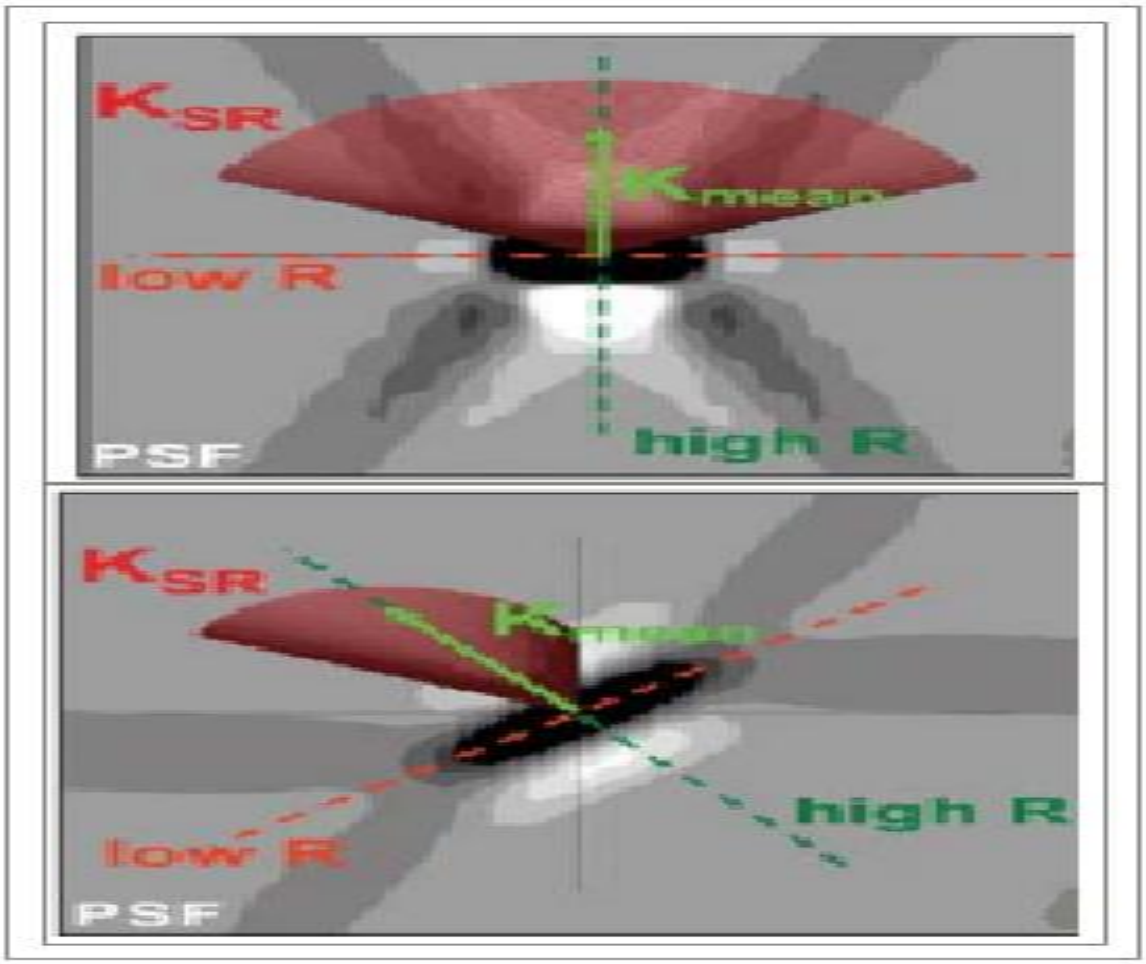

Figure 2.9 *Shows scattering wave number vectors KSR and PSF top zero offset survey and bottom at certain incident angle. Modified from (Lecomte I 2008).*

3. Data and Methodology

3.1 Data

This chapter includes data used in the study and methodology followed to find the result. These includes Models with geometry and property (Norsar model, SeisRoX model and background model), Survey parameters, wavelets selected and Target simulation PSDM parameters.

The geometry was done with assumed areal and section geometry. The properties are approximately estimated, properties of P–velocity and S- velocity. They were approximately estimated from gas hydrate study at Storegga slide OBS JM516 velocity profile data (Figure 3.1) from (Bünz et al, 2005). Density of sediment was approximately estimated from Gassmann diagram Figure 3.2 from *(*Andreassen et al. 1997*).*

The properties are given in models and tables. The modelling were done in Norsar 2D, Norsar 3D and SeisRoX. The density for background model was done in relative to the target density. Density increases with depth (Tenzer and Gladkikh, 2014). Velocities for background was obtained from the velocity profile of OBS JM 516, approximately estimated the illustration of the background model are in Figures 3.4-3.7 and the properties are in Table 3.1.

Velocity is more crucial than density concerning acoustic impedance in the case of pore fluid content gas in sand lower much more velocity than density of the rock (Andreassen, 2009).

Geometry of model was prepared for an area of (X, Y) (5 x 2) km and (Z) 2km depth with an assumed Azimuth 42° and UTM (X, Y) (572, 7175). Modelling section was selected from inline Figure 3. Property and geometry were inserted manually in Norsar 2D, the geometrical dimensions and descriptions of all models are in Table 3.2. Figure 3.8 and Figure 3.9 illustrate the target included in background model.

The model made in Norsar 2D was stored as SMIF file and exported to Norsar 3D and then to Seisrox Simulators to be processed for prestack depth migration (PSDM). The procedures followed are included in appendix.

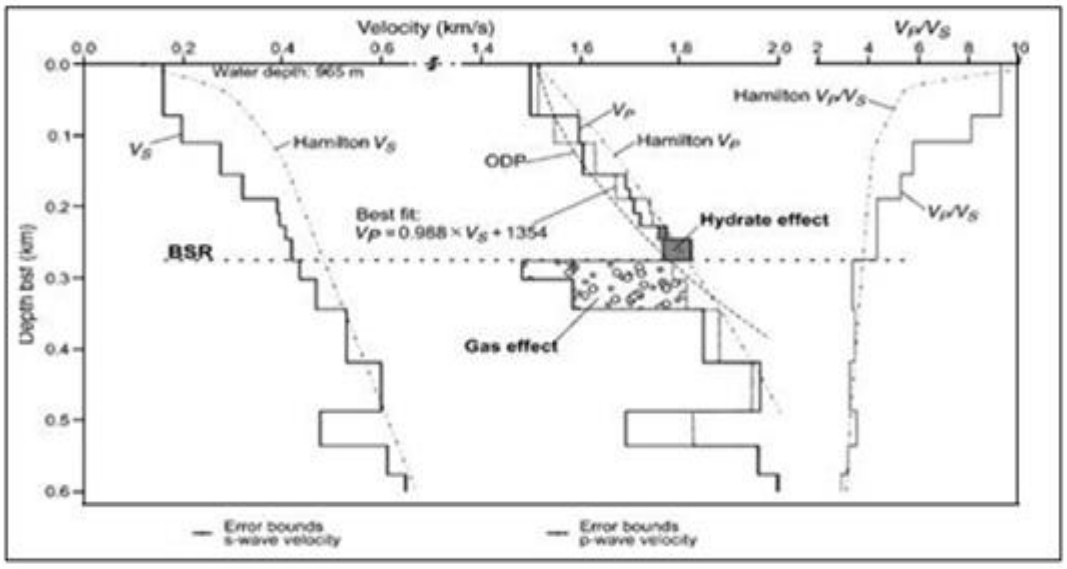

Figure 3.1 *showing p velocity and s velocity profile at OBS JM 516 from (Bünz et al. 2005).*

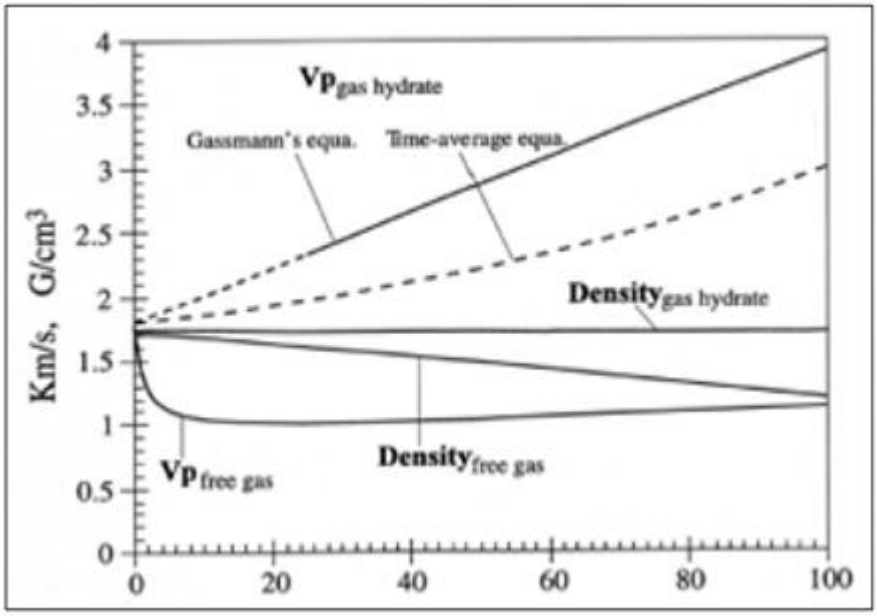

Figure 3.2 *shows Computed compressional wave velocity (km/s) and bulk density G/cm³ for sediments partially saturated with hydrate or with free gas. A velocity of 1780 m/s and bulk density of 1.74 ton/m³ for absences of hydrate and free gases (water-saturated sediments). Modified from (Andreassen et al. 1997).*

3.2 Methodology (Norsar 2D modelling program)

Norsar 2D modelling program was used for manually inserting the interface and the properties (P-velocity, S- velocity and D, density). After all the properties are inserted, it was possible to control over all properties by moving the curser at each required point. The coordinates and all the properties can be displayed at a point. The procedures are included in the appendix.

Property of Back ground Model

Depth in m	Vp (m/s)	Vs(m/s)	(ρ) ton/m^3	Remark
0-500	1500	0	1	water
500-1000	1600-1650	400	1.6-1.70	Layer 1
1000-1500	1700-1750	500	1.7-1.78	Layer 2
1500-2000	1750-1900	500	1.75-1.90	Layer3

Table 3.1 *shows the background properties P- velocity S- velocity and density verse depth.*

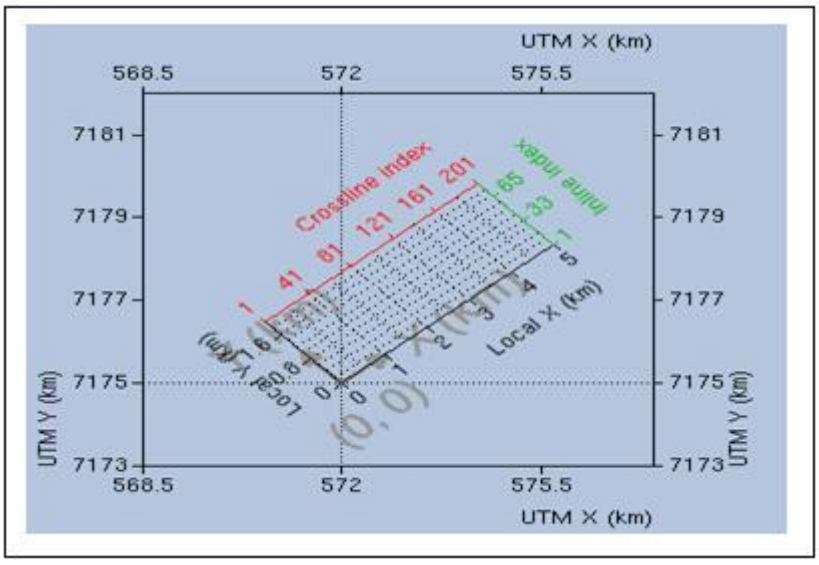

Figure 3.3 *shows Geometry of the area with assumed datum (UTM), in km (X, Y) (572, 7175) and azimuth 42.*

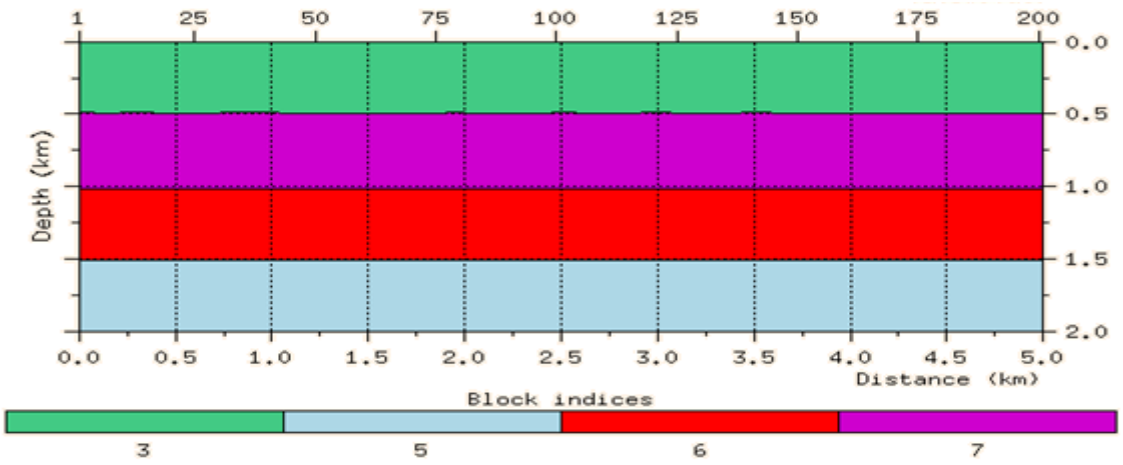

Figure 3.4 *shows the geometry of layers of blocks for the background model.*

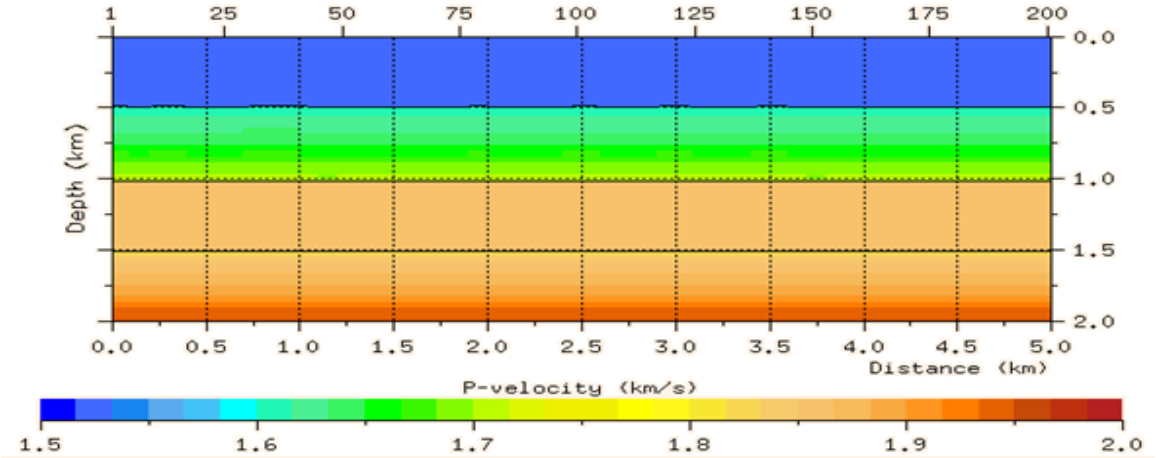

Figure 3.5 *shows p –velocity versus depth of the background model.*

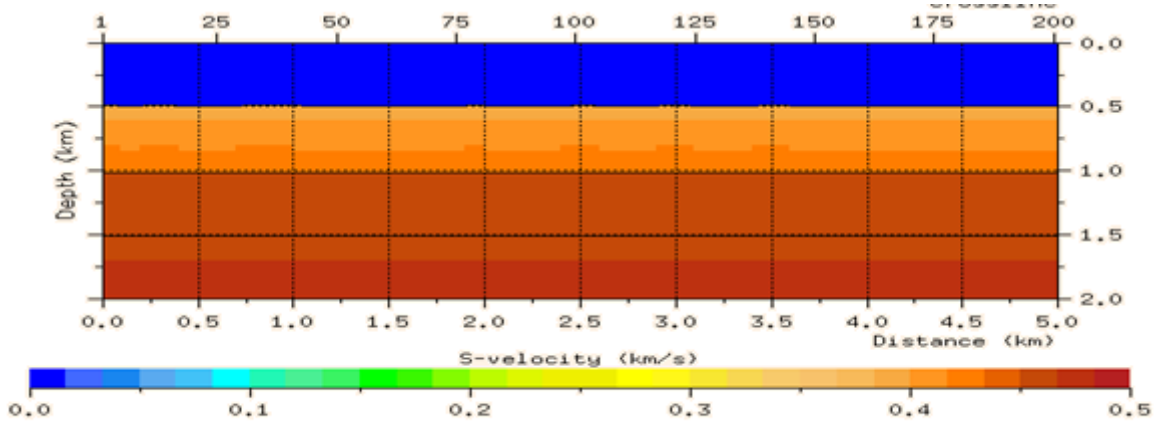

Figure 3.6 *shows S –velocity versus depth of the background model.*

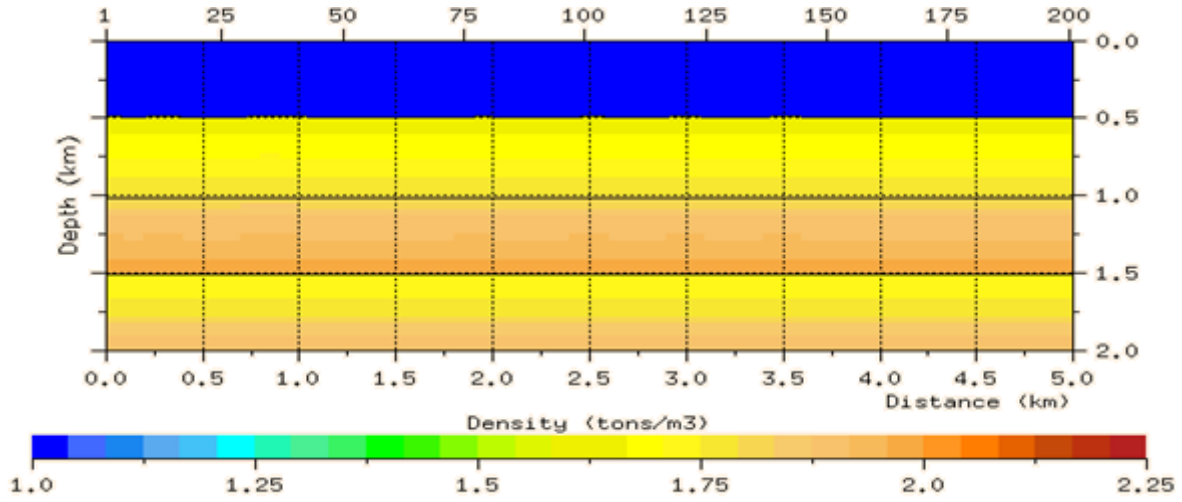

Figure 3.7 *shows density versus depth of the background model.*

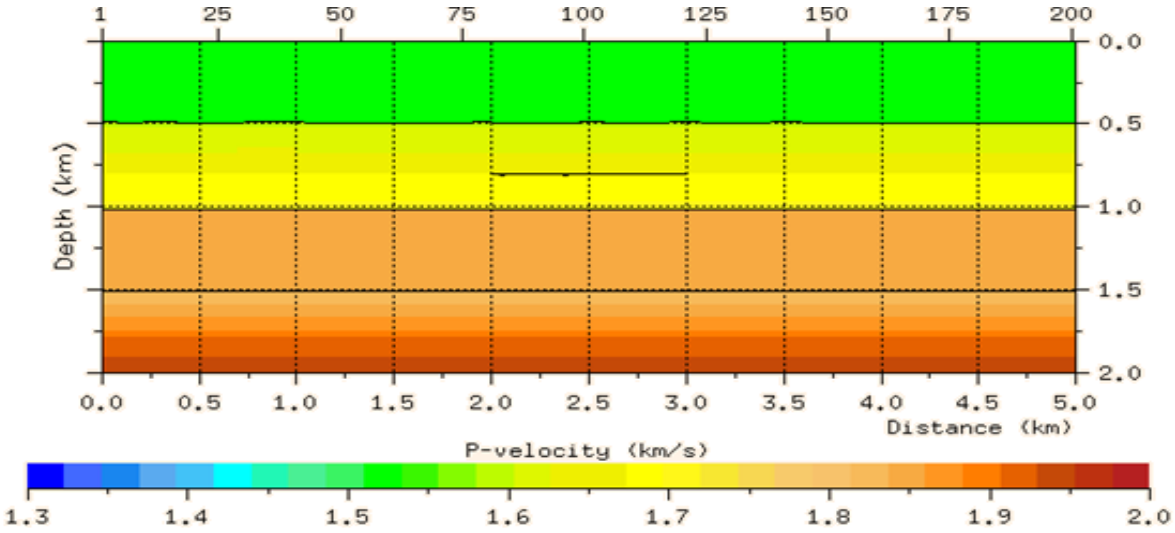

Figure 3.8 *shows background including Target.*

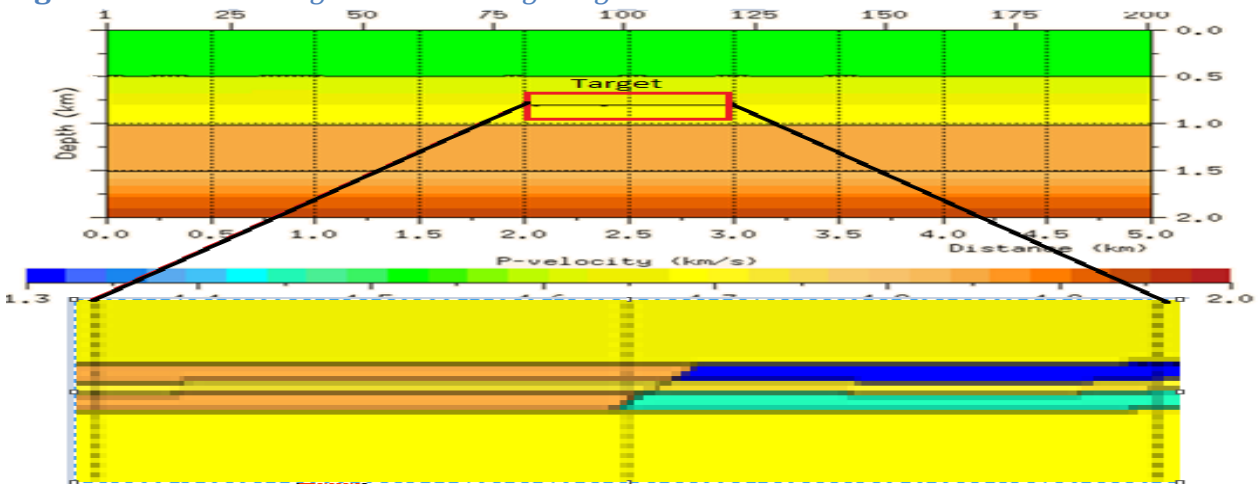

Figure 3.9 *shows magnifid image of the target between 2 and 3 km at x-axis and 0.8km z-axis or depth.*

Geometrical parameters used in the targets

model	thickness	width	Contact (dip)	Remark
Model 1	5m	1 km	horizontal	Thin layer
Model 2	5m	1km	Near horizontal	Thin layer
Model 3	5m	1km	Dipping	Thin layer
Model 4	10m	1km	Dipping	Thicker layer
Model 5	15m	1km	Dipping	continous reservior
Model 6	15m	1km	Dipping	Noncontinous reservior
Model 7	30m	1km	Near horizontal	continous reservior
Model 8	30m	1km	Dipping	continous reservior
Model 9	30m	1km	Near horizontal	Noncontinous reservior
Model 10	1m	1km	Dipping	Thin layer
Model 11 and Model 12	Different thickness	Total about 1km	Anticlinal	Anticlinal BSR

Table 3.2 *shows geometrical parameters used in the targets.*

3.2.1 Reservoir model 1, model 2 and model 3 (5m thick layer targets)

Three layers of 5m thickness and 1km width models was made, the three models includes, gas hydrate bearing sediment and free gas bearing sediments at contacts of different angle.

Model 1, (Figure 3.10) 5m gas hydrate bearing sediment at the top of 5m free gas bearing sediment horizontal contacts.

Model 2, (Figure 3.11) gas hydrate bearing sediment and free gases bearing sediment at near horizontal contact.

Model 3, (Figure 3. 12) gas hydrate bearing sediment and free gas bearing sediment at a dipping contact dip. The target is located at a depth of 800m below sea level. The same sediment background surrounds the targets. The elastic parameter used are table 3.3 model 1, Table 3.4 model 2, Table 3.5 model 3.

Reservoir Model 1

Properties used in the target			

Target layer	P velocity m/s	S velocity m/s	Density ton/m^3
Free gas bearing sediment	1450	600	1.72
Hydrates bearing sediment	1850	400	1.75
Sediment free of gases	1750	500	1.74

Table 3.3 *shows the properties P- velocity S- velocity and density* ***used in model 1.***

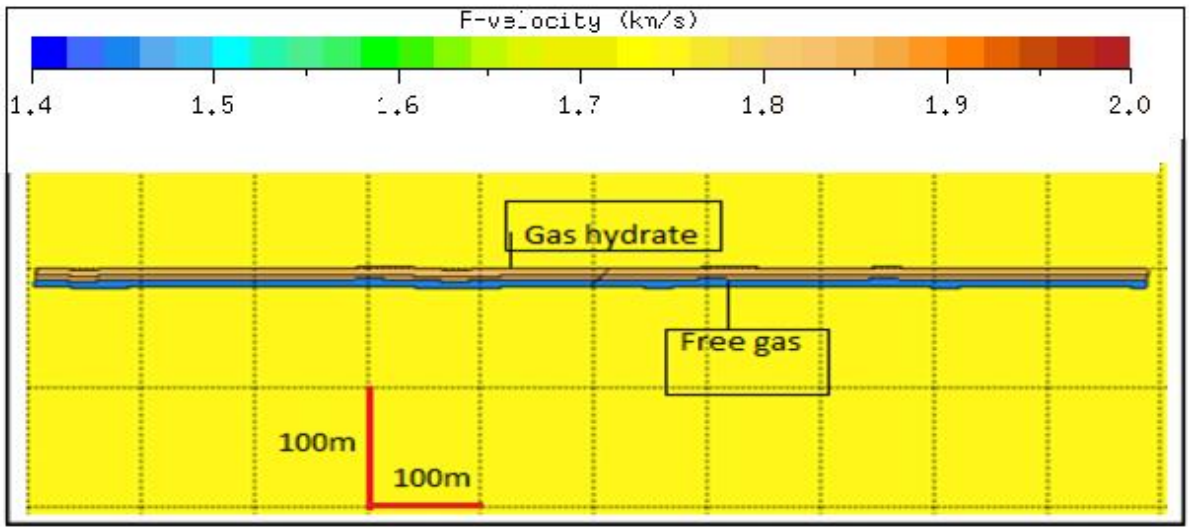

Figure 3.10 *shows horizontal contact between gas hydrate bearing and free gas bearing sediments model1.*

Reservoir Model 2

Properties used in the target

Target layer	P velocity m/s	S velocity m/s	Density ton/m^3
Free gas bearing sediment	1400	600	1.72
Hydrates bearing sediment	1850	400	1.75
Sediment free of gases	1750	500	1.74

Table 3.4 *showing the properties P- velocity S- velocity and density used in model 2.*

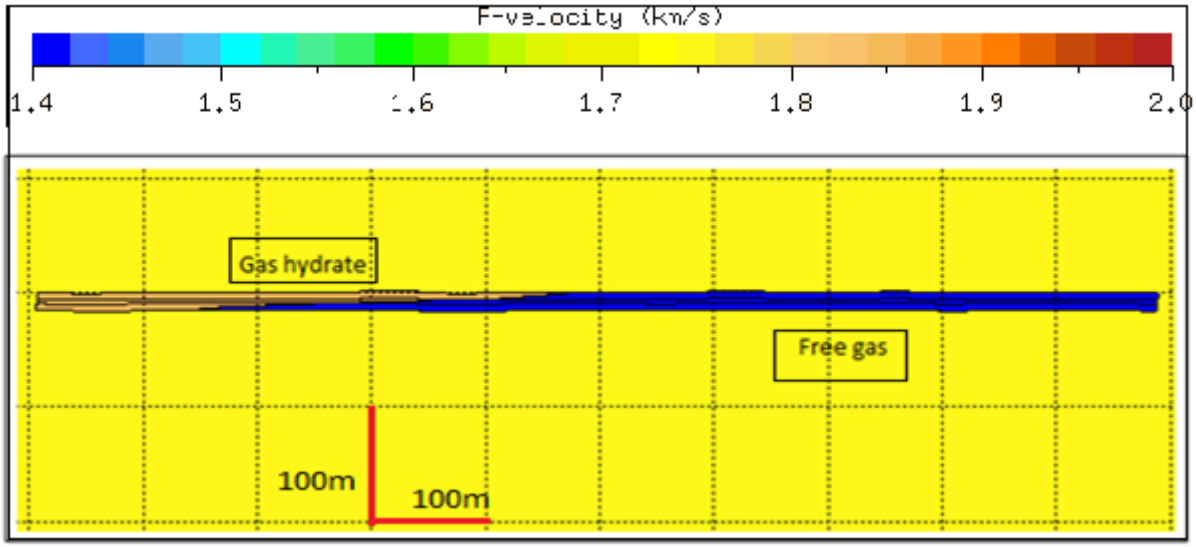

Figure 3.11 *showing near horizontal dipping contacts between gas hydrate bearing sediment and gas bearing sediment 5m thickness is mostly at the middle of the contact model 2.*

Reservoir Model 3

Properties used in the target

Target layer	P velocity m/s	S velocity m/s	Density ton/m^3
Free gas bearing sediment	1350	600	1.72
Hydrates bearing sediment	1850	400	1.75
Sediment free of gases	1750	500	1.74

Table 3.5 *shows the properties P- velocity S- velocity and density used in model 3.*

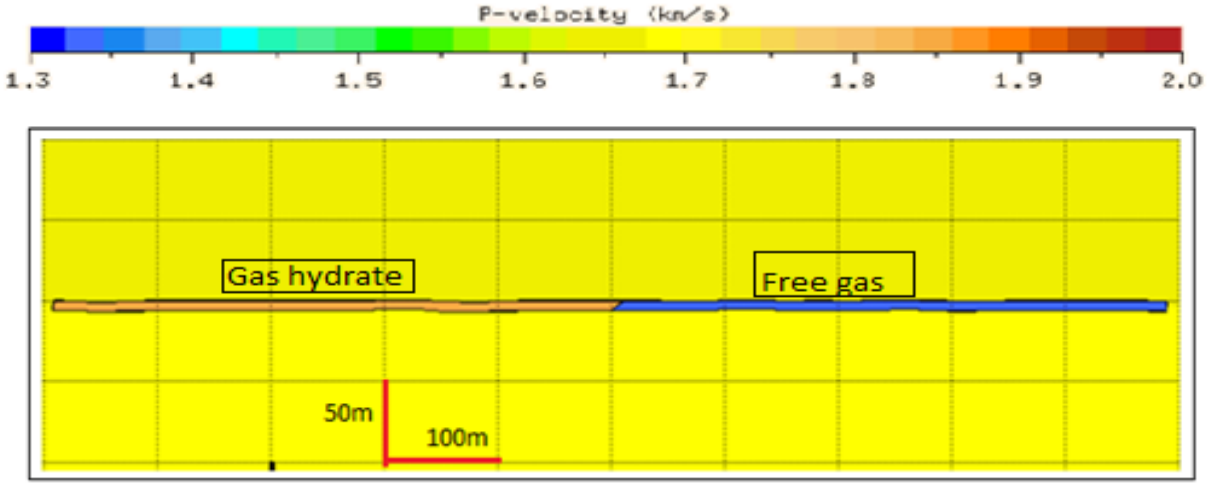

Figure 3.12 *shows dipping contacts between gas hydrate bearing sediment and gas bearing sediment model 3.*

3.2.2 Reservoir model 4, (10m) thick layer target

The 10m thick free gas bearing sediment and gas hydrate bearing sediment Figure 3.13 has made with a dipping contact and it has done for the purpose of comparing the change in thickness if it could give different result at a given incident angle and sampling in km in contrast to the 5m thick model properties are given in Table 3.6.

Reservoir Model 4 (10) m

Properties used in the target

Target layer	P velocity m/s	S velocity m/s	Density ton/m^3
Free gas bearing sediment	1350	600	1.72
Hydrates bearing sediment	1850	400	1.75
Sediment free of gases	1750	500	1.74

Table 3.6 *shows the properties P- velocity S- velocity and density used in model 4.*

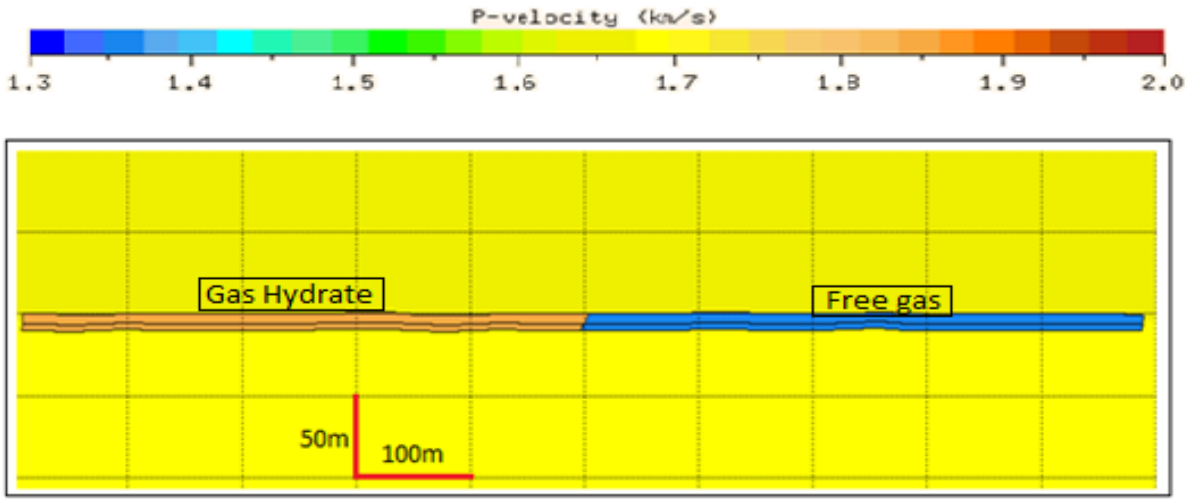

Figure 3.13 *shows dipping contacts between gas hydrate bearing sediment and gas bearing sediment 10m thick model 4.*

3.2.3 Reservoir model 5 and model 6 (15 m thick layer target)

Two 15m thick layers was made for studying the result change that could give from different geometrical contact, thickness and occurrences of hydrate bearing sediment and gas bearing sediment in continuous and non-continuous reservoir.

Model 5 Figure 3.14 15m thick layer gas bearing sediment and hydrates bearing sediment at a dipping contact, gas concentration decreases down in contact with 15m homogenous gas hydrate the properties are in Table 3.7.

Model 6 Figure 3.15 intercalation of 5m thick free gas bearing sediment and 5m thick sediment free of gas and lower layer gas bearing sediment with lower concentration. The hydrate side is also intercalation of 5m hydrate bearing sediment and 5m thick sediment free of gas (assumed non porous and impermeable) the properties are in Table3.8.

Reservoir Model 5 (15m)

Properties used in the target

Target layer	P velocity m/s	S velocity m/s	Density ton/m^3
Free gas bearing sediment	1300-1450	600	1.72
Hydrates bearing sediment	1850	400	1.75
Sediment free of gases	1750	500	1.74

Table 3.7 *shows the properties P- velocity S- velocity and density used in model 5.*

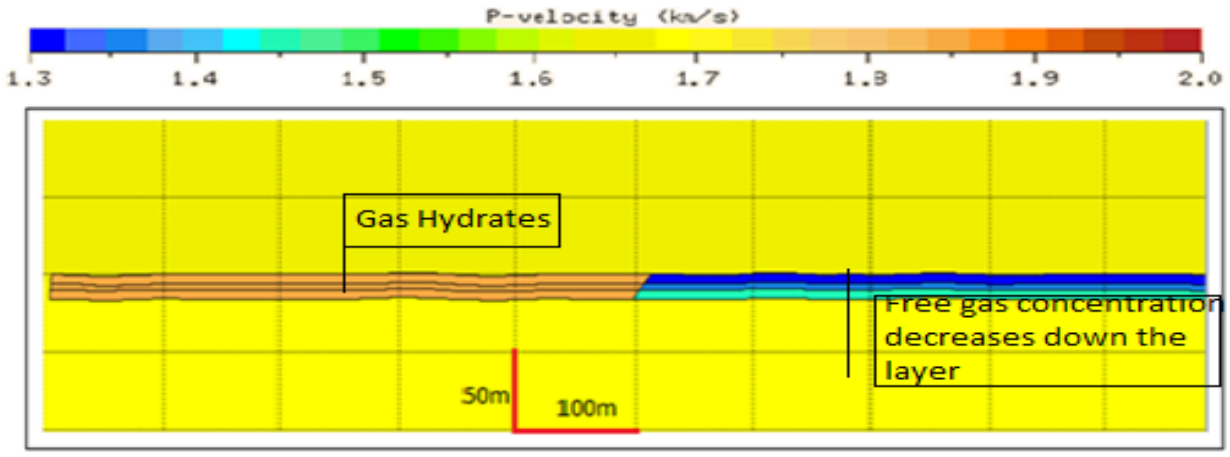

Figure 3.14 *shows dipping contacts between gas hydrate bearing sediment and gas bearing sediment 15m thick homogenous reservoir model 5.*

Reservoir Model 6

Properties used in the target

Target layer	P velocity m/s	S velocity m/s	Density ton/m^3
Free gas bearing sediment	1300-1450	600	1.72
Hydrates bearing sediment	1850	400	1.75
Sediment free of gases	1750	500	1.74

Table 3.8 *shows the properties P- velocity S- velocity and density used in model 6.*

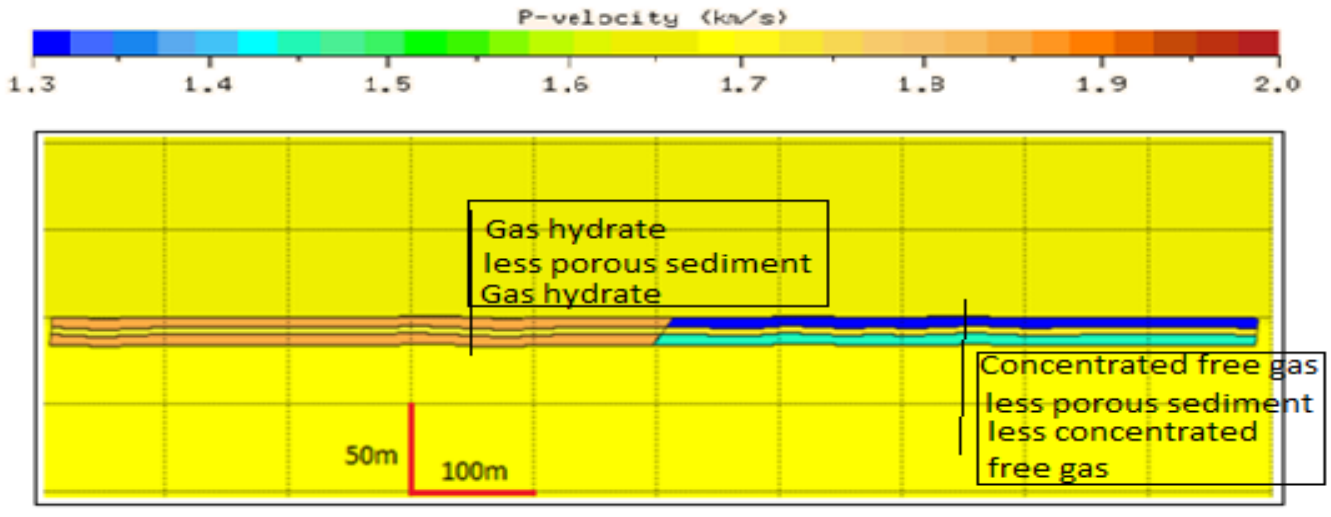

Figure 3.15 *shows a dipping interaction of gas hydrate and sediment, free gas and sediment. Model 6.*

3.2.4 Reservoir model 7, model 8 and model 9

Three 30m thick reservoir were generated to analyse the reflectivity character of the contact between hydrates bearing sediment and free gas bearing sediment as the reservoir thickness enlarged from model 2 to model 7 and model 3 to model 8 with different nature of occurrences and contact angle.

Model 7 Figure 3.16 is homogenous reservoir of hydrate and gas at near horizontal contact or gentling dipping contact the properties are in Table 3.9.

Model 8 Figure 3.17 the contact is steeply dipping and the properties are given in table 3.10.

Model 9A Figure 3.18 shows the intercalation of gas hydrate bearing sediment and sediment without hydrate or gas and the intercalation of gas bearing sediment and sediment without gas. It includes three thin layers of gases bearing sediment and two-sediment without gas at gradually dipping contact with hydrates bearing sediment, the model totally includes five layers each with thickness about 5m. The gas free sediments extends to the HSZ and free gas zone the properties are given in Table 3.11.

Model 9B figure 3.19 the HSZ is fully covered by hydrate bearing sediment, the free gas-bearing region is intercalation of different concentration of gas, very low gas in the less porous sediment layers. The properties are in Table 3.12.

Model 9C Figure 3.20 shows the intercalation of different concentration of gas bearing layers and hydrate bearing layers the highest concentration of gas is assumed to form higher concentration of hydrates. The lower concentration of gas is assumed to form lower concentration of hydrates the properties are in Table 3.13.

Reservoir Model 7 (30m)

Properties used in the target

Target layer	P velocity m/s	S velocity m/s	Density ton/m^3
Free gas bearing sediment	1350	600	1.72
Hydrates bearing sediment	1850	400	1.75
Sediment free of gases	1750	500	1.74

Table 3.9 *showing the properties P- velocity S- velocity and density used in model 7.*

Reservoir Model 7 (30m)

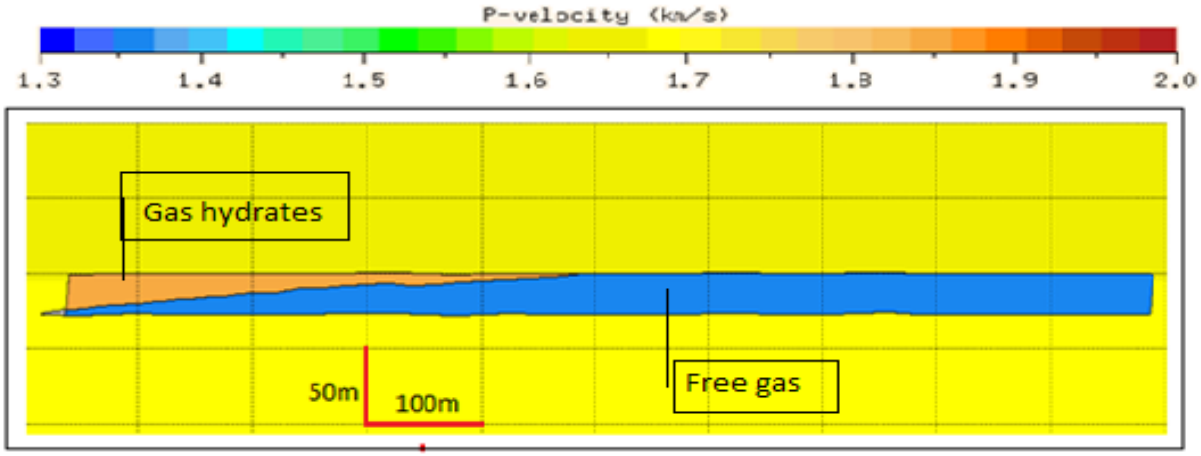

Figure 3.16 *shows a near horizontal dipping contact of gas hydrate and sediment and free gas (30m thick) Model 7.*

Reservoir Model 8 (30m)

Properties used in the target

Target layer	P velocity m/s	S velocity m/s	Density ton/m^3
Free gas bearing sediment	1300	600	1.72
Hydrates bearing sediment	1850	400	1.75
Sediment free of gases	1750	500	1.74

Table 3.10 *shows the properties P- velocity S- velocity and density used in model 8.*

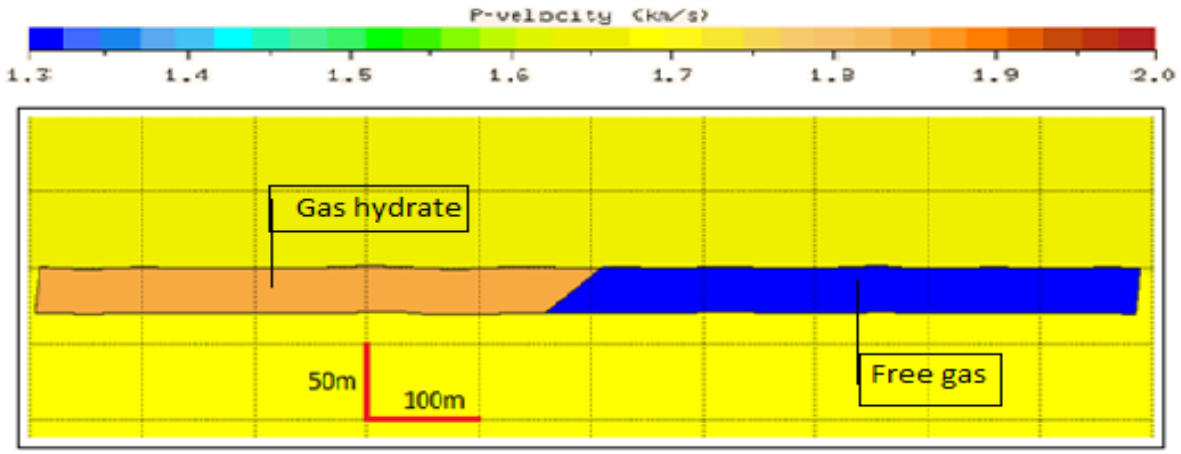

Figure 3.17 *shows a dipping contact of gas hydrate and sediment and free gas (30m thick). Model 8.*

Reservoir Model 9 (30m) intercalation every 5m

Properties used in the target

Target layer	P velocity m/s	S velocity m/s	Density ton/m^3
Free gas bearing sediment	1350	600	1.72
Hydrates bearing sediment	1850	400	1.75
Sediment free of gases	1750	500	1.74

Table 3.11 *shows the properties P- velocity S- velocity and density used in model 9A.*

Reservoir Model 9 A (30m)

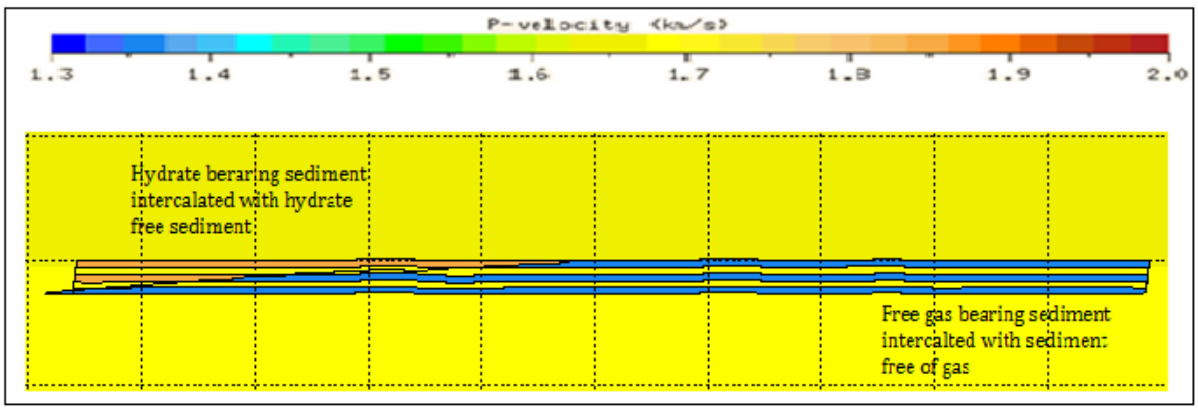

Figure 3.18 *shows near horizontal dipping contact of gas hydrate, sediment and free gas (30m thick). Model9.*

Model 9B Properties used in the target

Target layer	P velocity m/s	S velocity m/s	Density ton/m^3
Free gas bearing sediment	1350	600	1.72
Hydrates bearing sediment	1850	400	1.75
Sediment free of gases	1750	500	1.74

Table 3.12 *shows the properties P- velocity S- velocity and density used in model 9B.*

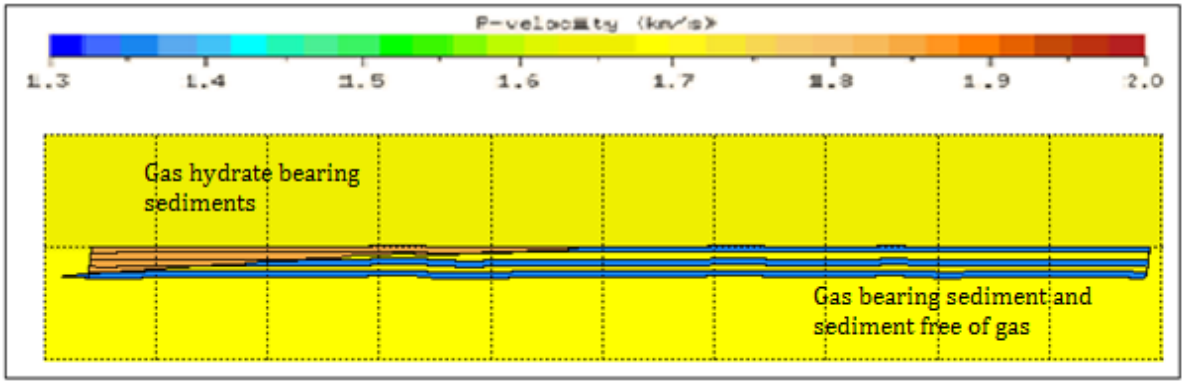

Figure 3.19 *shows near horizontal dipping contact of gas hydrate, sediment and free gas (30m thick). Model 9B.*

Model 9C Properties used in the target

Target layer	P velocity m/s	S velocity m/s	Density ton/m^3
Free gas bearing sediment	1350-1550	600	1.72
Hydrates bearing sediment	1780-1850	400	1.75
Sediment free of gases	1750	500	1.74

Table 3.13 *shows the properties P- velocity S- velocity and density used in model 9B.*

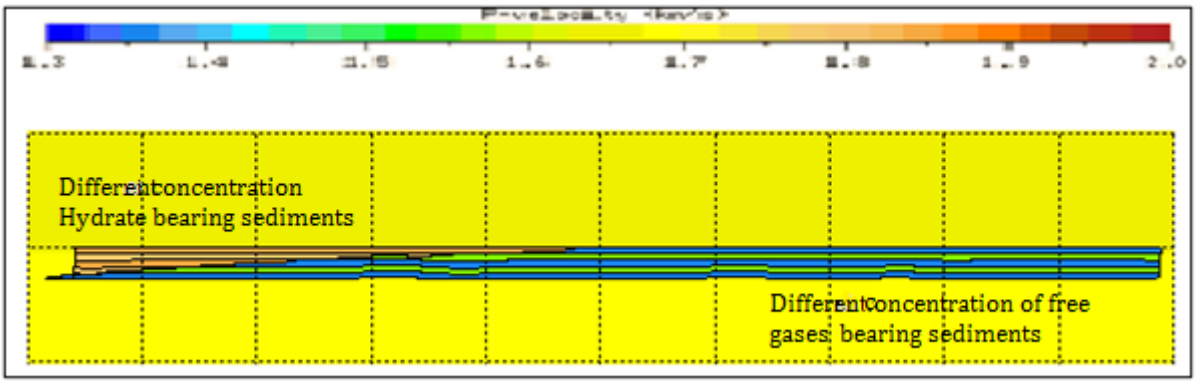

Figure 3.20 *shows near horizontal dipping contact of gas hydrate, sediment and free gas (30m thick). Model 9C.*

3.2.5 Reservoir model 10, 1m thick

Model 10 Figure 3.21 shows Very thin layer of 1m was generated for the purpose studying their reflectivity character at narrow contact of gas bearing sediment and hydrate bearing sediment occurrences between bedding planes or as a thin layer, the properties are in Table 3.14.

Reservoir Model 10 (1m)

Properties used in the target

Target layer	P velocity m/s	S velocity m/s	Density ton/m^3
Free gas bearing sediment	1350	600	1.72
Hydrates bearing sediment	1850	400	1.75
Sediment free of gases	1750	500	1.74

Table 3.14 *shows the property used in model 10.*

Reservoir model 10

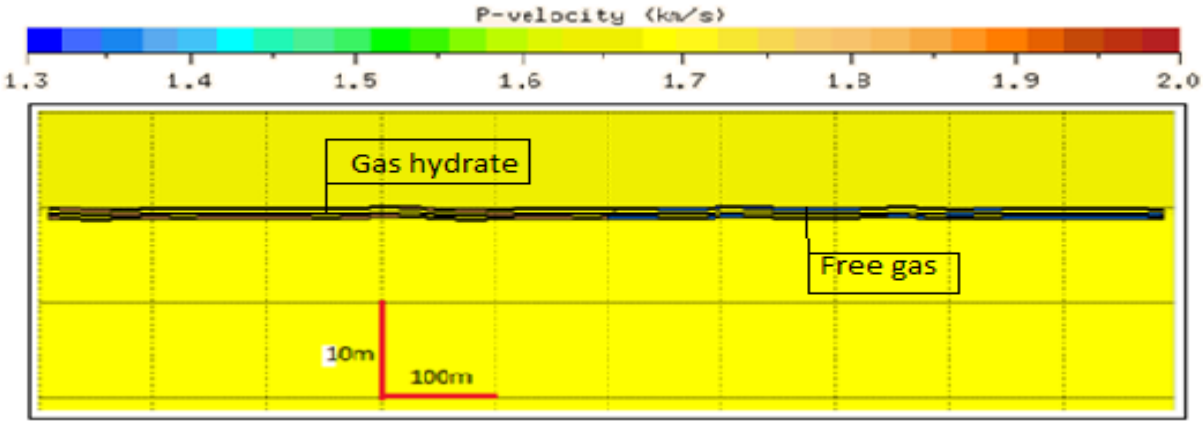

Figure 3.21 *shows very thin layer of gas hydrate and free gas in a dipping contact.*

3.2.6 Reservoir model 11 and model 12

Models made for different mode of geological occurrences of hydrate bearing and gas bearing sediments.

Model 11 Figure 3.22 an anticlinal shaped BSR cross cutting intercalated layers including free gas bearing sediment and less porous sediment without gas. The thickness varies from 2m – 20m less porous layer and 20- 200m layers with gas. This has been made to see the effect in the presences of different thickness of less porous layers. It was assumed the hydrate bearing sediment was formed at the top of the layers of both type the properties are given in table 3.16. Model 12 Figure 3.23 was made for analyzing of Significant enough thick absences of gas and hydrates between thick layers of containing free gases and top covered with hydrate bearing sediment. The properties are given in Table 3.16.

Reservoir Model 11(Properties used in the target)

Target layer	P velocity m/s	S velocity m/s	Density ton/m^3
Free gas bearing sediment	1350	600	1.72
Hydrates bearing sediment	1850	400	1.75
Sediment free of gases	1750	500	1.74

Table 3.15 *shows the properties P- velocity S- velocity and density used in model 11.*

Reservoir Model 11 (Anticlinal BSR)

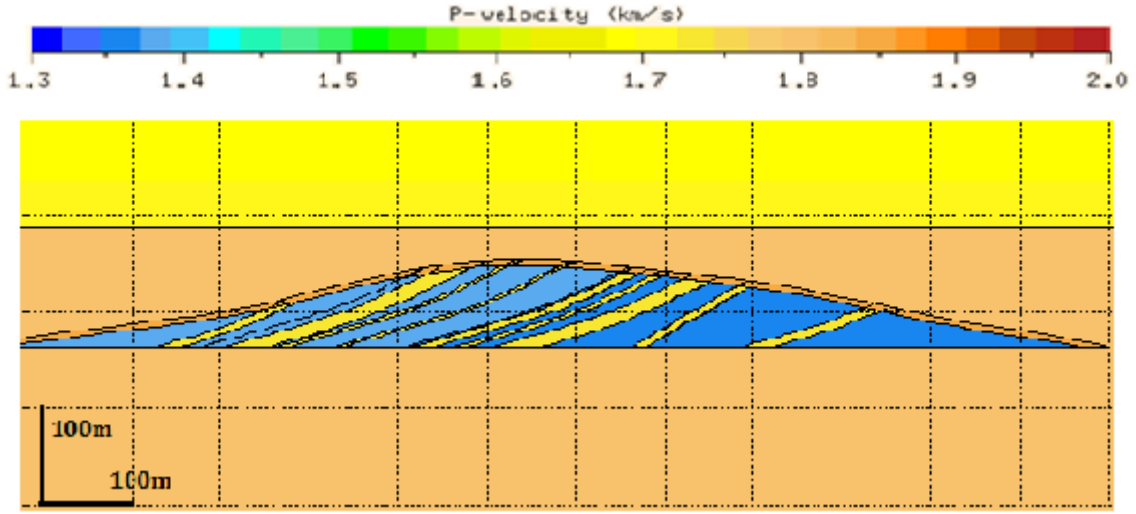

Figure 3.22 *shows anticlinal BSR cross cutting thicker strata with free gas and thin layers of less porous sediment covered by gas hydrate.*

Reservoir Model 12

Properties used in the target

Target layer	P velocity m/s	S velocity m/s	Density ton/m^3
Free gas bearing sediment	1350	600	1.72
Hydrates bearing sediment	1850	400	1.75
Sediment free of gases	1750	500	1.74

Table 3.16 *shows the properties P- velocity S- velocity and density used in model 12.*

Reservoir Model 12 (Anticlinal BSR)

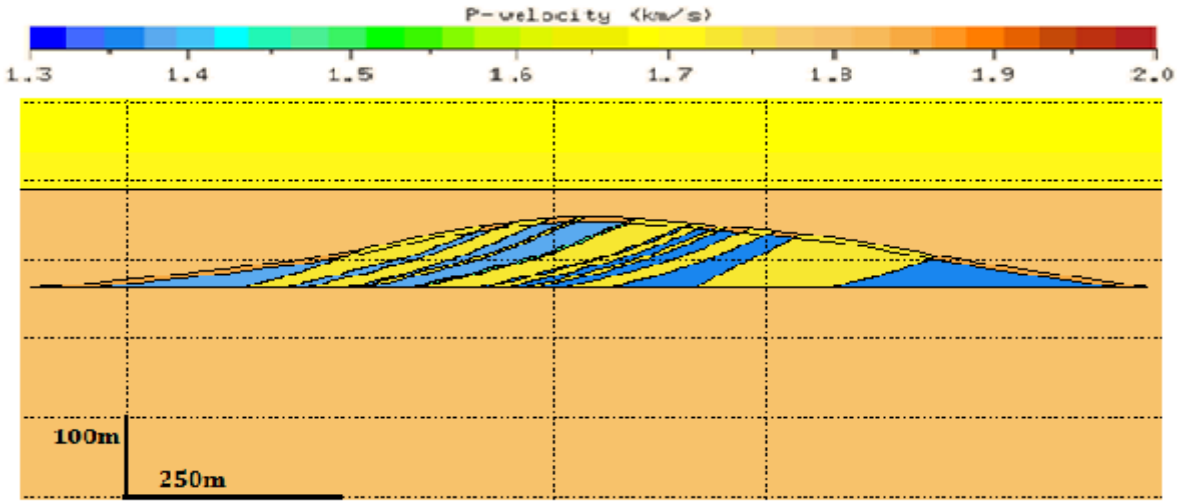

Figure 3.23 *shows Anticlinal BSR shows thick layers of free gas bearing sediment and thick layers of less porous sediment when the hydrate forms only at the top of free gas.*

3.3 Norsar 3D modelling

Model which was exported as SMIF from 2D and imported as SMIF in Norsar 3D. Then It was loaded as SMIF file in Norsar 3D. Then opened under model 2.5D afterward set element points 2D points. The 2D section extended uniformly in y direction, it is shown in Figure 3.24. Finally, the model is stored as a SeisRox file ready to open in SeisRox details as given as an appendix.

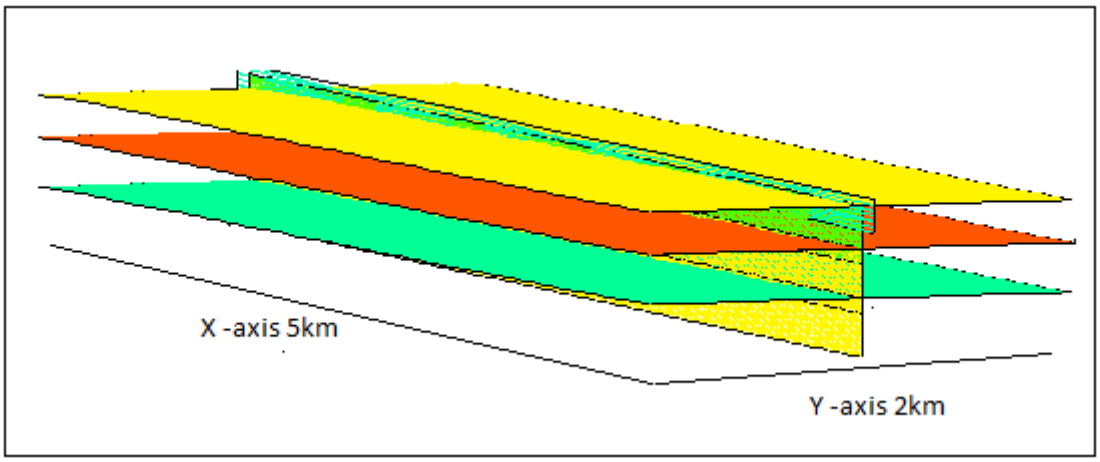

Figure 3.24 *shows 3D view of the background model used; It is illustrating the extension of 2D in y direction uniformly.*

3.4 SeisRoX modelling

The SeisRoX modelling process is a process where we can simulating seismic prestack Depth migration (PSDM) cubes by giving an input: SeisRox model, Background model, Seismic survey geometry, SeisRoX wavelet and, PSDM target. All the elements should be created in the object list in order to run the modelling process. The standard modelling method SimPLI (simulated pre-stack Local Imaging) was used for this study. The workflow in seisrox consists broad set up of the modelling process and the result catalogs.

In SeisRoX, we have options to use full field PSDM stimulator or local target PSDM stimulator. Local target simulator is chosen for this study. Under local target simulator, the 4D Reservoir is selected. 4D reservoir can be well defined as monitoring of a reservoir by using 3D acquisition through time. By Appling the same parameter or possibly the same parameters, it can help to study the change in amplitude of a reservoir as time lapse using 4D stimulator. The 4D reservoir simulator type is helpful to study change in amplitude at different type or condition of reservoir. The 4D reservoir simulator type has used for this study, all the important seisrox set are included under this category.

3.4.1 SeisRoX model

SeisRoX model different models, which has imported from Norsar 3D have used for this research, their details are mentioned in the above sub topic as Norsar models, the different models are converted in 2.5D and stored as seisrox file ready for simulation steps are include in appendix.

3.4.2 Background model

The SeisRoX background was also imported from Norsar 3D. A background geology, which consists of three layers, the sea floor and two-sediment layer (three horizons).

3.4.3 SeisRoX Surveys

A survey is the term used for a data set defining the shot and receiver positions (often-termed shot/receiver geometry) of the seismic experiments to be modelled (simulated). The survey can be two types: marine survey was where the receivers (streamer) are moving towed with shots and Land or (OBS) survey, where the receivers are in fixed positions relative to the shots. Marine survey has used for this study, properly selection the Survey parameter is very important to give accurate result. The survey on this study

has carried out parallel with the purposed target and background it is oriented at 0.0° rotation with x –axis. The center of the survey has done at the same coordinate with the center of the target, the center can be in UTM, Local or inline crosses line related, the local center is used for this study. The depth of the receiver and the shot are at 0.00 (sea level). The Figure 3.25 illustrate the streamer and the shot length in relation to the target and background center. The survey parameters are given in the Table 3.17.

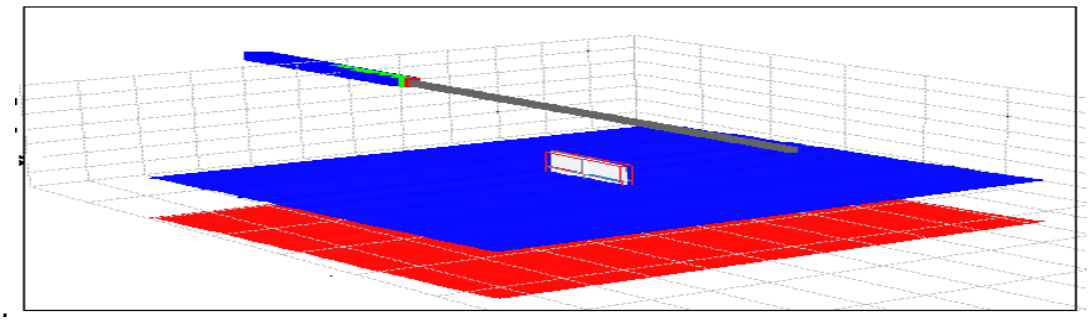

Figure 3.25 *shows Stimulation) PSDM setting SeisRox target background, survey setting (streamer and shot, green and gray lines at the top respectively), and target (red hallow rectangle) blue and red planes are interfaces.*

3.4.4 Survey parameters

For all of the study it is used common parameter in marine survey.

Shot configuration	Streamer/Receiver configuration
Center (x,y) (Local) (2.5,2.5) Depth(km) 0.00 Rotation(related X –axis) 0.00 Number of shot lines 1 Shot line length (km) 5 Shot line spacing(km) 0.025 Shot spacing 0.025	Depth(km) 0.00 Minmum offset(km) 0.1 Number of streamers 2 Streamer length (km) 2.5 Streamer spacing (km) 0.1 Reciver spacing (km) 0.0125

Table 3.17 *shows the parameters used in Survey.*

3.4.5 Wavelet

A wavelet is an object containing a single waveform sampled in time. It is also often termed a pulse, the wavelet are used when calculating seismic frequency. Zero phase has used for this study it is recommended a better resolutions by (Schoenberger, 1974) Figure 3.26 and 3.27 are illustration of wavelets.

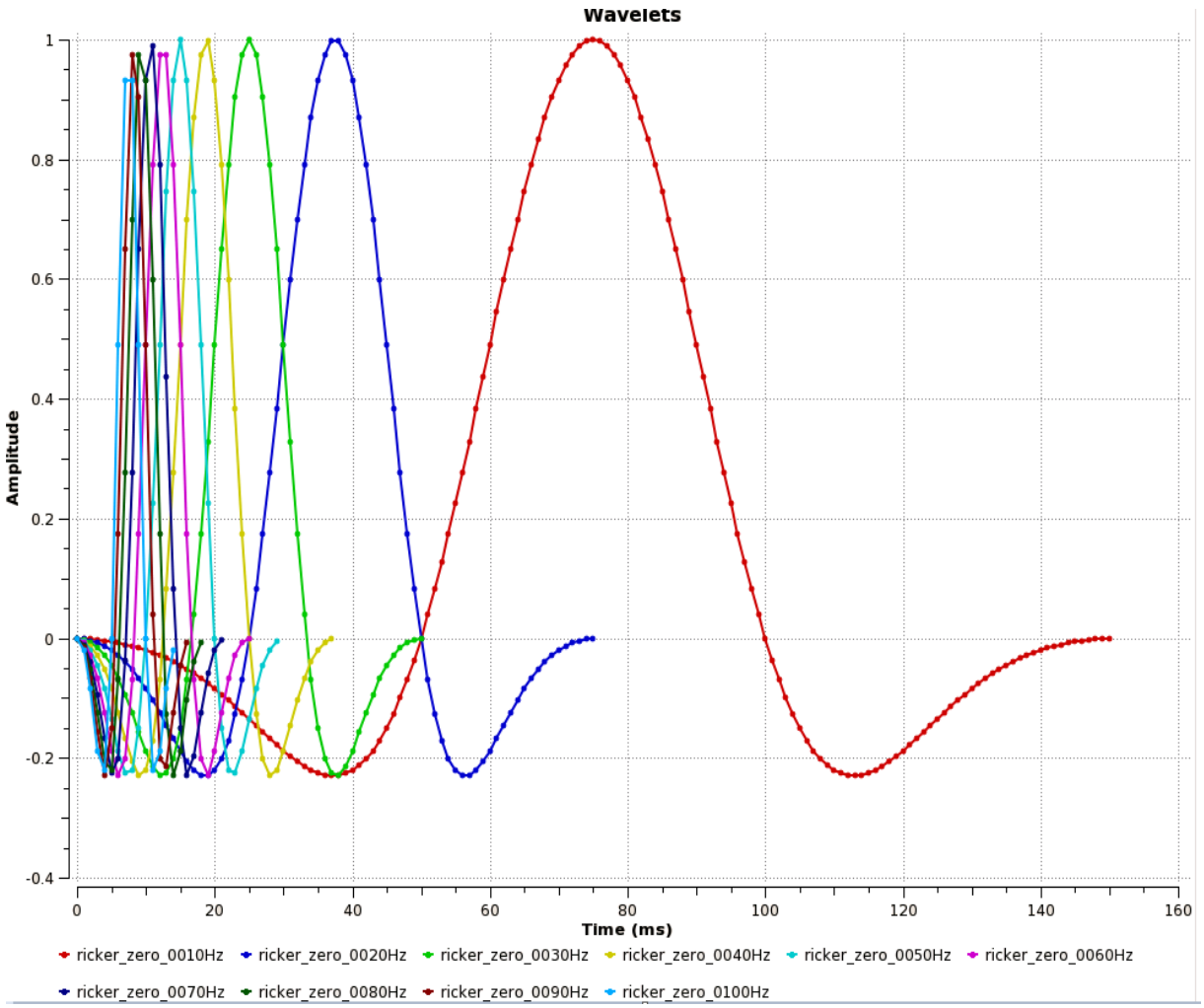

Figure 3.26 *shows amplitude verses time of wavelets riker zero from 10 Hz-100* Hz.

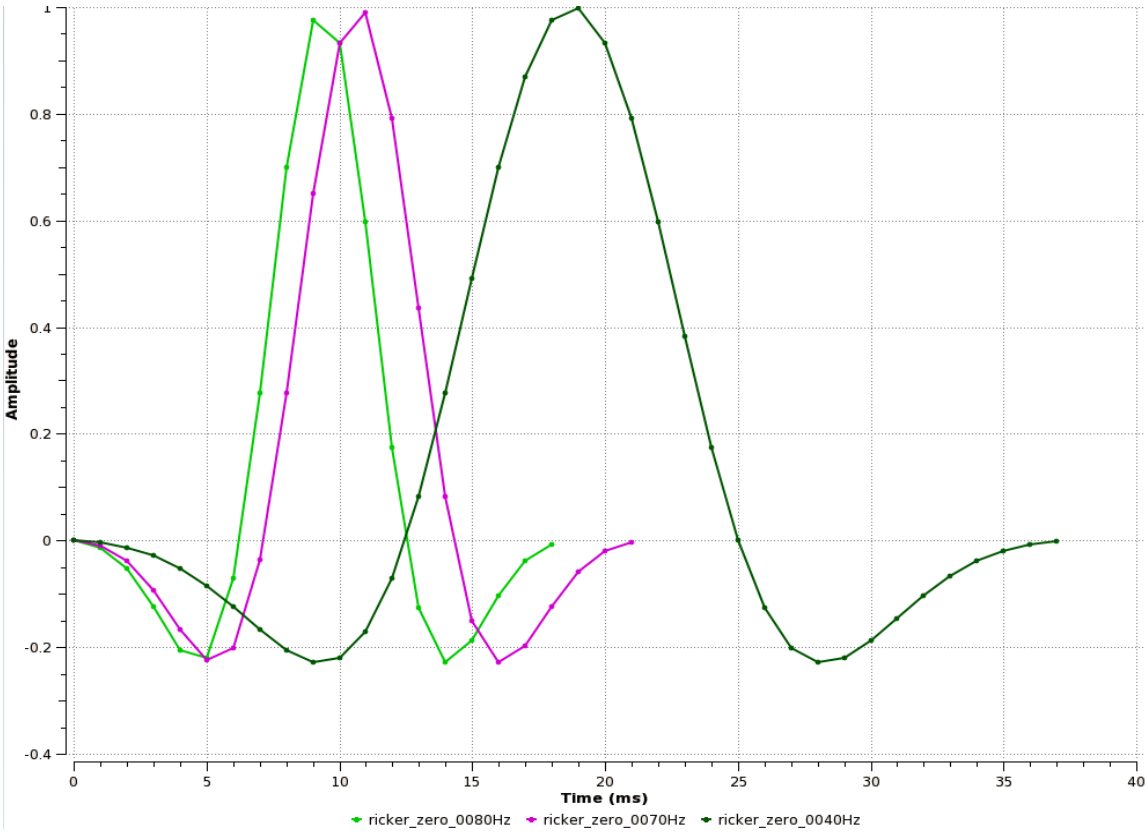

Figure 3.27 *show amplitude verses time of select wavelet 40 Hz, 70 Hz, 100 Hz.*

3.4.6 PSDM Target

The user specified cube can displayed in the 3D view Figure 3.28 is illustration of the PSDM cube.

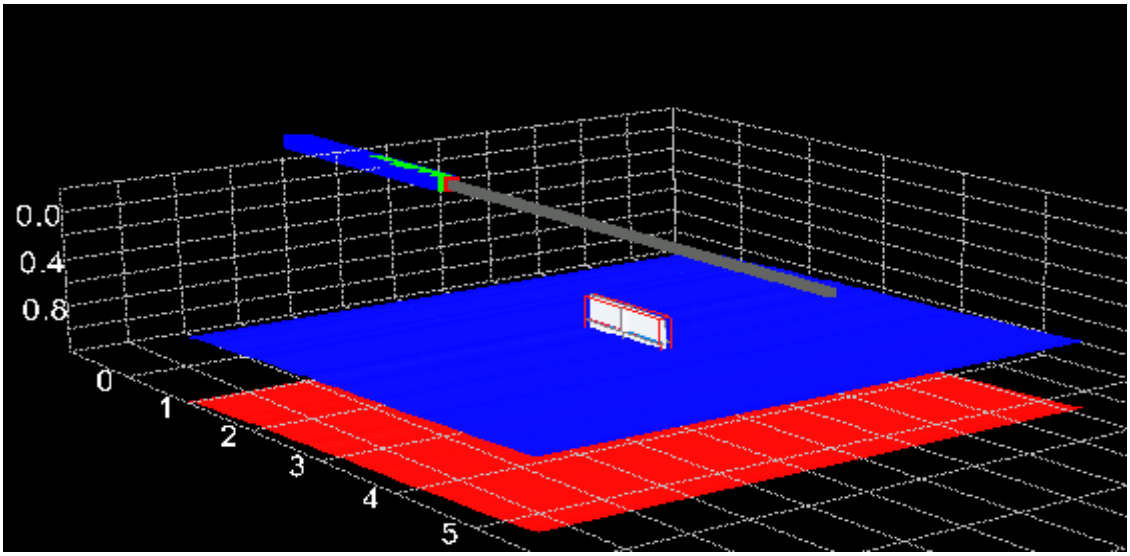

Figure 3.28 shows a survey oriented over target cube, white cube under red hollow red box the seismic cube.

The PSDM target includes different inputs of simulation. The center of the target can be defined under this folder. The grid defined in to 2D or 3D, the 3D grid was used for this study. The size of the target is recommended to be smaller to avoid mistakes since a single filter is used through the whole area. Though sampling (km) size recommended by Norsar SeisRoX are 0.01, x direction, 00.01, y direction and 0.005-z direction, small sampling gives better resolution, better coverage of wavenumber domain and make to escape truncated PSDM to give well gridded reflection. In addition to use the right sampling is vital because it has influence on the reflectivity and the PSDM filter (Nordahl,2015), so that sampling per km for this study has mainly chosen as in (x, y, z) (0.001, 0.01,0.001) and (0.005,0.01,0.005). The main target is parallel to x -axis and there for it was chosen small sampling in the x -axis (inline) rather than in y-axis in which the target extended uniformly.

Reflectivity

We have option of reflectivity selection in SeisRoX under PSLM target. The alternative are Zoeppritz (knott), Aki and Richards, 1980 or AVO-R0G (Shuey, 1985). The Zoeppritz gives closest values to real reflectivity so that the Zoeppritz has chosen on this study.

Incident angle selection. In SeisRoX, there are three option of incident angle selection:

1, Zero, here the incident angle is normal or at 0°,

2, The average angle, the average angle of all incident angle available the illumination vector calculated to produce one reflectivity.

3, Angle range: the incident angle differs between the angle range. The sampling angle delimit the sub range.

SIMPLI PSDM methods true amplitudes,

The default alternative allow using true amplitude. This do that all illumination vectors are well-thought-out equally same weight of 1(when making the SimPLl filter, supposing that all amplitude corrections, geometrical spreading, attenuation, transmission, etc. would have been done on the data (Norsar 2011). True amplitude denotes to faithfully preserve the reflectively strength of the reflectors in a seismic method.

PSDM Filter

This part comprises the aperture and travel time. The aperture is refers as horizontal spaces between the CMP of the (source receiver) couple attached to each illumination vector (survey dependent) and the target Center. It is highly recommended in (Norsar, 2011) to filter on aperture, as also done PSDM the default ideal value are 0 to 2km. The travel time is the sum of the travel time between source and target center and target center and receiver (the so-called scattering travel time) it is greatly suggested to use highest travel time 8s. If this does not taken, the illumination vectors involved to long travel time will be taken in to account, while in actuality, the reliable data would not be verified. Therefore an aperture between 0 and 2 km and travel time between 0 and 8s has used for all the processing done in this study.

A special type of filter is produced in the modeling method. The filter is called SimPLI filter (Illumination filter) it is shown in Figure 3.28 it comprises the total outcome of survey, background model, and seismic wavelet. The SimPLI filter automatically created from the input data. It is in the wavenumber domain and can be displayed in 2D or 3D viewer.

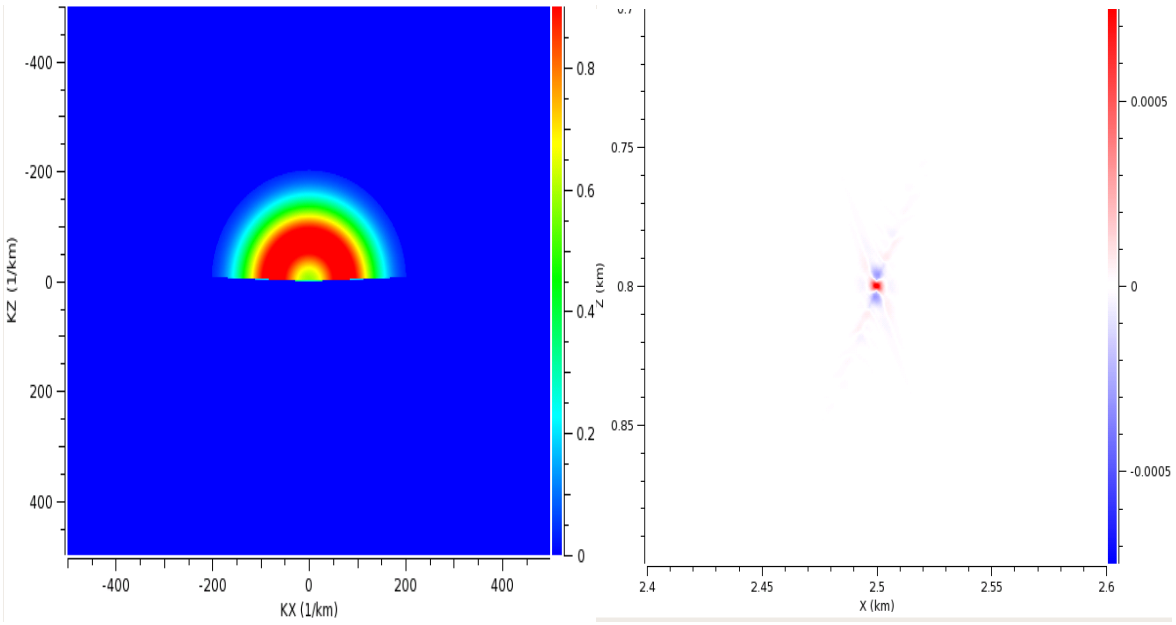

Figure 3.28 *shows SimPLl filter and PSF at 80 Hz frequency and 20°-incident angle.*

Optional result

On this part of the target there can be chosen different result to mention few of them PSF, reflectivity, VP, Vs and RHO. PSF and reflectivity has used on this study for purpose of estimation the resolution by producing psf images and Reflectivity coefficient producing from reflectivity images.

PSF

A Point spread function (PSF) can also calculated under optional results. The PSF is a seismic cube containing the seismic response of a model consisting of a single point scatter. It is the inverse 3D Fourier transform of the SimPLI filter.

Property gridding options

On this part one can choice among horizon interplotation and extraplotation to the boundries. Interplotation is calculate approximately a value when the near by value is known. Exptraplotation implies streching one value further in one direction. Intrplotation gridding has used for this study.

PSDM Target	
Center X,Y (km)	(2.5,2.5)
Depth Z (km)	defined depending on target
Grid type	3D y, size 0.100km
Size (km)	defined depending on target
Sampling (km)	defined depending on target
Reflectivity	Zoeppritz
Incident angle	defined depending on target
Simulated PSDM Method	
Method	True amplitude
PSDM Filters	
Aperture range (km)	0-2
Travel time range (s)	0-8

Table 3.19 *shows Simulation PSDM parameters used on this study.*

Result (4)

This chapter consists of input and results from different combination of synthetic seismic generating parameters (Local Target PSDM simulation). These are background model,survey, wavelet, seisrox target model and target parameter. Some of the important target parameters on this study which can affect results are:

- Depth of target
- Sampling per km
- Frequency with proper resolution for a give target thickness and different geological setting.
- Change in incident angle

Different thickness of free gas bearing sediments and gas hydrates bearing sediments in contact are analyzed on this study. The thickness of the targets used for this study are 1m (thin layer), 5m, 10m, 15m and 30m and anticline shaped targets.

The targets with 5m thickness (model 1, model 2 and model 3) and 10m (model 4) are homogenous layers of free gas bearing sediments and gas hydrate bearing sediments at different angle of contact between gas hydrate bearing sediments and free gas bearing sediments.

The targets with 15m (model 5 and model 6) consists of two type of input data; the first is homogenous gas bearing sediments and hydrates bearing sediments with 15m thickness and the second is intercalation of 5m gas bearing sediments and 5m sediments without gas (less porous sediment) and the other side intercalation of hydrate bearing sediments and less porous sediments.

The targets with 30m thick layer used in model 7, model 8 and model 9A, model 9B and 9C illustrates different results that are obtained due to variation to the frequency of the signal.

An anticlinal shaped model with BSR cross cutting slightly dipping sediments with intercalation of free gas and less porous sediments was developed in order to study the effects on the synthetic seismic data.

Mainly used Sampling per km are (x=0.001, y= 0.01, Z= 0.001),) (0.002, 0.01,0.001) (X= 0.005, Y= 0.01, Z=0.0025) and (0.01, 0.01, 0.005) for x= 0.001 stands for Common midpoint imaged every 1m and 0.005 displayed common midpoint imaged every 5m. The result are described as follow:

4. 1 Change in contact angle, from horizontal up to steeply dip contact of hydrate hydrates bearing and gas hydrates bearing sediments with up to 5m thick layer, thin to thick layer models used are (Model 1, model 2 and model 3).

4. 2 Changes in sampling per km with 5m and 10m thick layers used are (Model 3 and model 4).

4. 3 Changes in frequency for 30m thick layers. (Model 7 and model 9)**.**

4. 4 Changes in occurrences of hydrates bearing continuity and discontinuity of reservoir for 15m thick layer (Model 5 and model 6). For 30m layer model 7, model 9A, model 9B and model 9C and anticlinal BSR (model 11 and model 12).

4. 5 Changes in Incident angle (Model 3).

4.1 Change in contact angle Model 1, model 2 and model 3

Three Different models was generated as the different possible occurrences of gas hydrate bearing sediments and free gas bearing sediments. The wide horizontal and near horizontal contacts of hydrate bearing sediments and free gas bearing sediments gives strong proper reflection as in model 1 and model 2. The steeply dipping contacts of hydrate bearing sediments and gas bearing sediments contacts give proper reflectivity with small sampling in km of (x, z) (0.005,0.0025) as in Model 3. The illustration are in Figures 4.1-4.3.

5m thick gas bearing sediments horizontal and near horizontal contact with gas hydrate bearing sediments at **80Hz** frequency.

Depth	0.8
Size (km)	(x, y, z) 1, 0.1, 0.4(used on the processing)
Sampling (km)	0.005, 0.01,0. 0025

Model 1 and Model 2

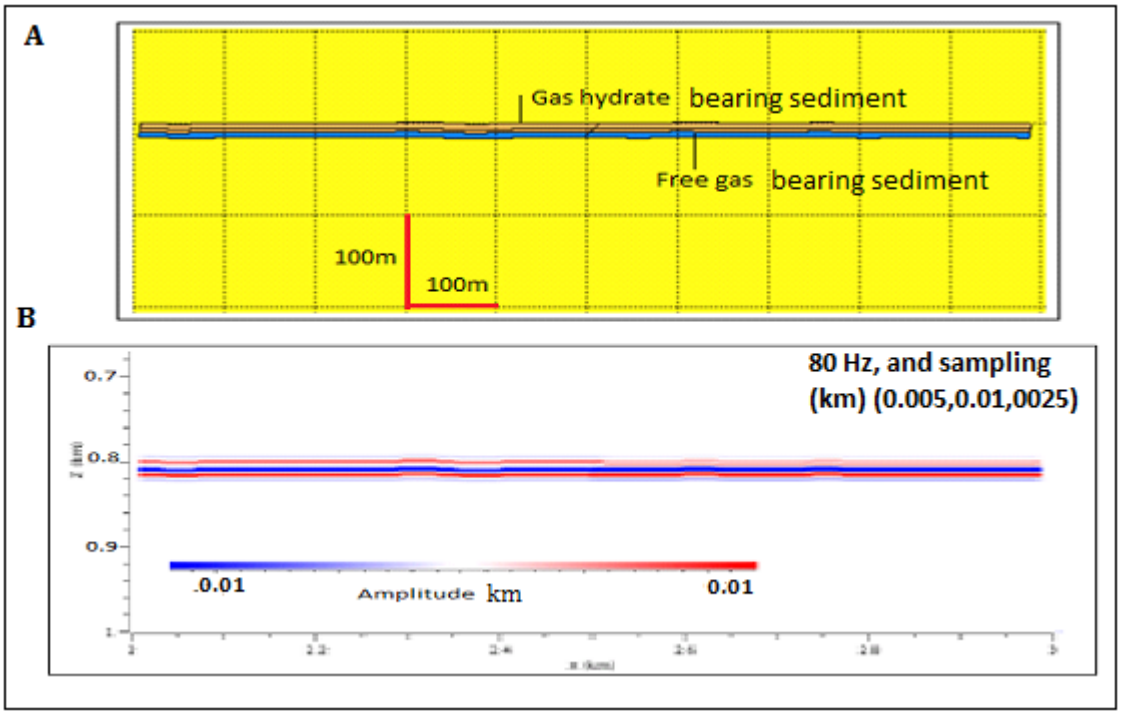

Figure 4.1 *shows two cross sections* **A,** *geological model 1(free gas-bearing sediments and below gas hydrate bearing sediments) and* **B,** *its synthetic seismic PSDM result a proper reflection at the top of free gas bearing sediments and below gas hydrate bearing sediments.*

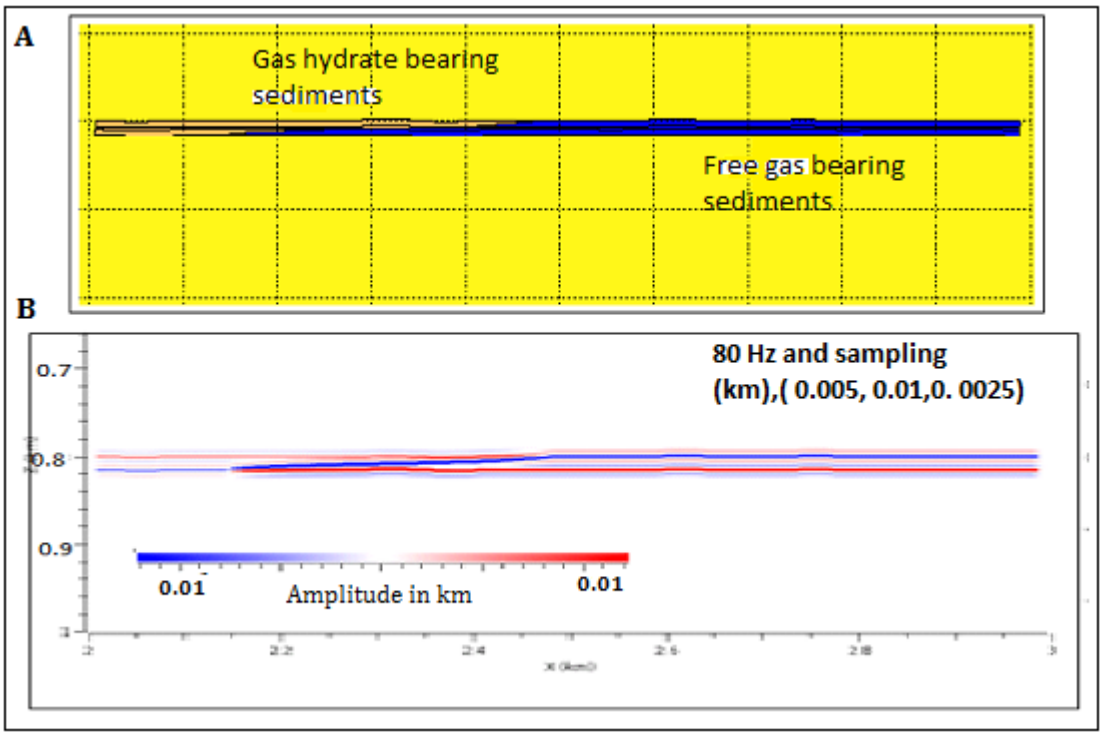

Figure 4.2 *shows two cross sections **A,** geological model 2 (free gas bearing sediments and gas hydrate bearing sediment at near horizontal contact and **B**, its synthetic seismic PSDM result enhanced reflection at the contact (proper BSR).*

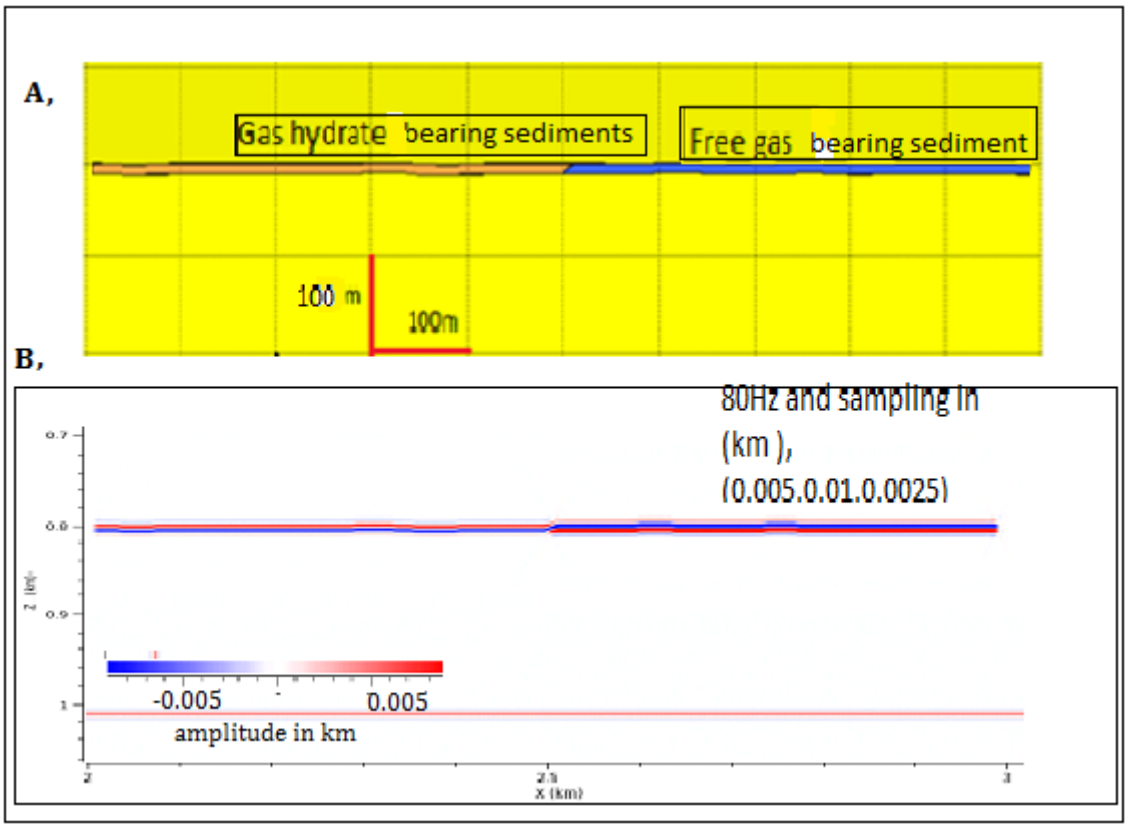

Figure 4.3 *shows two cross sections* **A,** *geological model 1(free gas-bearing sediment and below gas hydrate bearing sediment) and* **B,** *its synthetic seismic PSDM result seismic reflection at 0° angle 80Hz frequency and strong reflection for dipping contact of free gas bearing sediments and gas hydrates bearing sediments.*

4.2 Change in sampling in (km) at 0° and 100 Hz

Changing the Sampling per km also referred to as common mid-point distance and/or the thickness of gas hydrate bearing sediments and gas-bearing sediments has a profound effect on the appearance of a proper BSR on the synthetic seismic data. For the 5m thick sediments only the 1m (Figure 4.4) and 5m (Figure 4.5) common mid-point distances produced proper reflection, while the 10m common mid-point distance led to the termination of enhanced reflections (Figure 4.6). However, when the thickness of the sediments were increased from 5m to 10m, a proper BSR reflection was resulted with 10m common mid-point distance (Figure 4.7).

5m thick gas bearing sediment non-horizontal contact with gas hydrate bearing sediment studied with **100Hz** wavelet.

Depth	1.0	
Size (km)		(x, y, z) 1, 0.1, 0.2
Sampling	**0.001**, 0.01, **001**	

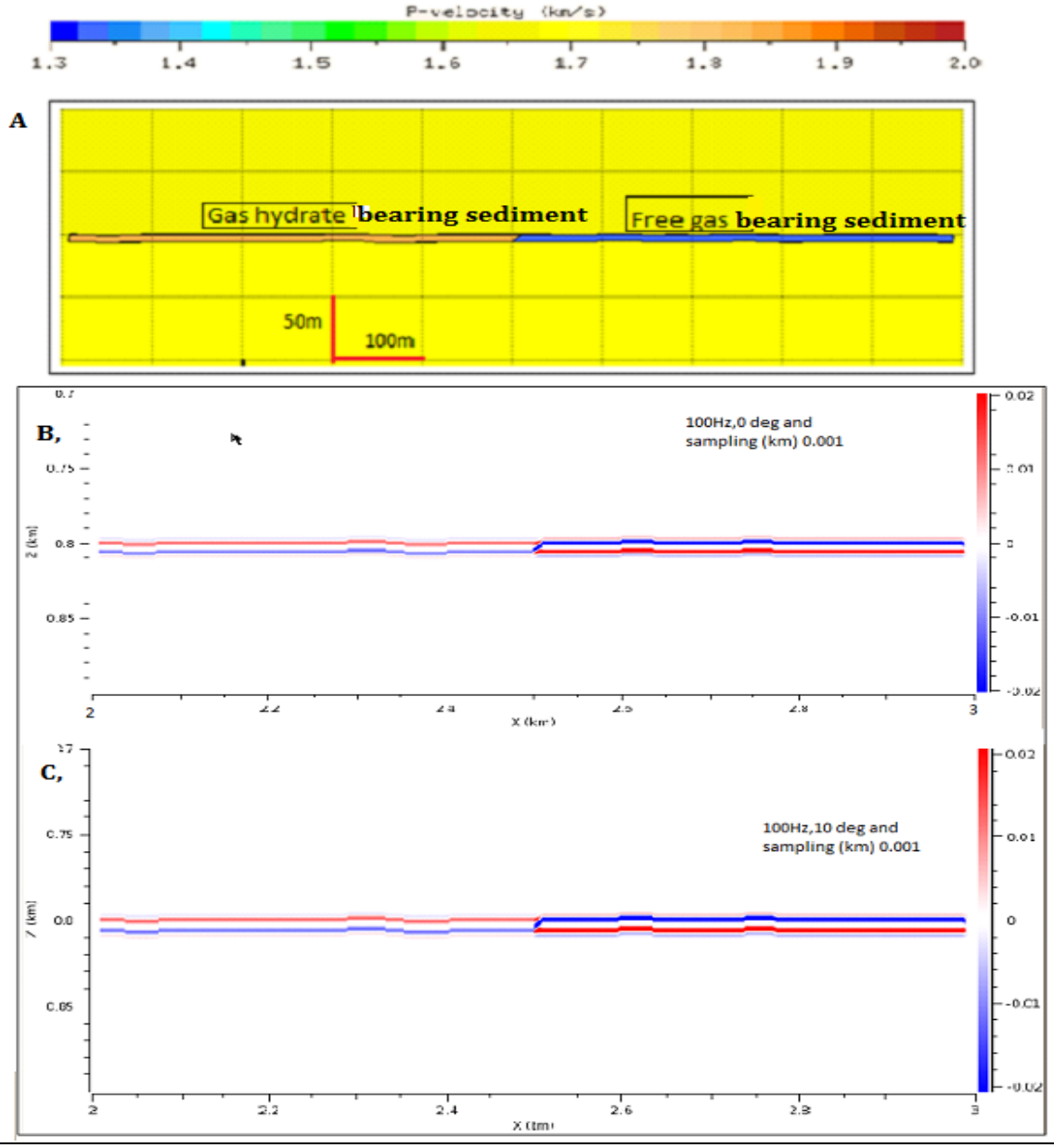

Figure 4.4 *shows three cross sections* **A,** *the geological model 3, gas hydrate bearing and gas bearing sediments at dipping contact.* **B,** *the synthetic seismic result at 0 deg 100 Hz sampling in km (x, z) (0.001, 001) the contact gives proper reflection.* **C,** *The synthetic seismic result at 10 deg gives proper reflection at the contact.*

5m thick gas bearing sediment non-horizontal contact with gas hydrate bearing sediment studied with **100Hz** wavelet.

Depth	1
Size (km)	(x, y, z) 1, 0.1, 0.2
Sampling (km)	**0.005,** 0.01, 0025

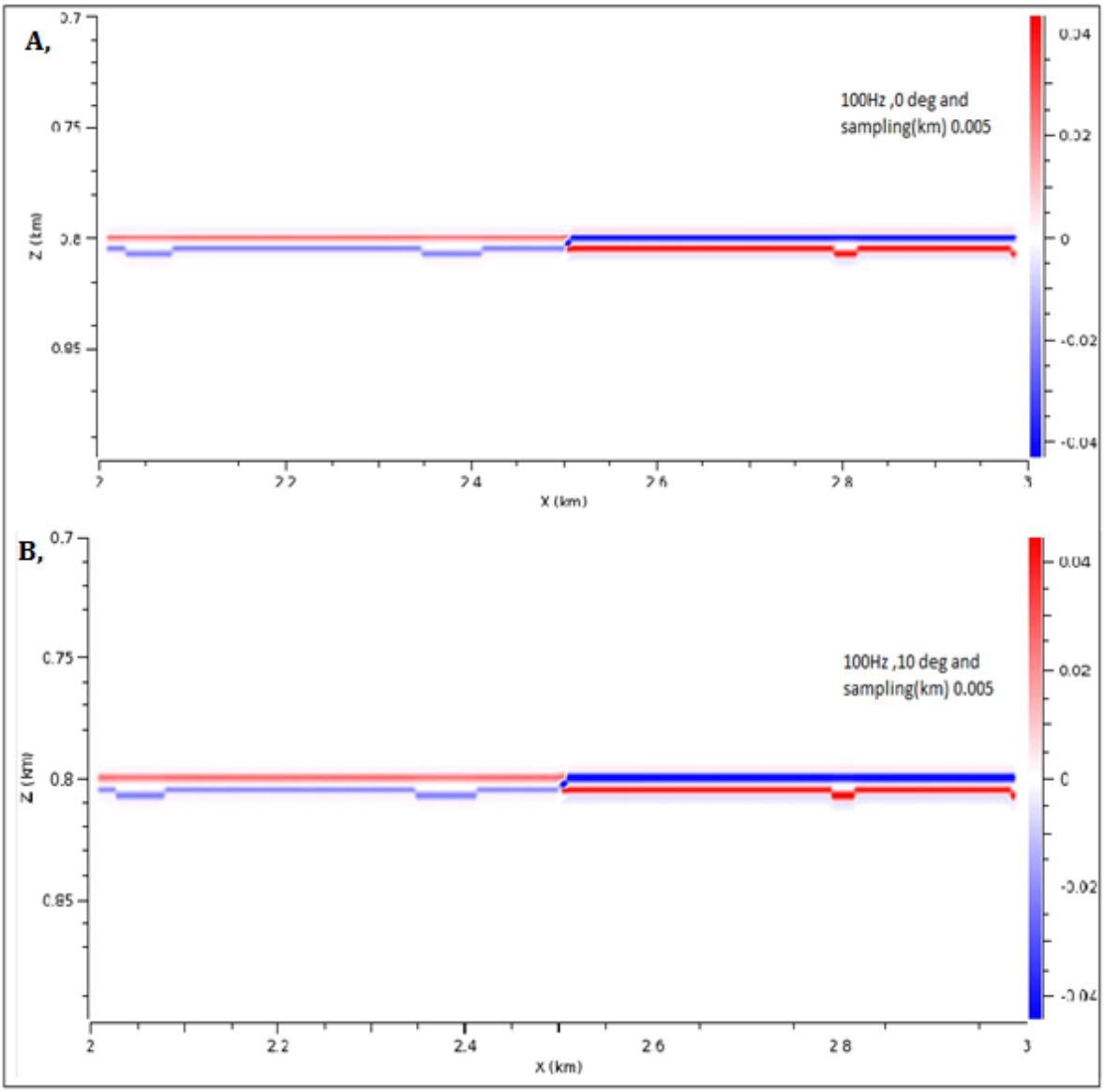

Figure 4.5 *shows two cross sections **A**, the synthetic seismic result at 0 deg. 100 Hz sampling in km (x, z) ,(0.005, 0025) gas hydrate bearing and gas bearing sediments at dipping contact gives proper reflection. **B**, The synthetic seismic result at 10 deg. gives proper reflection at the contact.*

5m thick gas bearing sediment non-horizontal contact with gas hydrate bearing sediment studied with **100Hz** wavelet.

Depth	1
Size (km)	(x, y, z) 2, 0.1, 0.2
Sampling	**0.01,** 0.01, 0025

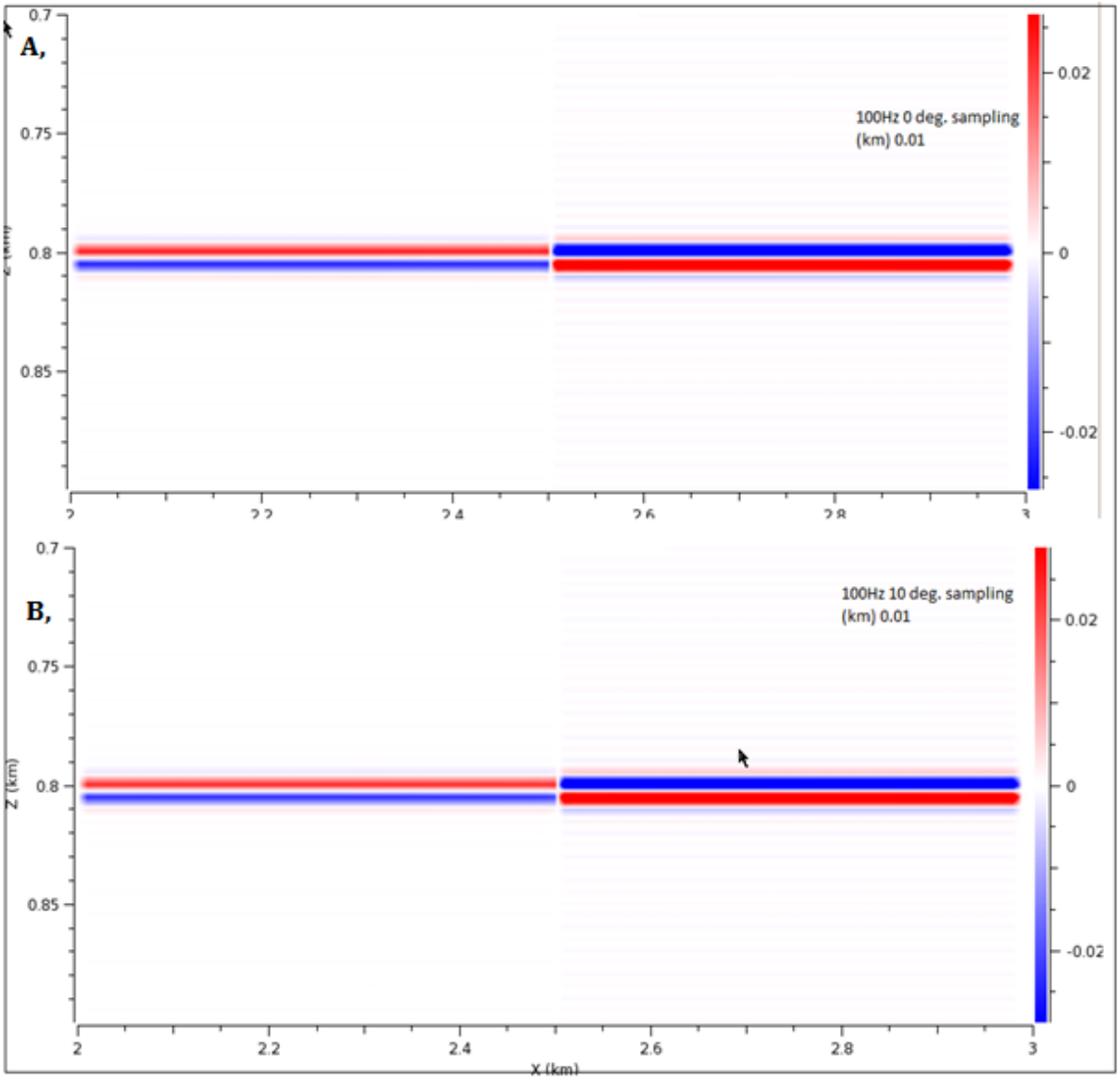

Figure 4.6 *shows two cross sections **A**, gas hydrate bearing and gas bearing sediments at dipping contact the synthetic seismic result at 0 deg. 100 Hz sampling in km (x, z) (0.01, 0025) the contact gives termination of enhanced reflection. **B,** The synthetic seismic result at 10 deg. gives termination of enhanced reflection.*

10m thick gas bearing sediment non-horizontal contact with gas hydrate bearing sediment studied with **100Hz** wavelet.

Depth	1
Size (km)	(x, y, z) 2, 0.1, 0.2
Sampling	**0.01,** 0.01, 0025

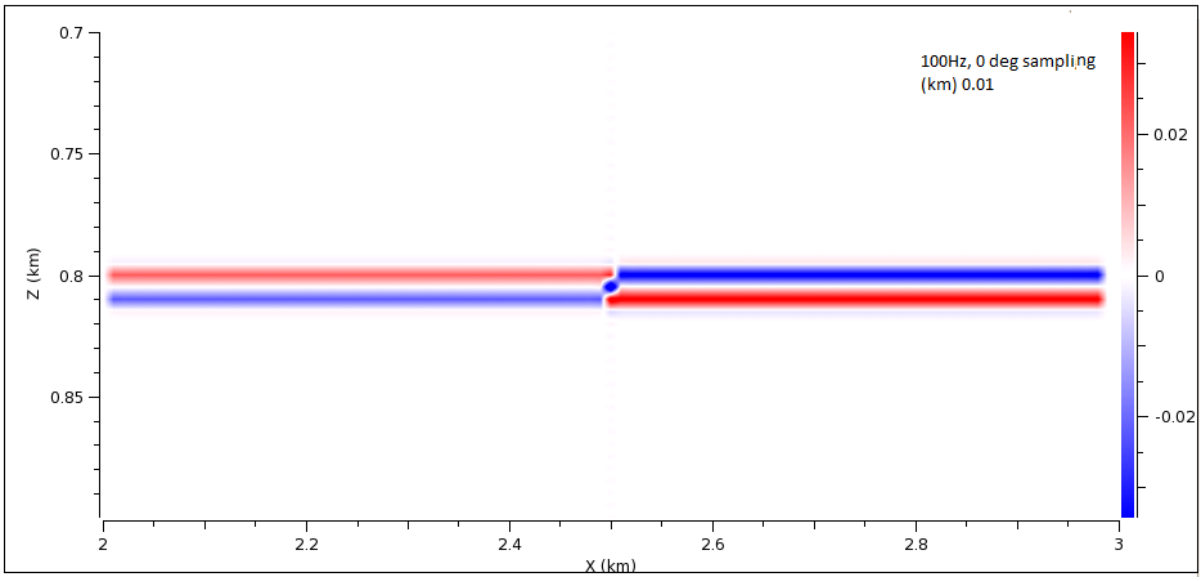

Figure 4.7 shows the synthetic seismic result of model 4 (10m layer thickness) at 0 deg, 100 Hz sampling in km (x, z) (0.01, 0025) gas hydrate bearing and gas bearing sediments at dipping contact gives proper reflection.

4.3 Changing in Frequency

This subtopic includes seismic image result by changing frequencies **10Hz**, **20Hz**, **30Hz**,**40Hz**, **50Hz**,**60Hz**, **70Hz**, **80Hz**,**90Hz**, **100Hz**, **150Hz** and **250Hz.** It is illustrated from Figure 4.8-4.14. It PSF images are included and illustrated in Figure 4.15. Estimated vertical and horizontal resolutions from PSF images Figure are given in table 4.1 and calculated tuning thickness are laid out on tables Table 4.2, Table 4.3 and Table 4.4.

Frequency change from lower to higher (**10Hz** to **100Hz**) and maximum frequency **250Hz** are described in this study. At higher frequency **250Hz** and **150Hz**, clear proper reflection between the thin layers of gas hydrate bearing sediment and free gas bearing sediments is shown. The enhanced reflection distinctly terminate at the end of the contact of layer with gas bearing sediments and gas free sediments. The reflection between gas bearing sediments and free sediments show strong reflection, but the gas hydrate bearing and the gas free sediments show lesser reflection than the first one.

Amplitude decrease from the higher frequency to the lower frequency. Amplitude at **250Hz** is about **20m**, while is decreased to 10 m at **100Hz** and a further decrease to 0.5m is observed at **10Hz**.

At lower frequencies, starting from **40Hz** to **10Hz** reflection at the bottom of the free sediments was strongly reduced and the reflection from top of gas bearing sediments started show strong interferences with the upper reflection. This is illustrated in Figure 4. 10 and Figure 4.11.

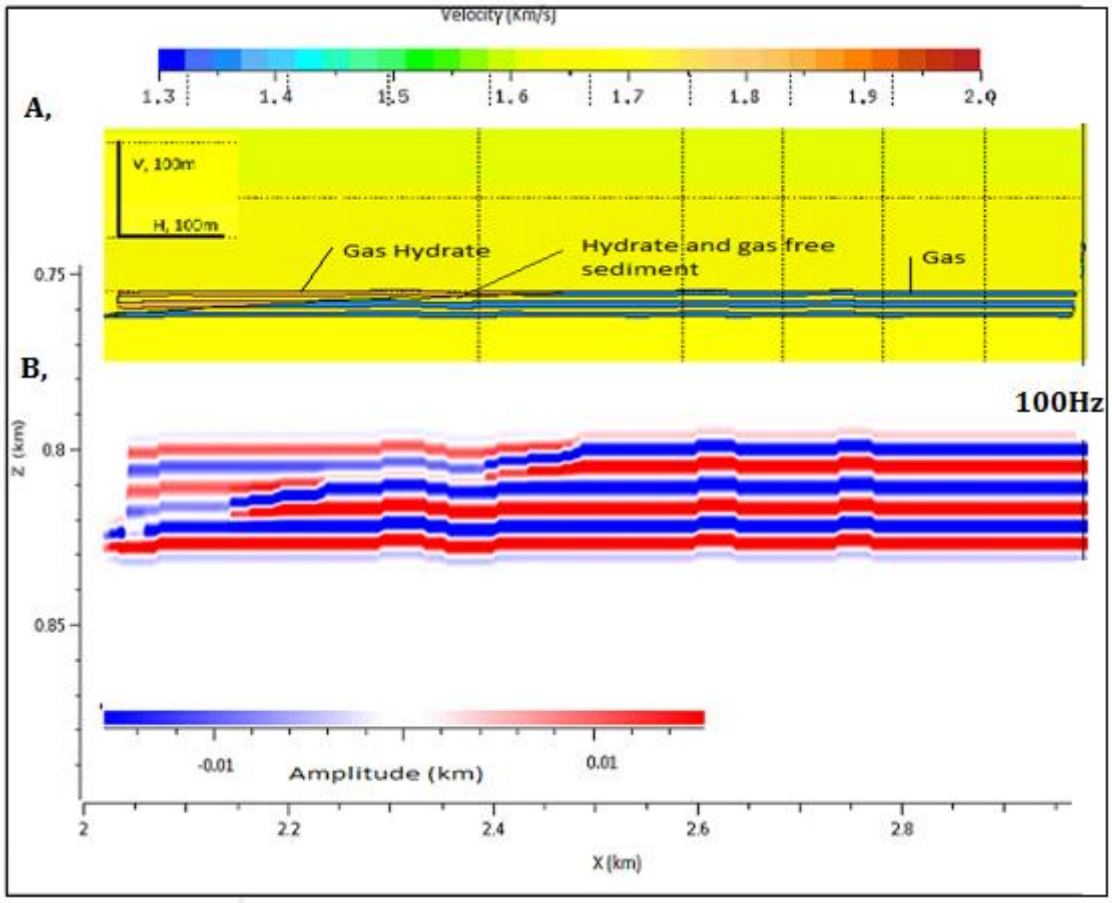

Figure 4.8 *shows two cross sections* **A,** *the geological model 9A (intercalated sediment with gas and without gas) and the background colored according p- velocity.* **B,** *The synthetic seismic result amplitude in km at* ***100Hz*** *frequency and* ***10°*** *incident angle at sampling (km)* ***(0.001, 0.001****). The seismic reflection show clearly strong reflection, the response from each layers, the enhanced reflection terminated at the end of the gas layer or at the triple junction point between gas hydrate free gas bearing sediments and less porous sediments (sediment without gas).*

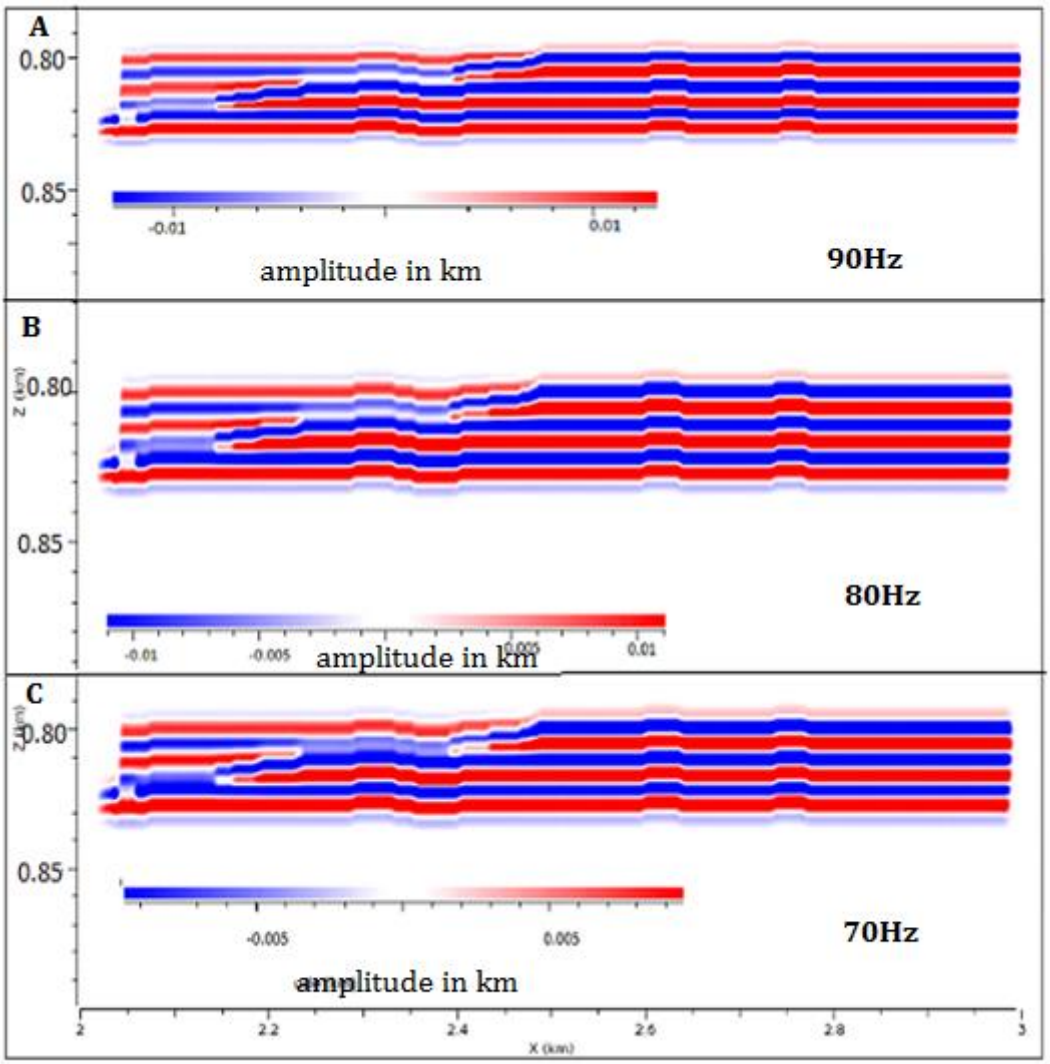

Figure 4.9 *shows three cross sections synthetic seismic result at a frequency* ***90Hz, 80Hz****, and* ***70Hz*** *respectively from top to bottom. A, At* ***90Hz*** *clear enhanced reflection termination at the end of gas layer. B, At* ***80Hz*** *dim reflection shows at top of the thinner part of the less porous layer and at* ***70Hz*** *dim reflection from the contact of hydrate bearing and the less porous gas free sediments started to interfere with top of the second gas bearing sediments layer.*

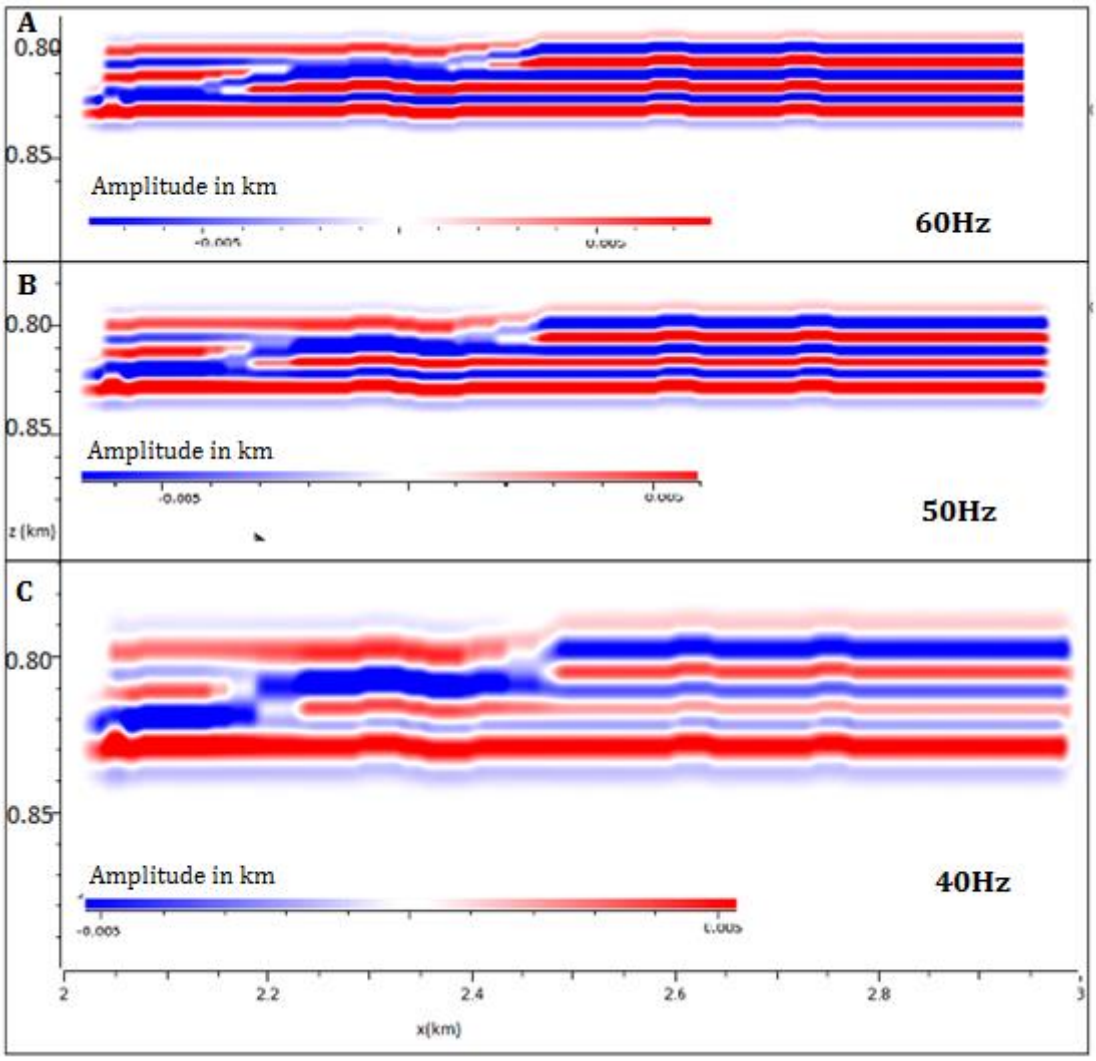

Figure 4.10 *shows synthetic seismic result at a frequency* ***60Hz****,* ***50Hz****, and* ***40Hz*** *respectively from top to bottom.* **A,** *At* ***60Hz*** *termination enhanced reflection at top gas layer dim reflection at a contact of hydrate and sediment less porous sediment and interferences at the top of thin layers.* **B,** *At* ***50Hz****, top free gas shows termination of enhanced reflection at hydrate and less porous sediments contact diming increases as well the interferences at the thinner part of the layers increases.* **C,** *At* ***40Hz*** *the top free gas shows termination of anomalously strong reflection termination, hydrate and less porous contact more dimmer the interferences also increases at thinner layers.*

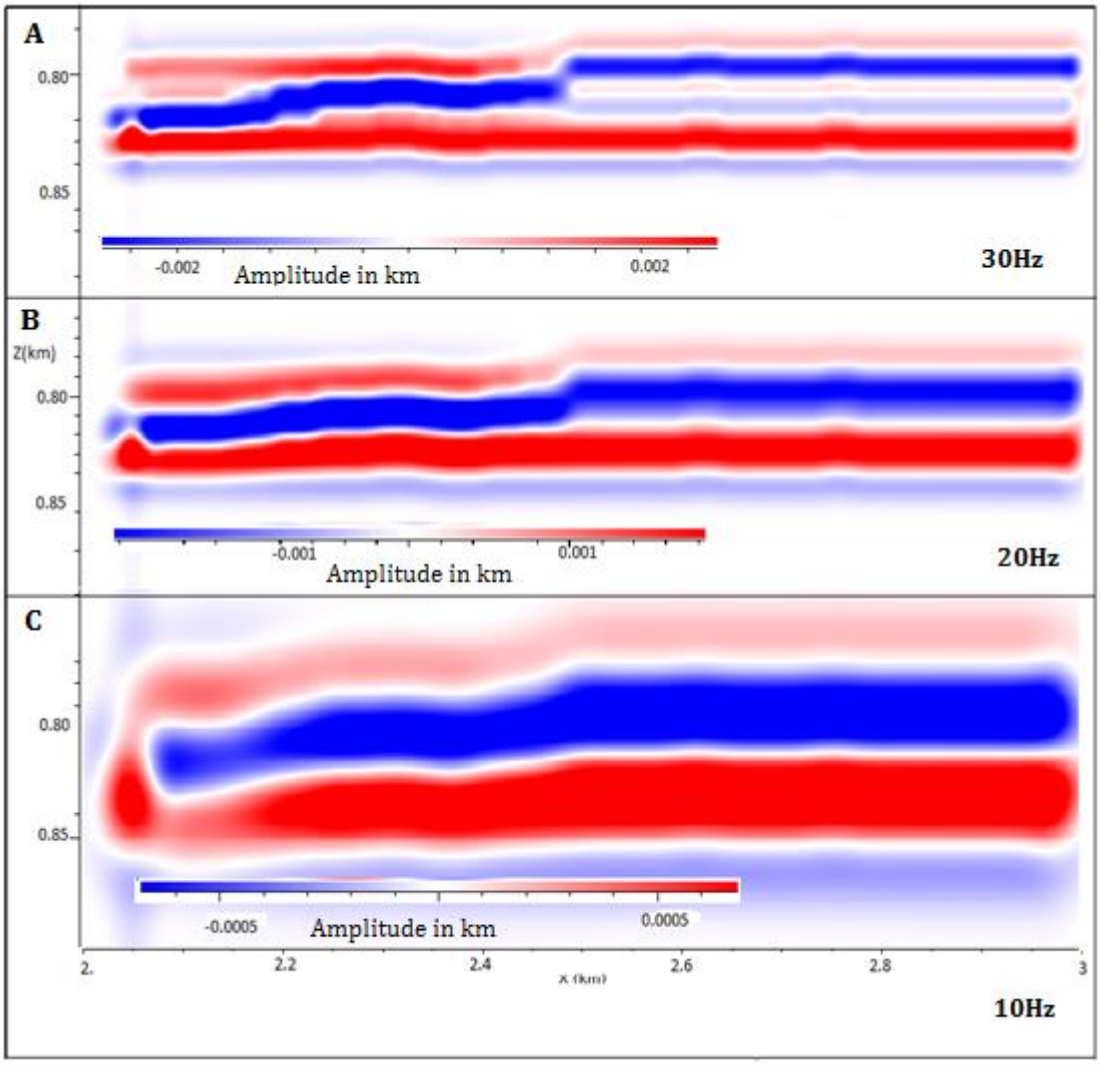

Figure 4.11 *shows synthetic seismic result at a frequency* ***30Hz, 20Hz,*** *and* ***10Hz*** *respectively from top to bottom.* **A**, *At* ***30Hz****, the contact of gas hydrate bearing sediment and the less porous sediment and the free gas bearing sediment not easily identified it show a homogenous contact of enhanced reflection. The layers under the top of gas bearing sediment at the right side shows dim reflection between layers.* **B,** *At* ***20Hz****, the contact is homogenous reflection it does not show the continuity of the less porous layer.* **C,** *At* ***10Hz*** *the layers are showing only two big reflections it look like only one layer top and bottoms.*

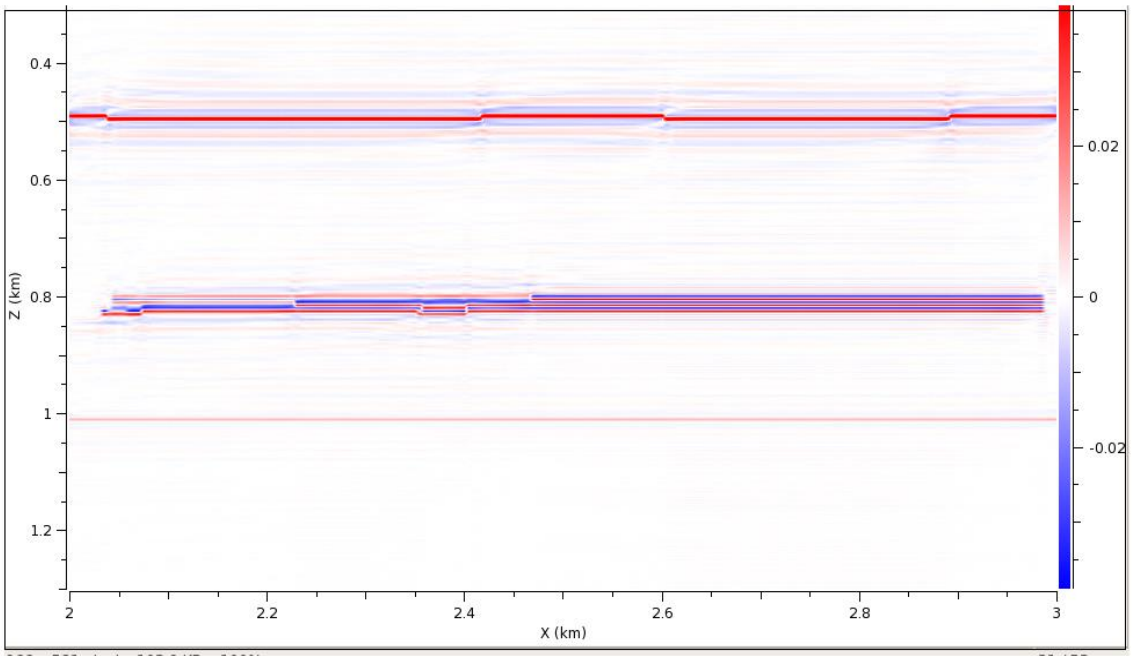

Figure 4.12 *shows seismic result at **250Hz**. The seismic response of model 9 included with background at a depth of 800m below sea level the 30m layer of less porous sediment, free gas and gas hydrate intercalated the contact of the hydrate and gas (BSR) is indicated by the termination of the enhanced reflections which resulted at the contact of hydrate and free gases bearing sediment .*

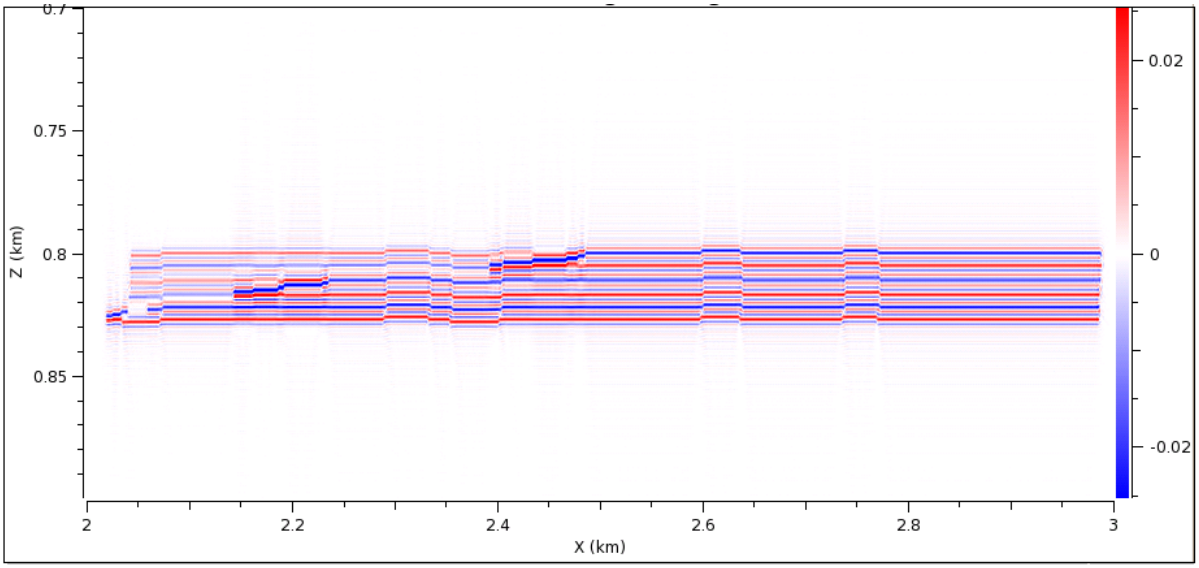

Figure 4.13 *shows synthetic seismic result at a frequency 250Hz processed in small window to give magnified images. The seismic response of each layers of 5m thick 5 layers shows a clear reflection. The contact between gas hydrate and free gas shows precisely limited strong reflection at BSR.*

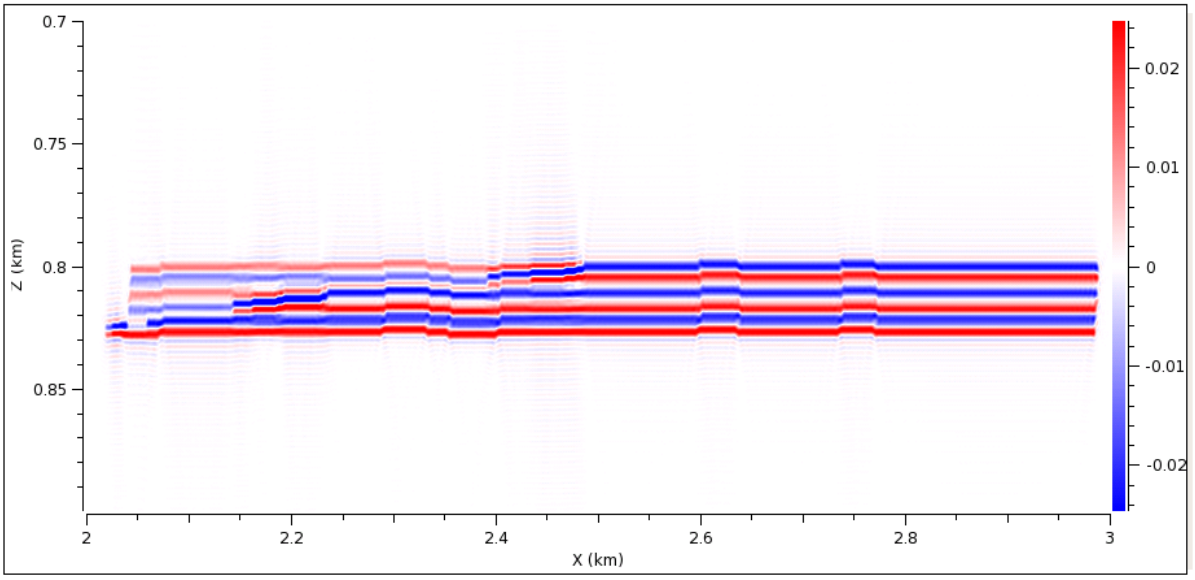

Figure 4.14 *showing seismic result at **150Hz** enhanced reflection terminate at or near the triple junction point of hydrate bearing, gas bearing sediment and less porous sediment.*

PSF as frequency changes

The psf changes from lower frequency to high frequency. The lowest frequency has lower resolution, and the highest frequency has high resolution. The changes to the psf images as frequency changes are shown in Figure 4.15, and the estimated resolutions are presented in Table 4.1.

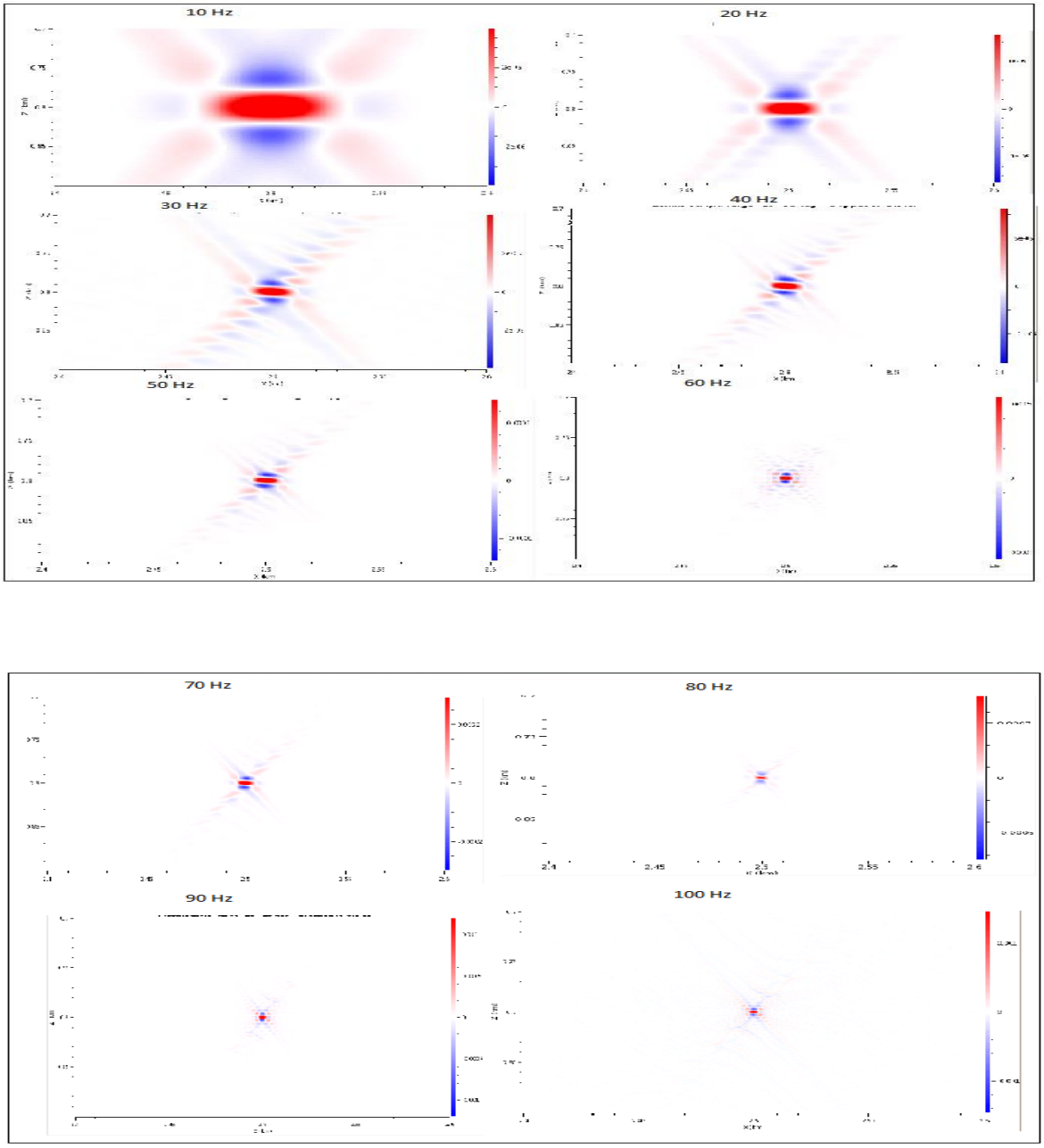

Figure 4.15 *shows the psf as frequency change from 10Hz to 100Hz.*

Frequency	Vertical resolution(m)	Horizontal resolution(m)
10	30	40
20	14	20
30	10	16
40	6	10
50	6	8
60	5	6
70	4	5
80	4	4
90	4	4
100	3	3
250	2.5	2
500	2	1.5
1000	1.5	1

Table 4.1 *Shows SeisRoX resolution estimated from psf image. For lower frequency starting 10 Hz and higher frequency 1000 Hz.*

Vertical resolution free gas layer.

Frequency	Wave length (m)=V/f, V= 1350m/s	Vertical resolution= λ/4 maximum tuning thickness'	Minimum thickness without interference λ/2
10	135	33.75	67.5
20	67.5	16.88	33.76
30	45	11.25	22.5
40	33.75	8.44	16.88
50	27	6.75	13.5
60	22.5	5.625	11.25
70	19.30	4.825	9.65
80	16.88	4.22	8.44
90	15	3.75	7.5
100	13.5	3.38	6.76

Table 4.2 *Resolution calculated free gasses with interval velocity of 1350m/s.*

Frequency	Wave length (m)= v/f=, V=1850m/s	Vertical resolution λ/4 maximum tuning thickness'	Minimum thickness without interference λ/2
10	185	46.25	92.5
20	92.5	23.125	46.25
30	61.66	15.42	30.84
40	46.25	11.56	23.12
50	37	9.25	18.5
60	30.83	7.70	15.4
70	26.43	6.61	13.22
80	23.13	5.78	11.56
90	20.56	5.14	10.28
100	18.5	4.63	9.26

Table 4.3 *Seismic Resolution for hydrate layer with interval velocity 1850m/s.*

Vertical resolution less porous sediment layer.

frequency	Wave length (m)=v/f,V=1750m/s	Vertical resolution λ/4 maximum tuning thickness'	Minimum thickness without interference λ/2
10	175	43.75	87.5
20	87.5	21.88	43.76
30	58.33	14.58	29.16
40	43.75	10.94	21.88
50	35	8.75	17.5
60	29.16	7.29	14.58
70	25	6.25	12.5
80	21.87	5.46	10.92
90	19.44	4.86	9.72
100	17.5	4.38	8.76

Table 4.4 *Resolution calculated with interval velocity of 1750m/s.*

4.4 Changing in the occurences of hydrate and free gas

Different models were generated to study the contact as the differently occurrences of hydrate and gas bearing sediments and synthetic seismic generated. These models processed are model 5, model 6, model 7, model 9, model 11, and model 12.

Two 15m thick layers were generated to examine the effects of different geometrical contacts, thickness and continuity of hydrate/gas free bearing sediments (discontinuous layers of hydrate bearing and gas bearing sediments) have on the synthetically produced seismic data.

Reservoir Model 5

Reservoir Model 5 intercalation of 5 m thick free gas and 5m thick sediment free of gas and lower layer gas with lower concentration. The hydrate side is also intercalation of 5m hydrate and 5m thick sediment free of gas assumed non-porous and impermeable. This is illustrate in geological model Figure 4.16 and synthetic seismic result 4.18.

Reservoir Model 6

Model 6 is made up of15m thick layer gas bearing and hydrate bearing sediments with a dipping contact. The given gas concentration decreases down in contact with 15 m thick homogenous gas hydrate bearing sediment. The homogenous contact gives proper reflection but the intercalated layers give an interrupted BSR. This is illustrated in Figure 4.17 in model and Figure 4.18 seismic result.

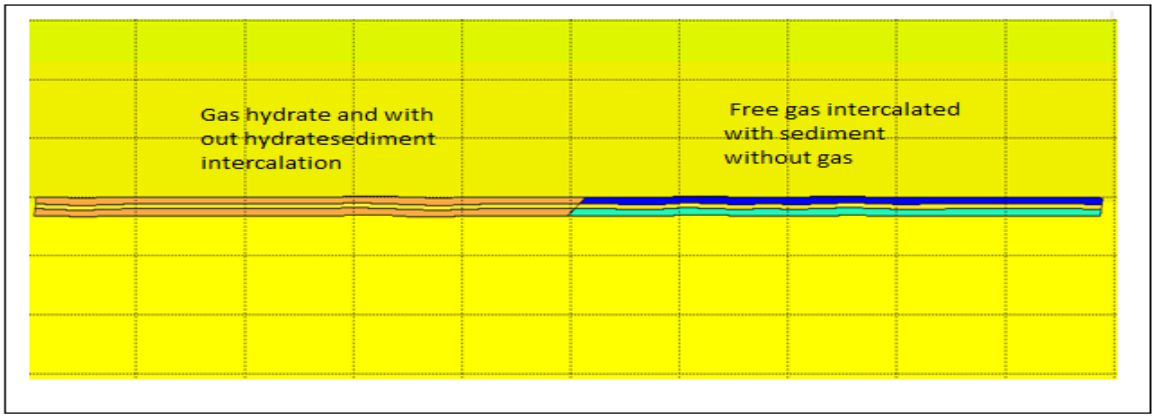

Figure 4.16 *shows a dipping intercalation of gas hydrate bearing and sediments left and free gas bearing sediments and sediment without gas right. Model 5.*

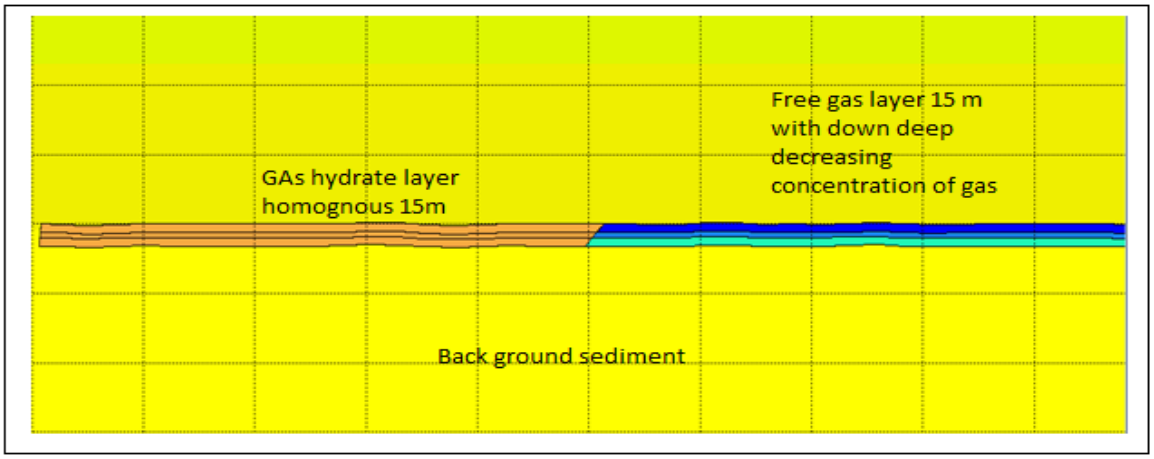

Figure 4.17 *showing dipping contacts at between gas hydrate bearing sediments and different concentration of gas bearing sediments 15m thick homogenous reservoir model 6.*

15m thick gas non-horizontal contact with gas hydrate with **40 Hz** and **normal** angle wavelet.

Depth	0.8
Size (km)	(x, y, z) 1, 0.1, 0.4
Sampling (km)	0.001, 0.01, 001

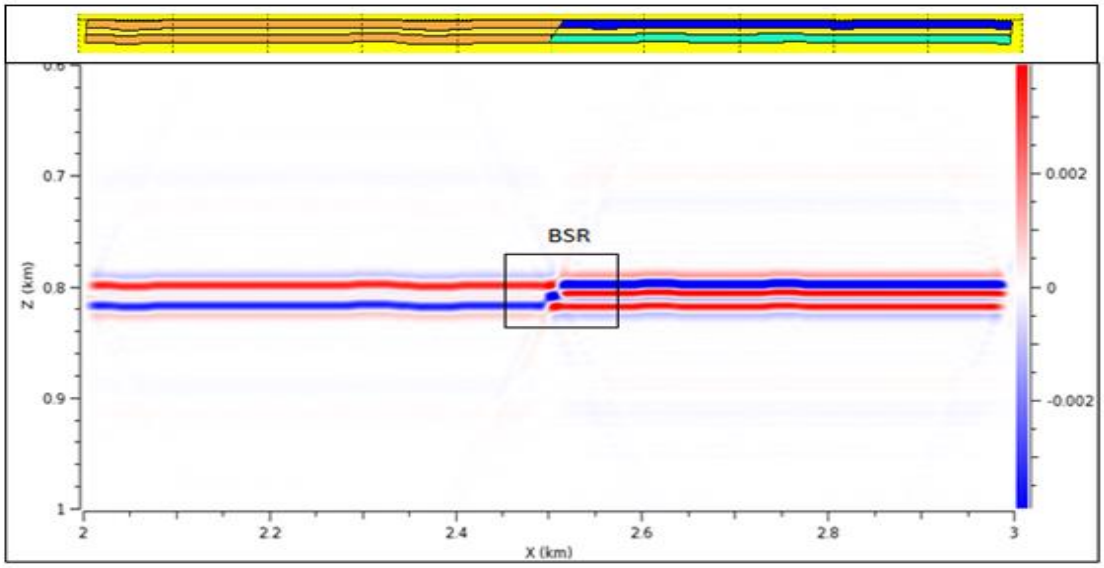

Figure 4.18 *shows the geologic model target Model 5 and the seismic image, intercalated layers of hydrate bearing and gas bearing sediments with less porous sediments. The seismic reflection at BSR is not continuous.* .

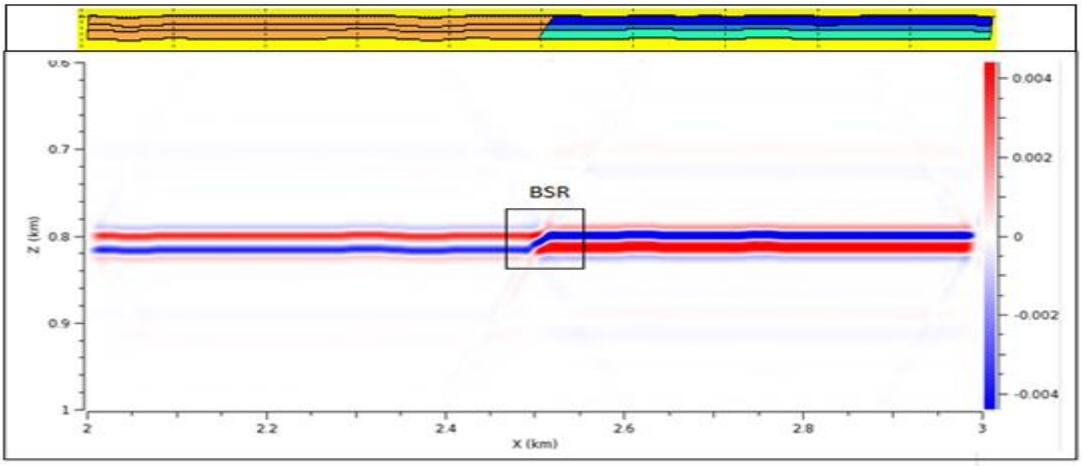

Figure 4.19 *shows the geologic model target model 6 and the seismic image of it, homogenous hydrate bearing contact with gas bearing sediments proper reflection at BSR.*

Reservoir Model 7

The synthetic seismic PSDM of 30m region of homogenous gas hydrate bearing sediment and gas bearing sediment model 7 gives strong enhanced reflection at contact. The model and the seismic images are given in Figure 4.24. Intercalation of five layers about 5m thick, each with near horizontal BSR are presented in model 9A, 9B and model 9C. The result at higher frequency is distinctictlty termination of the enhanced reflection at the point in the BGSZ near the triple junction point of hydrate and gas bearing sediments and sediments without gases. Figure 4.21 gives the illustration of the model 9 and Figure 4.22-4.26 the synthetic seismic result.

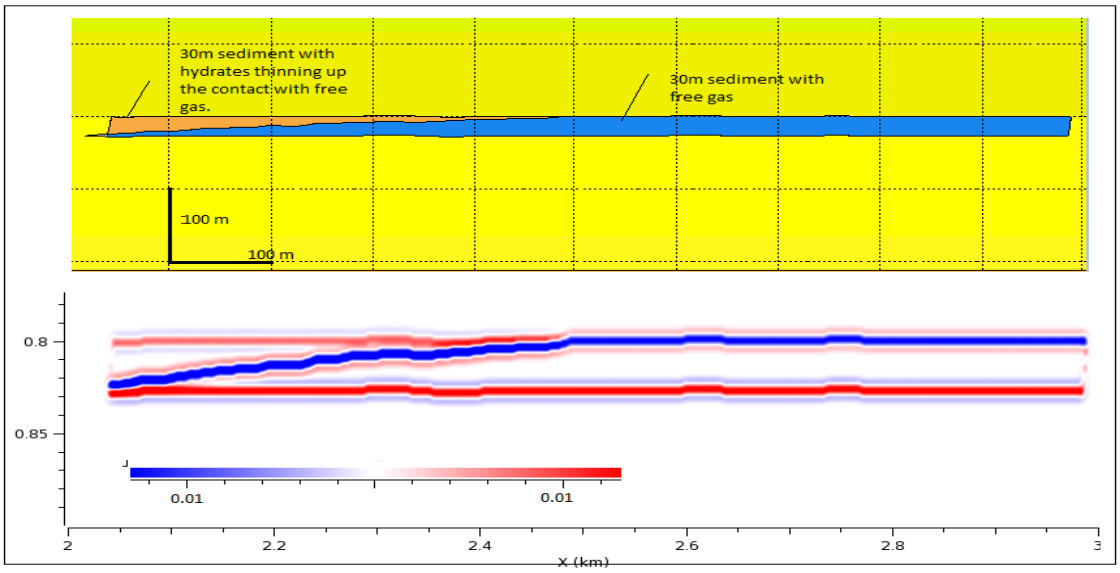

Figure 4.20 *shows the geological model (thick sediment layer 30m Gas hydrate and free gas at contact (BSR crosscutting 30m strata)) and synthetic seismic result at 100 Hz, the contact gives enhanced reflection.*

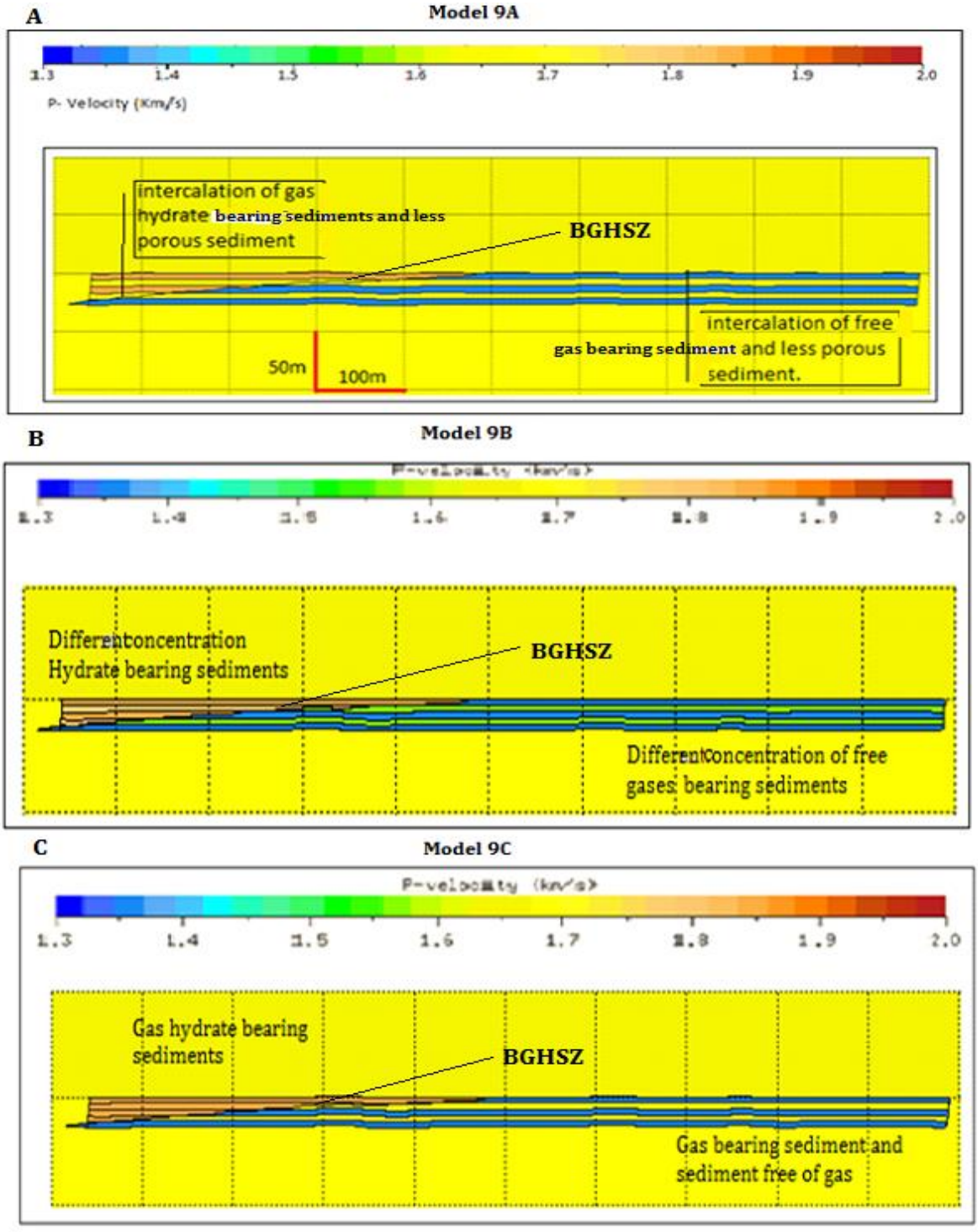

Figure 4.21 *shows three models A, the intercalation of hydrate and gas bearing sediment below and above BGHSZ with sediment free of gas , B, The intercalation of different concentration of hydrate and gases bearing sediments below and above BGHSZ and C, gas hydrates bearing layer above BGHSZ and gas bearing layers of high and very low gas concentration. The concentration is shown by velocity color.*

Reservoir Model 9

Frequency 40 Hz sampling in km (0.001, 001) at normal angle

The results of the three models 9A, 9B and 9C at sampling in km (0.001, 001) in x and z direction at normal angle with **40Hz**. The synthetic seismic result PSDM for model 9A and Model 9B is the same result the enhanced reflection terminates at near the top the triple junction points. However, 9C gives a proper reflection at the contact hydrate bearing 1850m/s and gas bearings layers 1350m/s -1550 m/s (proper BSR).

Low frequency (**40 Hz**) cannot identify model 9A and 9B. Model 9A is the gas free extended in the GHS region and on the free gas region, however 9B in the HSZ hydrates are formed there for contact of hydrates bearing sediment and sediment with very low gas with P- velocity 1750m/s and free gas bearing sediment 1350m/s P-velocity intercalated.

Frequency 40 Hz sampling in km (0.005, 0025) at normal angle

The results of the three models 9A, 9B and 9C at sampling in km (0.005, 0025) in x and z direction at normal angle with 40Hz.

The synthetic seismic result shows very similar results for the model 9A, 9B and 9C. The BSR shows, as it is undulating continuous proper reflection. A frequency of 40Hz and sampling in km (0.005, 0.0025) cannot identify the BSR in three different ideal models 9A, 9B and 9C.

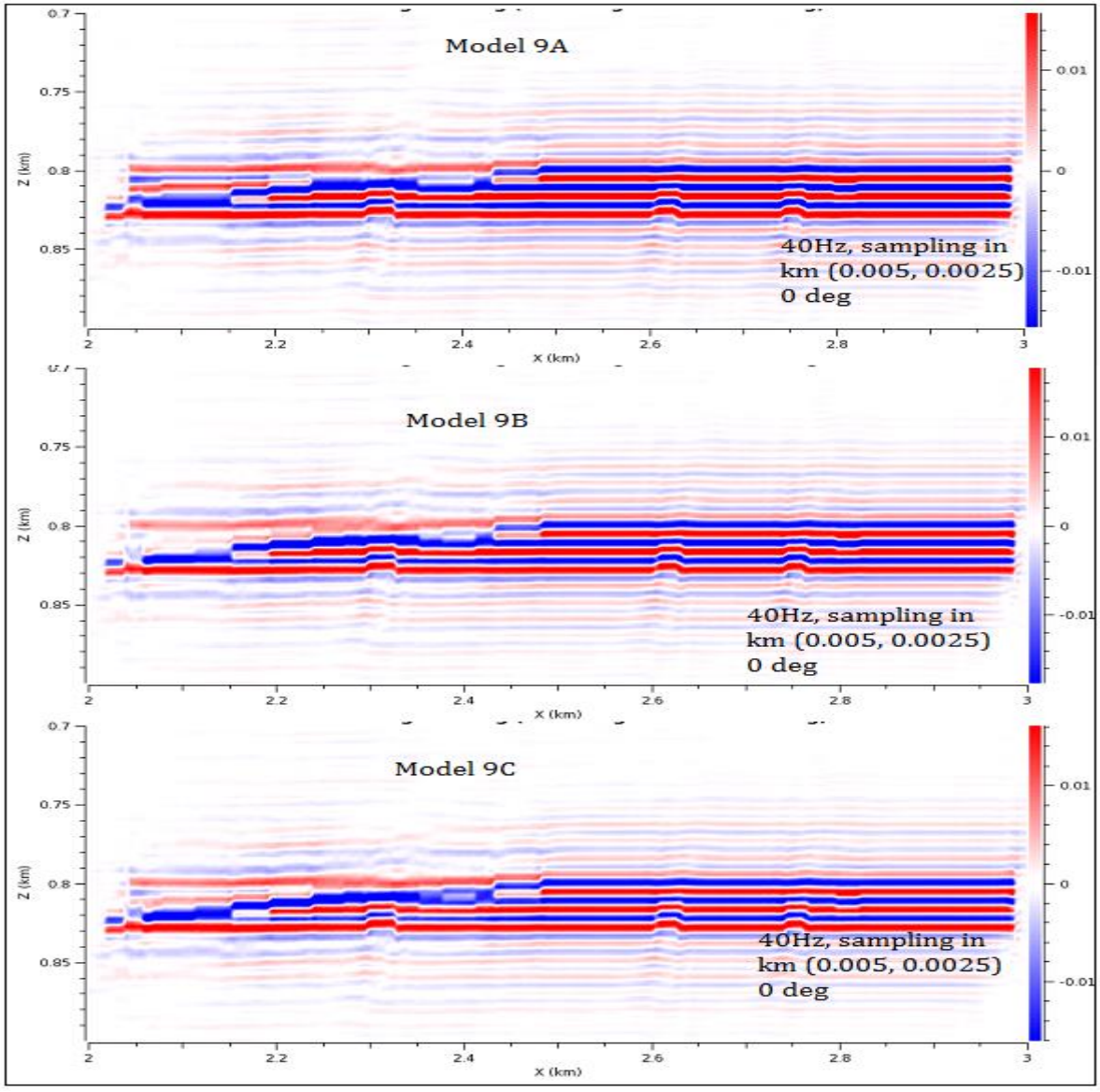

Figure 4.22 *shows three similar result the synthetic seismic result of model 9A, model 9B and model 9C undulating proper reflection BSR at three of the models show the same reflection.*

Frequency 40 Hz sampling in km (0.01, 005) at normal angle

The results of the three models 9A, 9B and 9C at sampling in km (0.01, 005) in x and z direction at normal angle with 40Hz.

The synthetic seismic result in Figure 4.23 results from all the three models show the termination of enhanced reflection at the contact or BSR. Frequency of 40 Hz and sampling (0.01, 0. 005) cannot identify the different model BSR appearances.

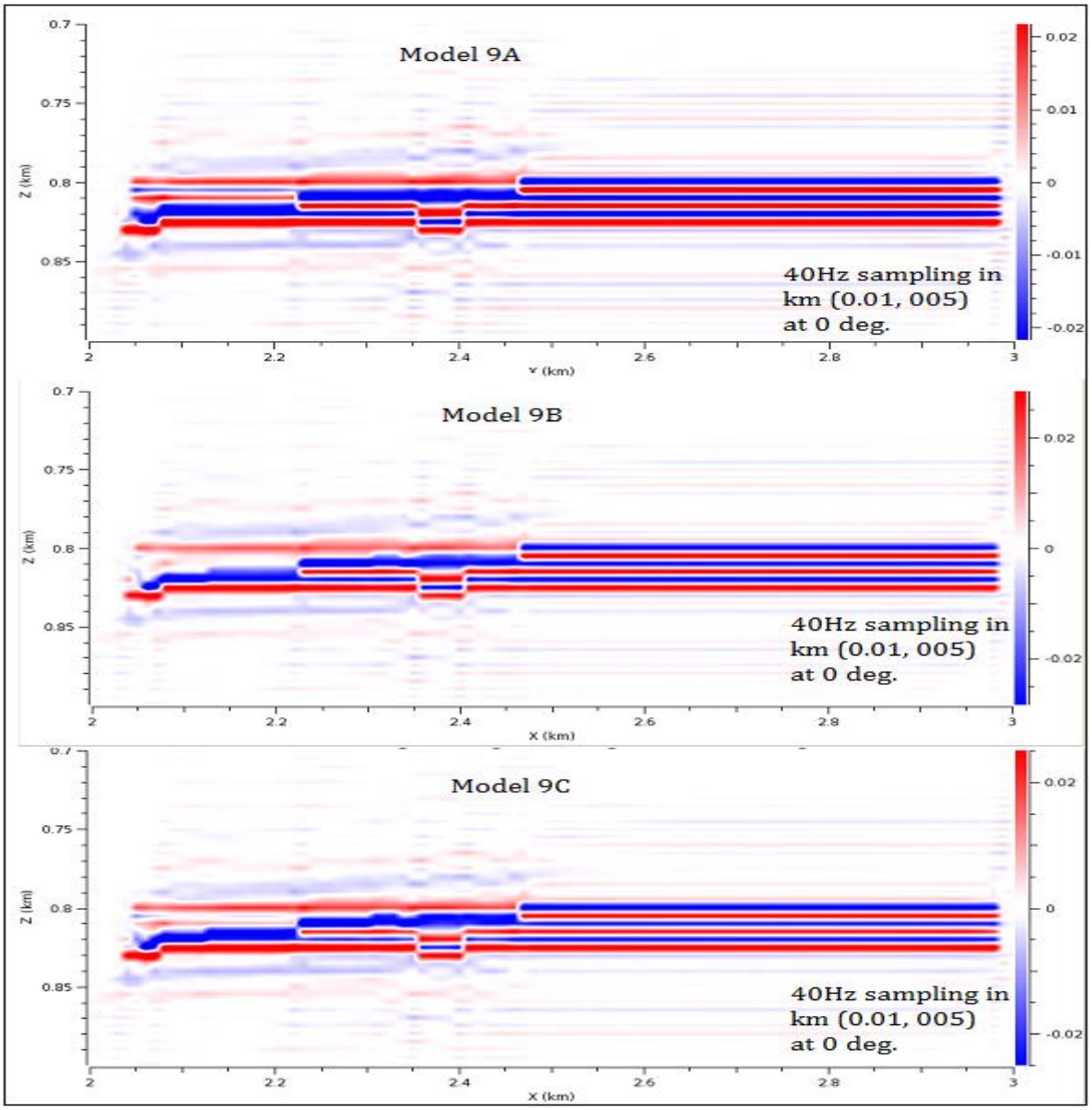

Figure 4.23 *shows three similar result the synthetic seismic result of model 9A, model 9B and model 9C shows termination of enhanced reflection at BGHSZ, three of the models show the same reflection.*

Frequency 80 Hz sampling in km (0.001, 001) at normal angle

The results of the three models 9A, 9B and 9C at sampling in km (0.001, 0. 001) in x and z direction at normal angle with 80Hz.

The synthetic seismic result in Figure 4.24 results from all the three models show the termination of enhanced reflection at the contact or BSR. The termination of enhanced reflection for model 9A and 9B is clearly observed but the termination for Model 9C is includes blur reflection at thinner parts of the layer. Frequency of 80 Hz and sampling in km (0.001, 0.001) cannot identify the different between model 9A and model 9B.

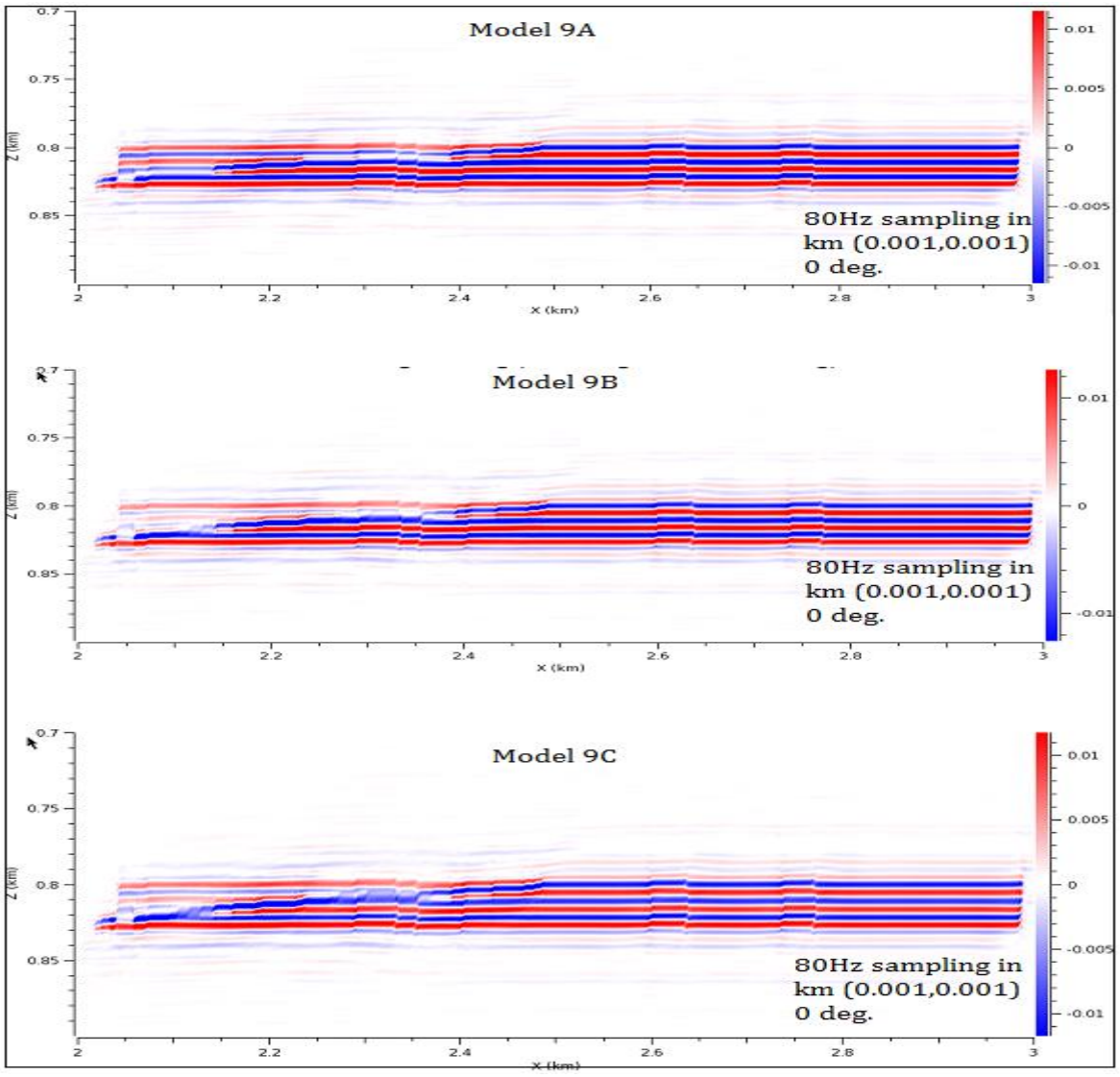

Figure 4.24 *shows three similar result the synthetic seismic result of model 9A, model 9B and model 9C shows termination of enhanced reflection at BGHSZ, three of the models show the same reflection.*

Frequency 80 Hz sampling in km (0.005, 0025) at normal angle

The results of the three models 9A, 9B and 9C at sampling in km (0.005, 0. 0025) in x and z direction at normal angle with 80Hz.

The synthetic seismic result PSDM in Figure 4.25 results from all the three models show the termination of enhanced reflection at the contact or BSR. The termination of enhanced reflection for model 9A, 9B, and 9C are clearly observed at BGHSZ. Frequency of 80 Hz and sampling in km (0.005, 0.0025) cannot identify the different between model 9A model 9B and model 9C.

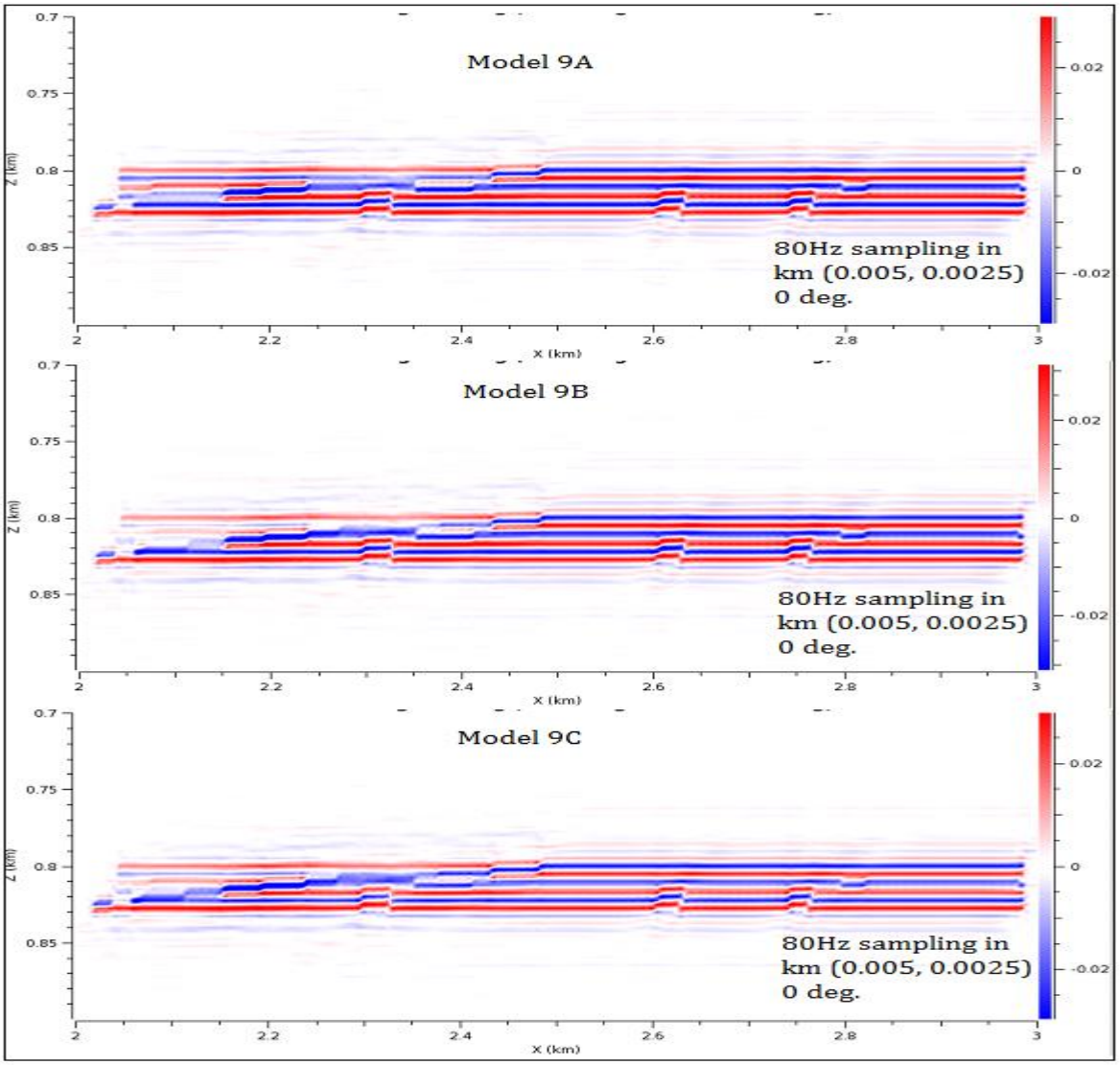

Figure 4.25 *shows three similar results, the synthetic seismic result of model 9A, model 9B and model 9C shows termination of enhanced reflection at BGHSZ, three of the models show the same reflection.*

Frequency 80 Hz sampling in km (0.01, 005) at normal angle

The results of the three models 9A, 9B and 9C at sampling in km (0.005, 0. 0025) in x and z direction at normal angle with 80Hz.

The synthetic seismic result PSDM in Figure 4.26 results from all the three models show the termination of enhanced reflection at the contact or BSR. The termination of enhanced reflection for model 9A, 9B, and 9C are clearly observed at BGHSZ. Frequency of 80 Hz and sampling in km (0.005, 0.0025) cannot identify the different between model 9A model 9B and model 9C.

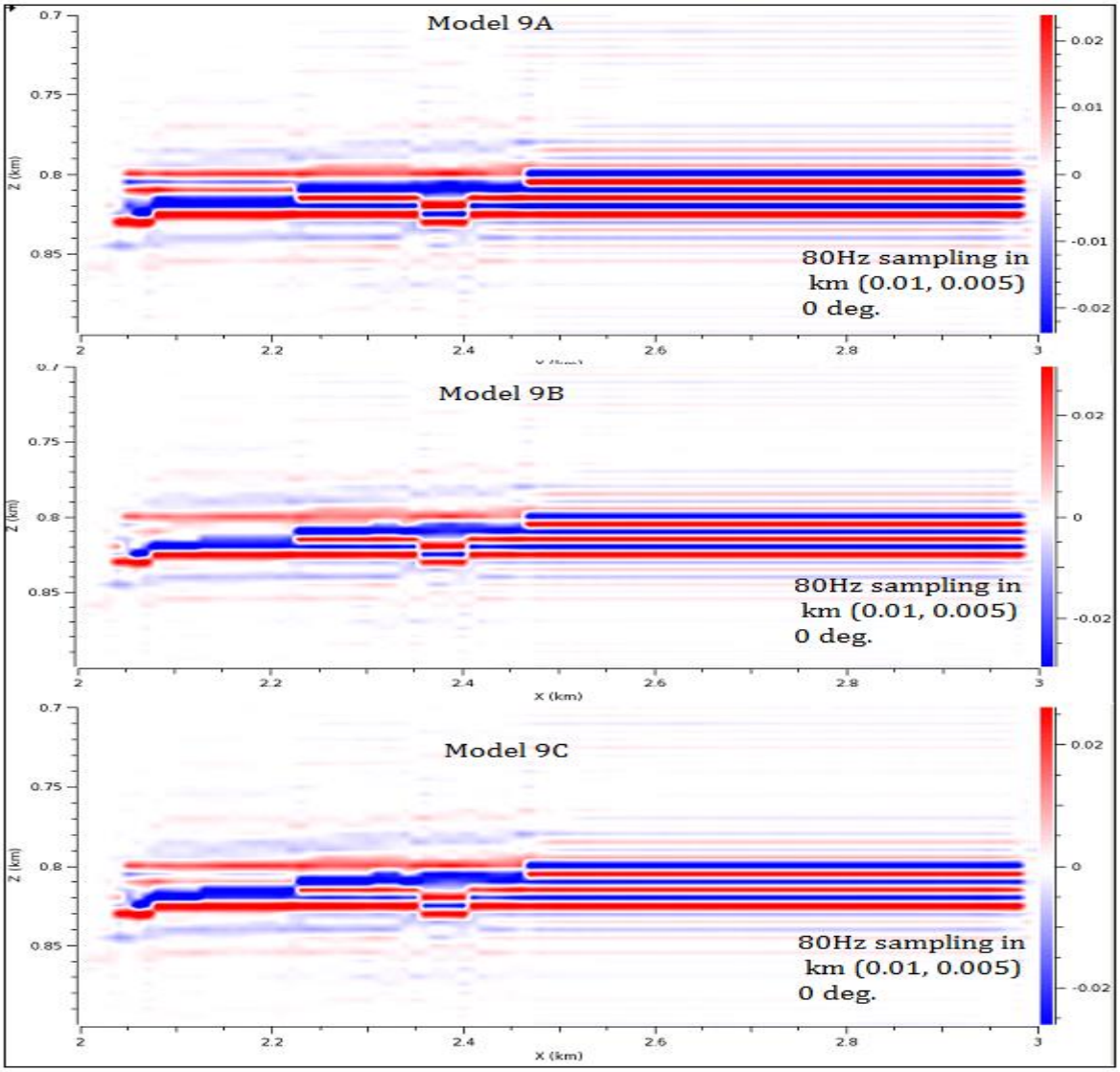

Figure 4.26 *shows three similar results, the synthetic seismic result of model 9A, model 9B and model 9C shows termination of enhanced reflection at BGHSZ, three of the models show the same reflection.*

Azimuth and dip

The azimuth and dip for workflows of model 9 is generated. The illumination vector shows the orientation of the illuminated reflectors in the survey. Reflectors are oriented between 40° and 60° northeast and 40° and 60° southwest. The highest of illumination was mapped to have with a dip value from 60°to 65° and from 50° to 55°. The red color denotes maximum number of illumination vectors and the deep blue minimum number of illumination vectors.

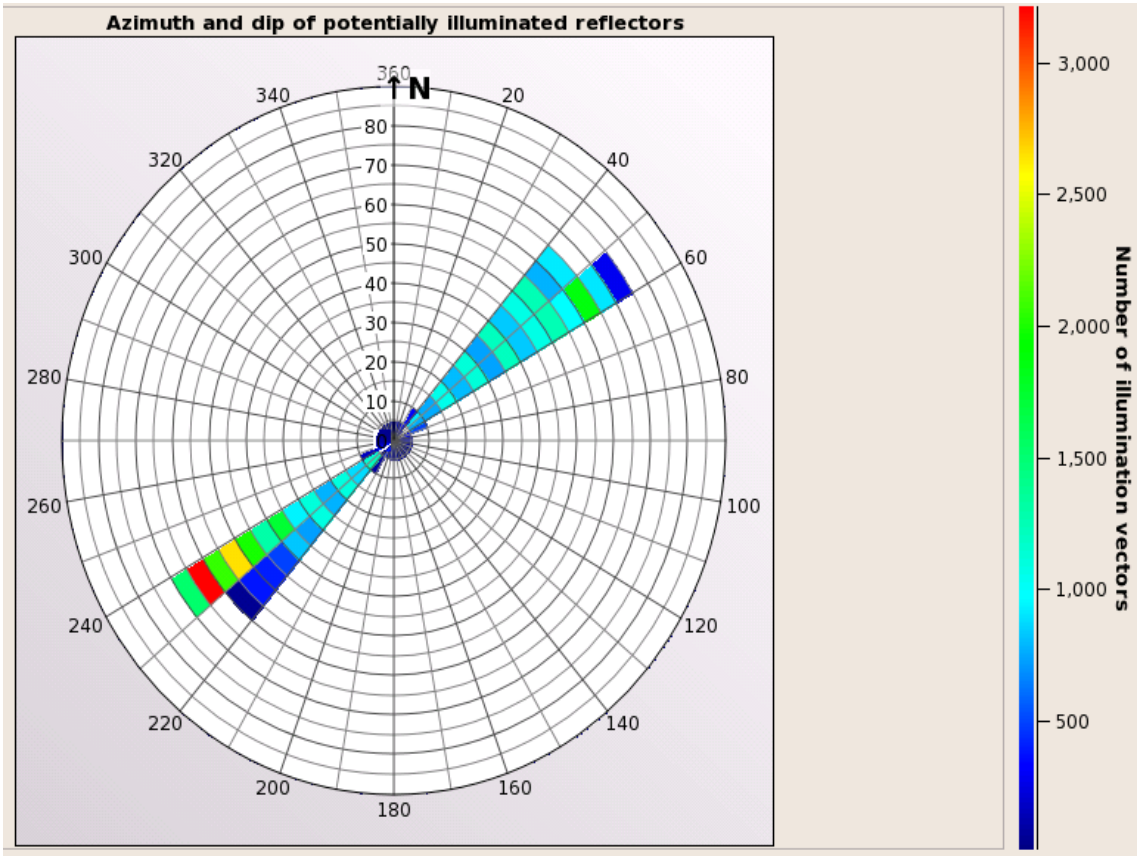

Figure 4.27 *shows the Azimuth and dip of illuminated vectors for the workflow used to illuminate model 9, red color maximum number illumination vectors and deep blue minimum number of illumination vectors.*

Reservoir model 11 and model 12

The anticlinal shaped BSR model 11 and model 12. The contacts between free gas bearing sediment and hydrate bearing sediment gives proper reflection and it is interrupted at the contacts between the less porous sediment. The interruption is not clear for thinner less porous layer at low frequency **40Hz** Figure 4.20 and 4.22 but it is sharply seen with higher frequency at **80Hz** Figure 4.21 and 4.23**.** The interruption of thick less porous sediment is seen by less reflection from the contact with gas hydrates, the illustration of the anticlinal BSR crosscutting strata. The absences of proper reflection is clearly seen, as the less porous sediment layer are thicker Figure 4.22 and Figure 4.23.

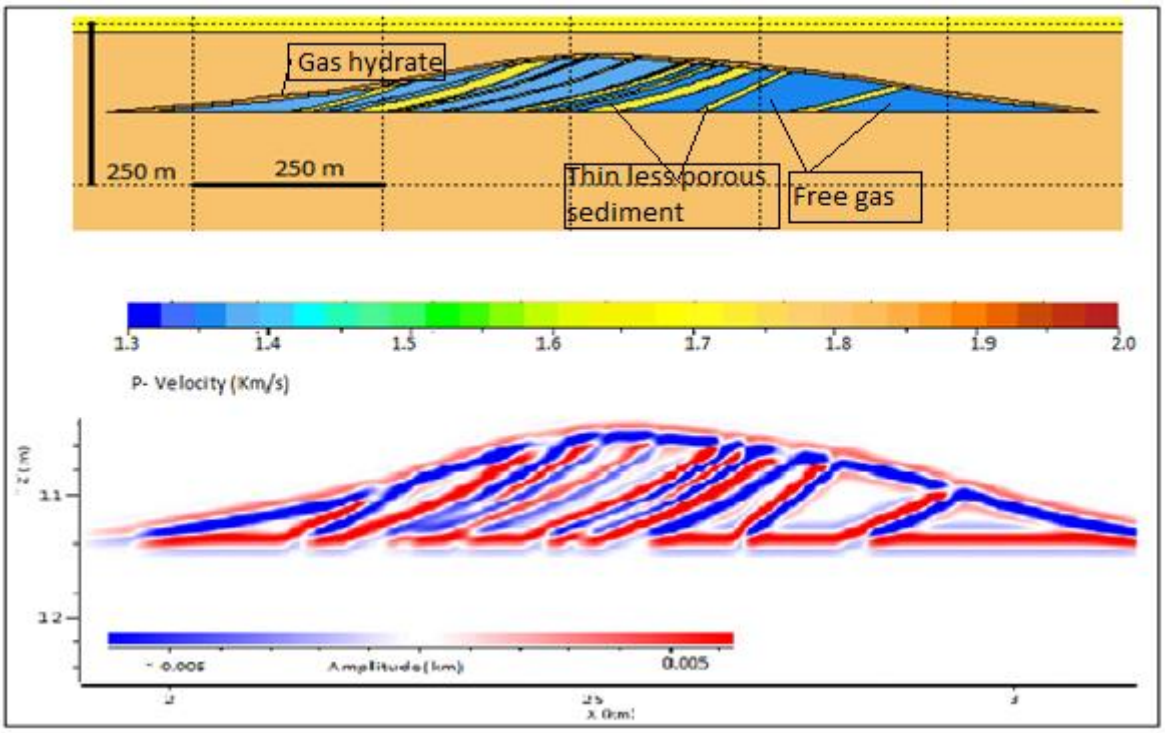

Figure 4.28 *shows Anticlinal BSR cutting dipping thick layers of sediment with gas and thin layers without gas, the case hydrate formed at the top of gas free sediment and less porous sediment with gas. Seismic result at* ***40 Hz*** *and* ***normal*** *angle, sampling at (0.001, 0.001) (x, z). The seismic reflection show strong enhanced reflection at gas hydrate free gas contact but it terminate at triple Junction contact of gas hydrate ,free gas and less porous sediment with significant thickness it seems negligible effect from very thin less porous layers.(at center of the anticline the effect of thin layers of less porous seen negligible).*

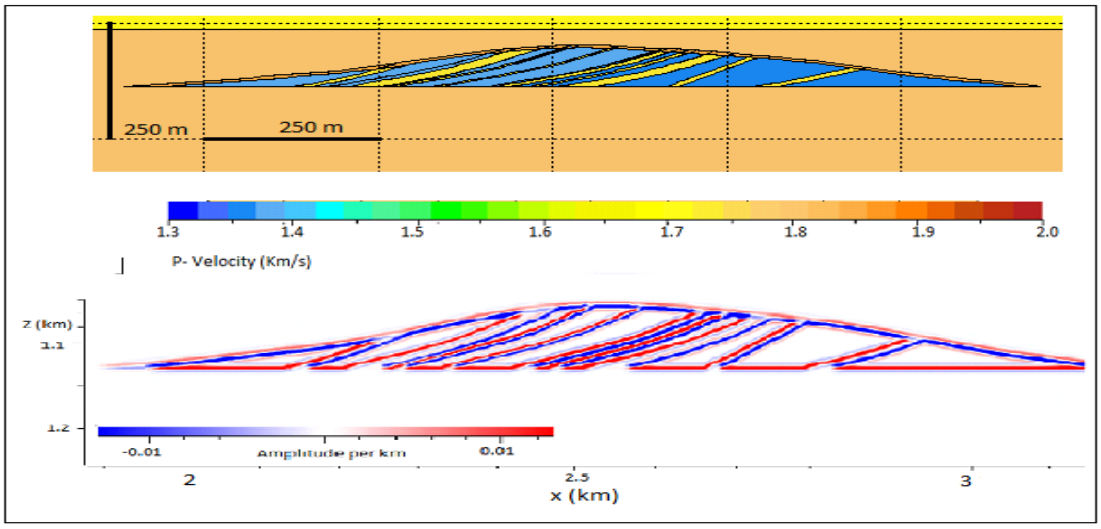

Figure 4.29 *shows Anticlinal BSR cutting dipping thick layers of sediment with gas and thin layers without gas, the case hydrate formed at the top of gas free sediment and sediment with gas. Seismic result at* ***80 Hz and normal*** *angle, sampling in km at 0.001, 0. 001 (x, z). The seismic reflection shows termination of enhanced reflection at BSR free gas, gas hydrate and less porous sediment contact (triple Junction contact). Even the very thin layer of less porous sediments shown termination of enhanced reflection.*

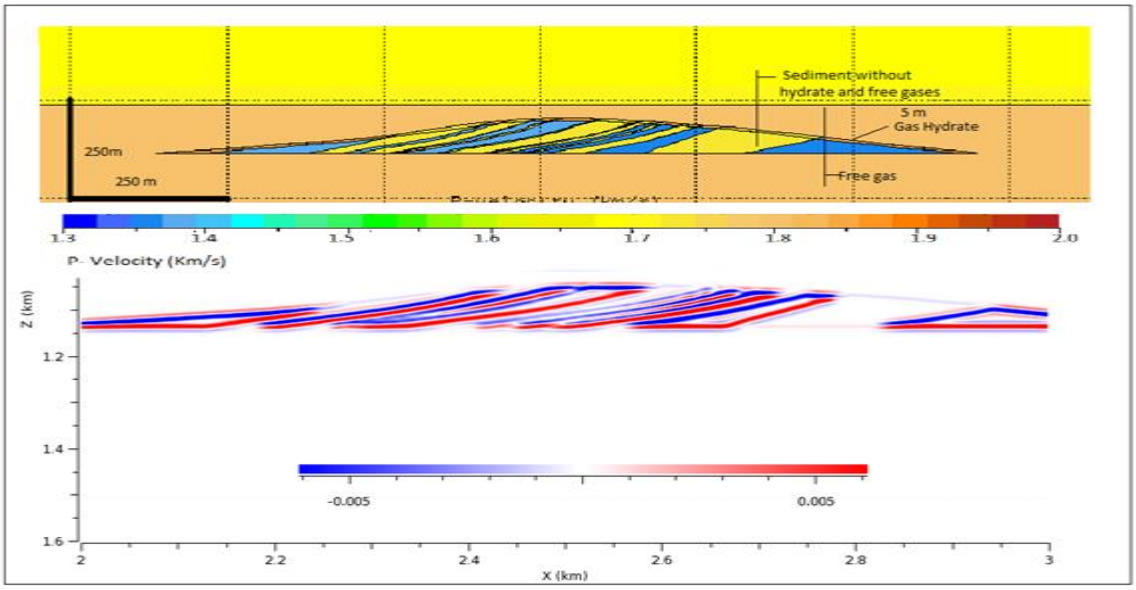

Figure 4.30 *shows Anticlinal BSR cutting dipping thick layers of sediment with gas and without gas, the case hydrate not formed at the top of gas free sediment Seismic result at* ***40 Hz*** *at* ***normal*** *angle, sampling at 0.001, 001 (x, z). The seismic result shows termination of enhanced reflection by the gas layers very less reflection at the top of the less porous*

sediments.

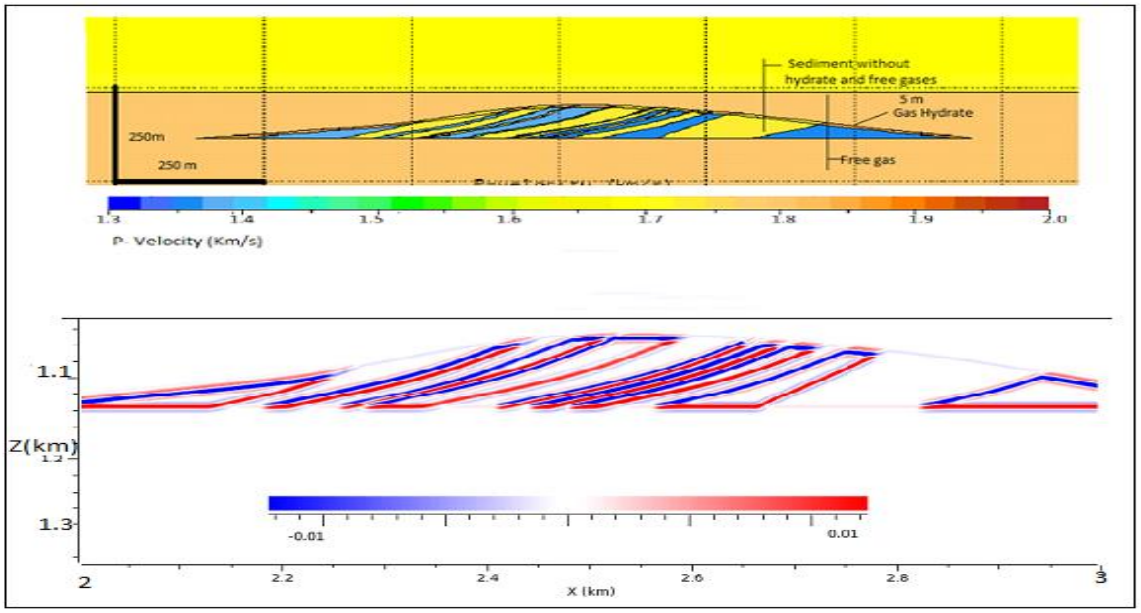

Figure 4.31 *shows Anticlinal BSR cutting dipping thick layers of sediment with gas and without gas, the case hydrate not formed at the top of gas free sediment. Seismic result at* ***80Hz*** *and* ***normal*** *angle, sampling at 0.001, 001 (x, z). the seismic reflection show strong reflection at the contact of gas hydrate and free as well as free gas and less porous sediment the termination or the absences of reflection or less reflection even at a very the thin less porous sediments is clearly seen.*

4.3 Seismic result by incident angle change

The 5m thick free gas bearing sediments and gas hydrate bearing sediments investigated by using frequency dominant at **70 Hz**. The incident angle changes from **0°** to **60°,** at **0°, 10°,20°,30°,40°,45,50°** and **60°**. The result for horizontal and near horizontal contacts of gas and hydrates was similar from the above subtopic **4.1** one example of the angle changes Figures 4.1and 4.2 at **0°** it gives proper enhances reflection at the contact.

The result for model 3 contact between gas and hydrate steeply dipping contact are gradual changing at a given frequency **70 Hz**.

- Anomalous strong reflection are observed At **0°** and **10°,** at **20°** less strong reflection at the bottom of the contact ,
- At **30°** dim reflection
- At **40°** and **50°,** it shows no reflection at the contact, the contact is identified by the termination of the enhanced reflection at the top and bottom of the free gas.
- At **60°** strong reflection of the top of gas bearing sediment but does not show reflection at the bottom of the gas bearing sediment.
- At **60°** it shows over critical reflection gives polarity reversal. The seismic results are given below; Figure 4.16- 4.18 illustrates the seismic result by changing the incident angle at a given frequency. The reflectivity are illustrated in Figure 4.21 and 4.22, Figure 4.23 and 4.24 shows the magnified seismic images.

Target dipping contact of gas hydrate and free gasses (model 3)

5m thick gas non horizontal contact with gas hydrate at **80 Hz** wavelet

Incident angle (**0°,10°, 20°,30°, 40°, 50° and 60°)**

Depth	1
Size (km)	(x, y, z) 2, 0.1, 1
Sampling	0.005, 0.01, 0025

Model 3

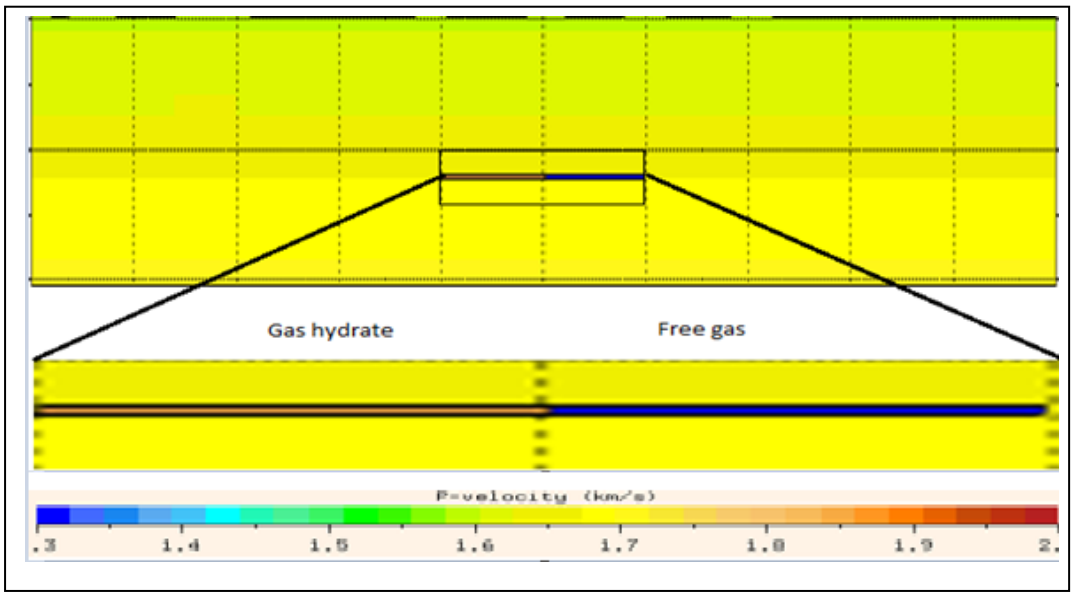

Figure 4.32 *shows magnified size of model 3*

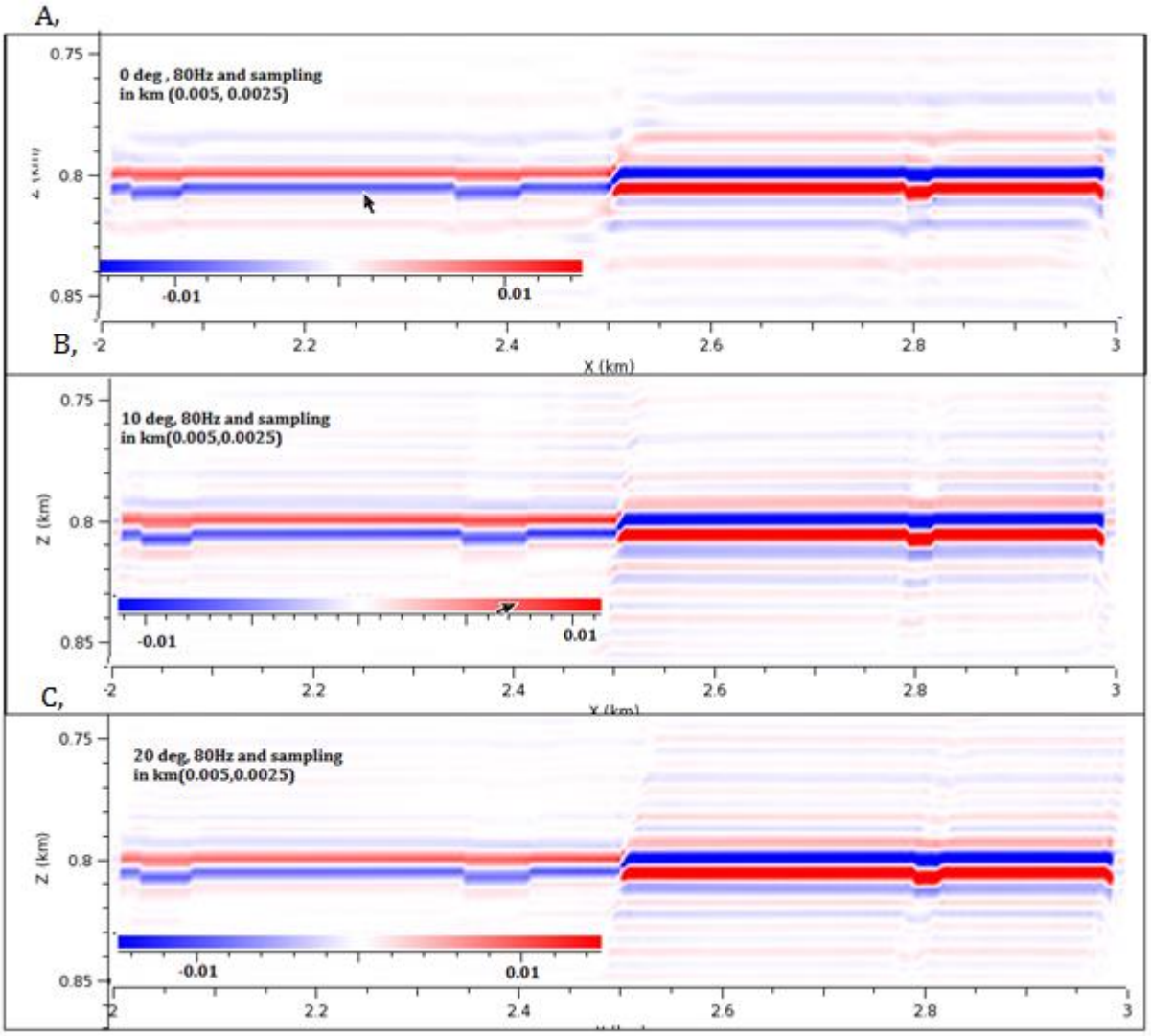

Figure 4.33 *shows seismic reflection at 80Hz frequency and incident angles* ***A,*** *at 0° strong reflection at contact.* ***B,*** *at 10° strong reflection and C, at 20° bottom contact dim.*

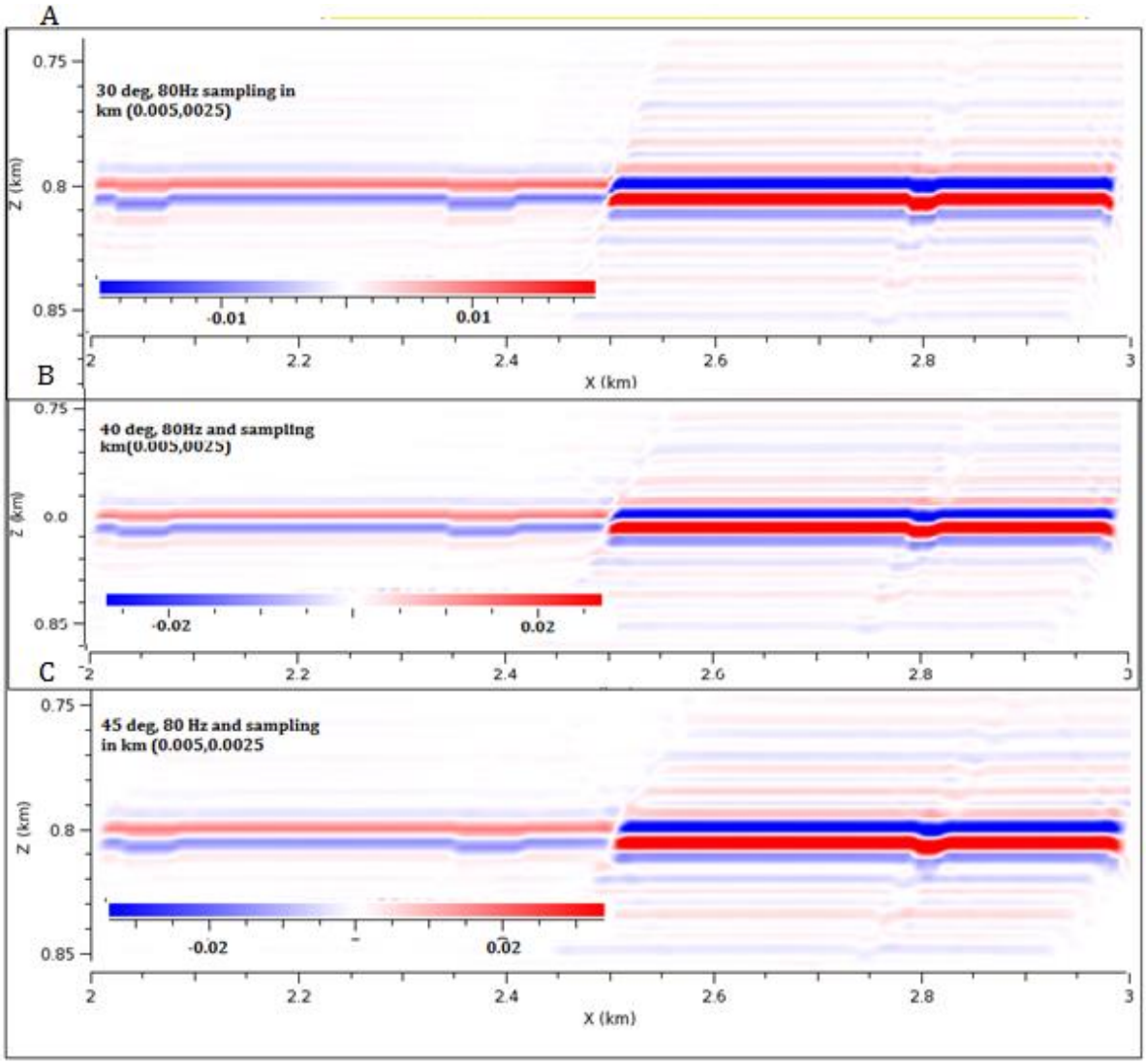

Figure 4.34 *shows seismic reflection at 80 Hz and an incident angles **A**, 30° shows termination of reflection at contact enhanced reflection seen on the free gas side **B**, 40 termination at contact and C, 45° termination at contact for dipping contact of free gas and hydrates bearing sediments.*

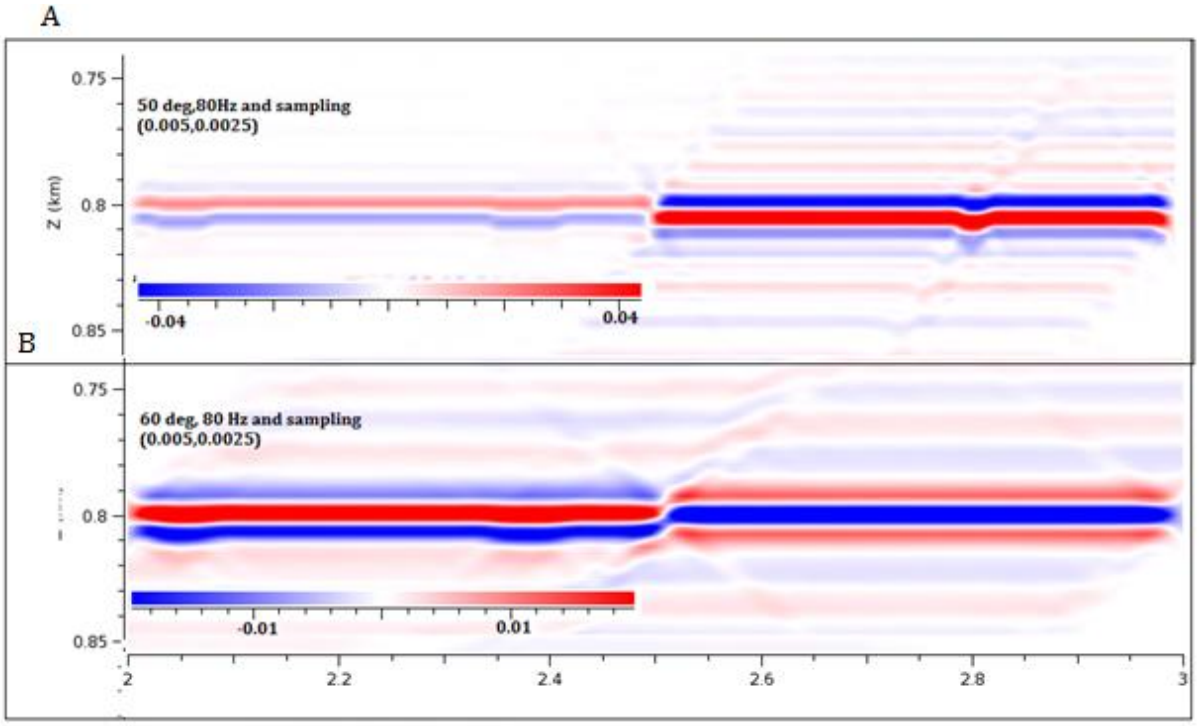

Figure 4.35 *shows seismic result at 80 Hz **A**, at 50° termination of enhanced reflection and **B**, at 60° it shows a reversed polarity.*

PSF as incident angle change.

Point of scattering function is incident angle dependent the result are illustrated in psf image figure 5.36 and the estimated resolution table 4.5 shows as the incident angle increases vertical resolution increases or the highest angle give better vertical resolution. As the incident angle increase horizontal resolution decreases lower angle give better horizontal resolution.

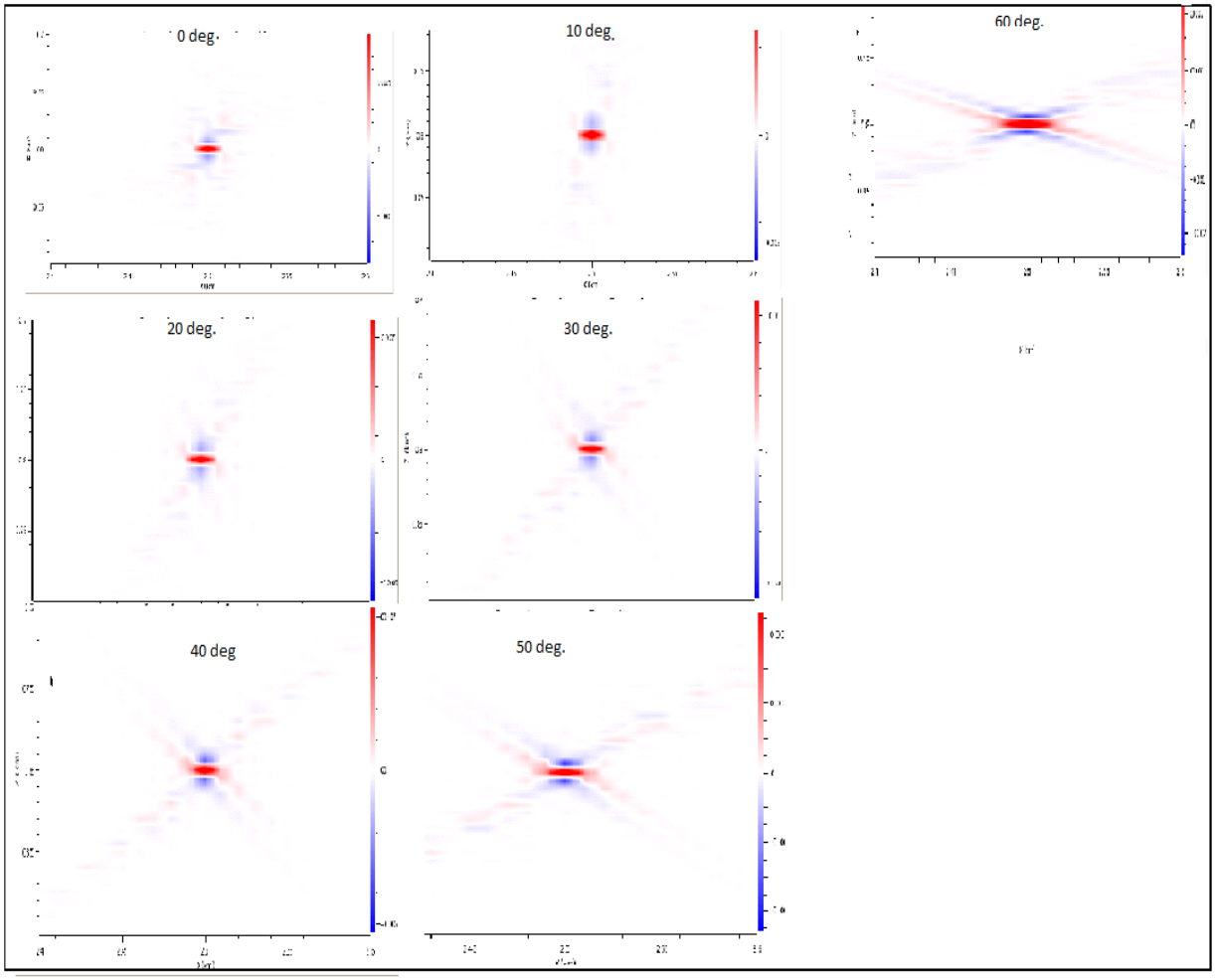

Figure 4. 36 *shows the Psf as incident angle changes from 0 deg to 60 deg at 80Hz.*

Incident angle	Vertical resolution	Horizontal resolution
0	9 m	18 m
10	8 m	18 m
20	8 m	18 m
30	7 m	18 m
40	6 m	20 m
50	6 m	20 m
60	5 m	40 m

Table 4.5 *Estimated Seisrox vertical and horizontal resolution at different angel with 80 Hz frequency.*

5 Discussion

This chapter will primarily discuss the parameters that affect the reflectivity of the BSR to give proper reflection or indicates by the termination of enhanced reflection at the bottom gas hydrates stability zone.

On marine reflection seismic data the BSR can show as a proper, coherent reflection with enhanced amplitudes However, some seismic data, mostly that with larger and higher frequency bandwidth show the BSR as the termination of enhanced reflection (Vanneste et al. 2001).

The parameters that affect BSR reflectivity are classified in this study into two groups. The first group are controlled parameters, these we can change. The second are uncontrolled parameters, which are found in nature, (which are beyond our control in a real world). The way the acoustic impedance of the gas-filled portion of the reservoir influences a reservoir appears like in seismic data depends on the water-filled reservoir portion, the cap rock, and the thickness of the gas-filled interval (Andreassen 2009).

5.1 Change in Controlled Parameters

The parameters that can be changed will be discussed from the results in sections: 4.2 change in sampling in (km) 4.3, change in frequency and 4.5 change in incident angle.

5.2 Uncontrolled parameters

The occurrences and the thickness will be discussed from results in sections: 4.1 and 4.4 changing in dipping angle in model and changes in occurrences.

The controlled parameters and the uncontrolled parameters affect the resolution of the seismic reflection as well as the results of PSDM. The reflection from a reflector depends on the acquisition and processing system. (Andreassen, 2009). Some of the main factors, which affect appearances of the synthetic seismic result of (PSDM), are the survey, the wavelet the sampling space in km and the incident angle given. The uncontrolled parameter are the thickness and occurrences of the BSR or the geological setting that are beyond our control. Seismic resolution is the crucial for understanding seismic stratigraphic detail from seismic data.

5.1 Change in Controlled parameters

5.1.1 Change in sampling in m

In SeisRoX, sampling in km laterally in the x- axis is the same as in conventional seismic common midpoint distance (CMP).

Lateral resolution cannot be shorter than the bin spacing (12.5-15m) of the 3D data set, while it may be more applicable to take in account the limit between the bin spacing and the principal wavelength (Cartwright and Huuse, 2005). Multi-channel seismic line in mid Norwegian margin NH9651-202 recorded at 80-90Hz resulted CMP 12.5m, it is shown in figure 5 .(Buenz and Mienert, 2004) and the Hydratech high-resolution data was taken with a bin of 6m wide as shown in Figure 5. (Bjørnøy, 2015).

The sampling in km in SeisRox gives different resolutions, because sampling in km in the SeisRoX increases the resolution decreases. Figure 4.4-4.6 is an illustration of the synthetic seismic PSDM result processed at different sampling in km. The appearances of BSR is strongly related to the resolution of the seismic system (Champman et al, 2002; Wood et al., 2002). Small sampling in km gives a better resolution in seismic reflection. This is shown on the Table 5.1.

Sampling in km	0.001 0.001	0.0025 0.005	0.005 0.01
Horizontal resolution	5m	8m	20m
Vertical resolution	2m	6m	6m

Table 5.1 *Sampling in km computed at 100Hz 0 degree.*

5.1.2 Changing in frequency

The frequency used for seismic reflection is very important to the resolutions. Higher frequencies give higher resolutions and low frequencies give lower resolutions. As seismic wave penetrates further down, the frequency of the sound signal will reduce while the velocity and wavelength will increase. This reveals that with increasing depth the seismic resolution will be poorer. High frequencies that reflect from shallow depths have higher resolutions, lower frequencies can penetrate to a deeper depth, but they will have a lower resolution (Andreassen, 2009).The results in section 4.3 at higher frequencies shows strong BSR reflection at the contact of hydrate bearing and free gas bearings sediment. This BSR is indicated as the termination of enhanced reflection at approximately of the triple junction point between the hydrate bearing sediments, the free gas bearing sediments and gas free sediments.

As frequency is lowered down from **100H** to **50Hz,** the thinner part of the gas-free sediments starts to interfere with the second layers of the free gas-bearing sediment as shown in Figure 4.8 and Figure 4.9. At **70Hz, 60Hz** and **50Hz** the reflection similar to the continuous gas hydrate-bearing sediment with different strengths of reflection from strong to dim continuous BSR. At **30Hz,** the top of the gas bearing sediment is similar as proper reflection. The sediment without gas is not easily identified with this frequency. Calculated resolutions from PSF in SeisRoX lower frequencies **30Hz, 20Hz**. and **10Hz** cannot identify layers less than 5m thickness .This is shown in Figure 4.11 which are calculated frequencies for sediment with 1750 m/s. these frequencies cannot identify 5m layers and is illustrated in Tables 5.2 and 5.3 shaded by red colors. The amplitude decreases from the higher frequencies to the lower frequencies. The amplitude at **250Hz** is about **20m**; at **100Hz** is about **10m** it decrease to **0.5 m** at **10Hz**.

Frequency	Vertical resolution(m)	Horizontal resolution(m)
10	30	40
20	14	20
30	10	16
40	6	10
50	6	8
60	5	6
70	4	5
80	4	4
90	4	4
100	3	3
250	2.5	2
500	2	1.5
1000	1.5	1

Table 5.2 *shows vertical and horizontal resolution estimated from the psf result psf figure 4.15 given in chapter 4.*

frequency	Wave length (m)=v/f,V=1750m/s	Vertical resolution λ/4 maximum tuning thickness'	Minimum thickness without interference λ/2
10	175	43.75	87.5
20	87.5	21.88	43.76
30	58.33	14.58	29.16
40	43.75	10.94	21.88
50	35	8.75	17.5
60	29.16	7.29	14.58
70	25	6.25	12.5
80	21.87	5.46	10.92
90	19.44	4.86	9.72
100	17.5	4.38	8.76

Table 5.3 *shows vertical and horizontal resolution calculated using eqn.1.7 for sediment with P-velocity 1750m/s.*

5.1.3 Change in incident angle.

The BSR reflectivity in relation to the incident angle depends on the property of the interfaces. As incident angle changes, reflectivity also change (Sheriff and Gedart, 1995; Ecker et al.1998; Yuan et al., 1999*).* Model 3 in this thesis is used to study changes in incident angles. It yields different response as incident angle changes. The result as the incident angle increase from **0°** to **60°** gives progressivly change from proper reflection at the contact(BSR) to the termination of enhanced reflection Figure 4.33-4.35. This can be related to the resolution that is estimated from PSF as incident angle changes from **0°** to **60°**. It is given in Table 5.4. The pattern of changing the appearances of the BSR is directly related to the resolutions given on the psf Table 5.4 as horizontal resolution increase from **18m** to **20m** reflection terminated at dipping contact of the 5m hydrate bearing and gas bearing layer happened.

Incident angle	Vertical resolution	Horizontal resolution
0°	9 m	18 m
10°	8 m	18 m
20°	8 m	18 m
30°	7 m	18 m
40°	6 m	20 m
50°	6 m	20 m
60°	5 m	40 m

Table 5.4 *shows the estimated vertical and horizontal resolution at different angle lower horizontal resolution colored red which give reflection termination at the given model 3.*

Illumination and survey

Survey parameters

For all workflows on this study a common parameter in marine survey was used as in Table 5.5 The illumination vector in seisrox calculated in the background model for a given shot / receiver couple and ray types .The survey parameter is shown on Figure 5.1 (Norsar, 2011).

Shot configuration		Streamer/Receiver configuration	
Center (x,y) (Local)	(2.5,2.5)	Depth(km)	0.00
Depth(km)	0.00	Minmum offset(km)	0.1
Rotation(related X –axis)	0.00	Number of streamers	2
Number of shot lines	1	Streamer length (km)	2.5
Shot line length (km)	5	Streamer spacing (km)	0.1
Shot line spacing(km)	0.025	Reciver spacing (km)	0.0125
Shot spacing	0.025		

Table 5.5 *Survey parameters used on seisrox workflows of this study.*

Azimuth and dip (Illumination)

The azimuth and dip for workflows of model 9 is generated. The illumination vector scale shows in Figure 5.1 that the orientation of the illuminated reflectors in these survey reflectors are oriented between 40°, 60° northeast, 40°, and 60° southwest. The highest illumination is mapped to have dip of 60°-65° and 50°-55°. This tell us that if there is a reflector perpendicular to that vector near the calculation point. This reflector will indeed be illuminated in real acquisition (Norsar, 2011) by using the same parameters as in this study. The red color denotes maximum number of illumination vectors and the deep blue minimum number of illumination vectors. For the high-resolution receiver spacing 0.006 km is used. The Hydratech high-resolution 3D seismic data collected by a cruise led by Ifremer, to the mid Norwegian margin in 2002 (Nouzé et al., 2004). The size of the bin was~6m of the dataset and the Dominant frequency (~80 Hz) provides better horizontal and vertical resolution related to conventional industry 3D seismic data. (Hustoft et al., 2007).

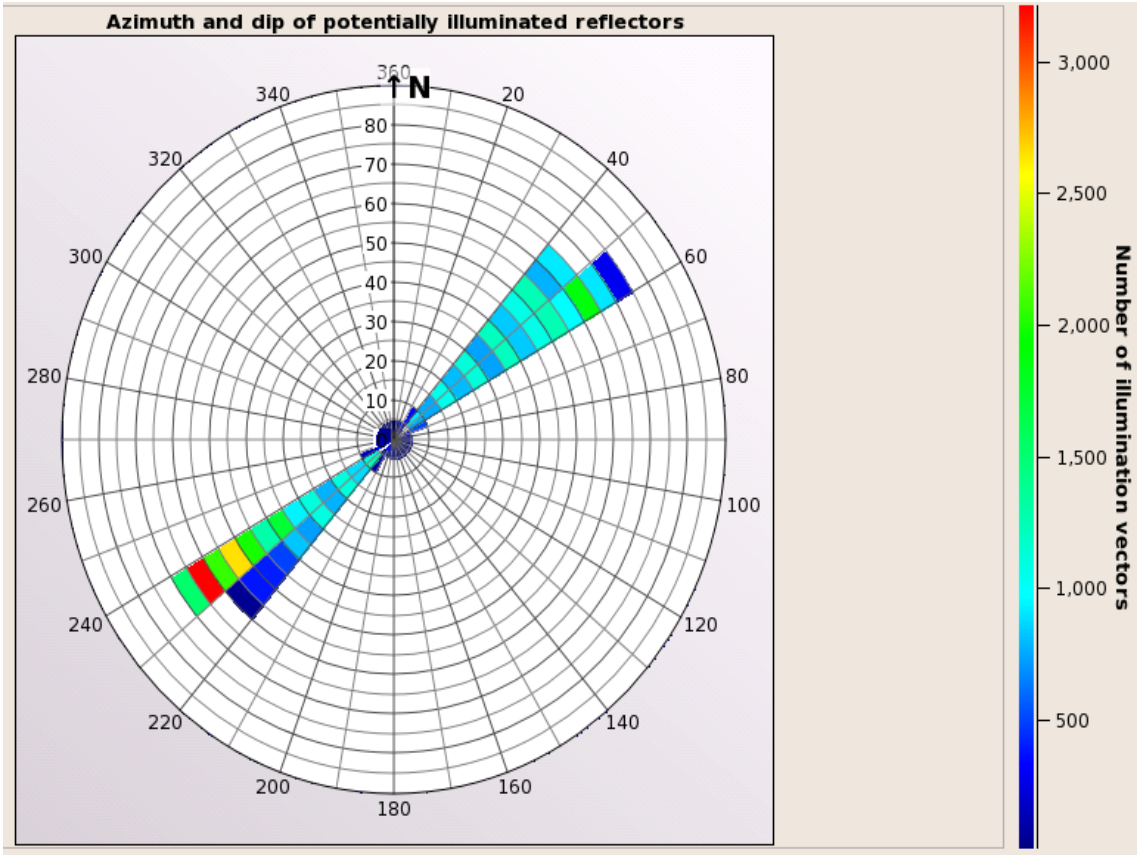

Figure 5.1 *shows the Azimuth and dip of illuminated vectors for the workflow used to illuminate model 9, red color maximum number illumination vectors and deep blue minimum number of illumination vectors.*

5.2 The uncontrolled parameters

The uncontrolled parameters used in this thesis (which are beyond our control in a real world) are the occurrence and thickness of the sediments. The reflectivity of BSR depends on the resolution and the thickness of the layer. Models on this study have been made by many assumptions because of the limitation of real data. Model 7 is made with the assumption if gas hydrate is formed uniformly in a gas bearing sediment resulting in physical boundary at the bottom of gas hydrates stability zone, as interstial hydrates are favoured in coarse sediments (Henry et al, the issue). Figure 5.2A illustrates a homogenous gas hydrate bearing and gas bearing layer model 7, Figure 5.3B shows model 7 with the background model. These significant thickness and width results show anmoalously strong reflection at the contact or BSR. The gas bearing and hydrate bearing zones have the same thickness as the seismic section taken from the real data but the assumtion does not gives a Synthetic seismic reflection that can matched with the real data. Figure 5.8.

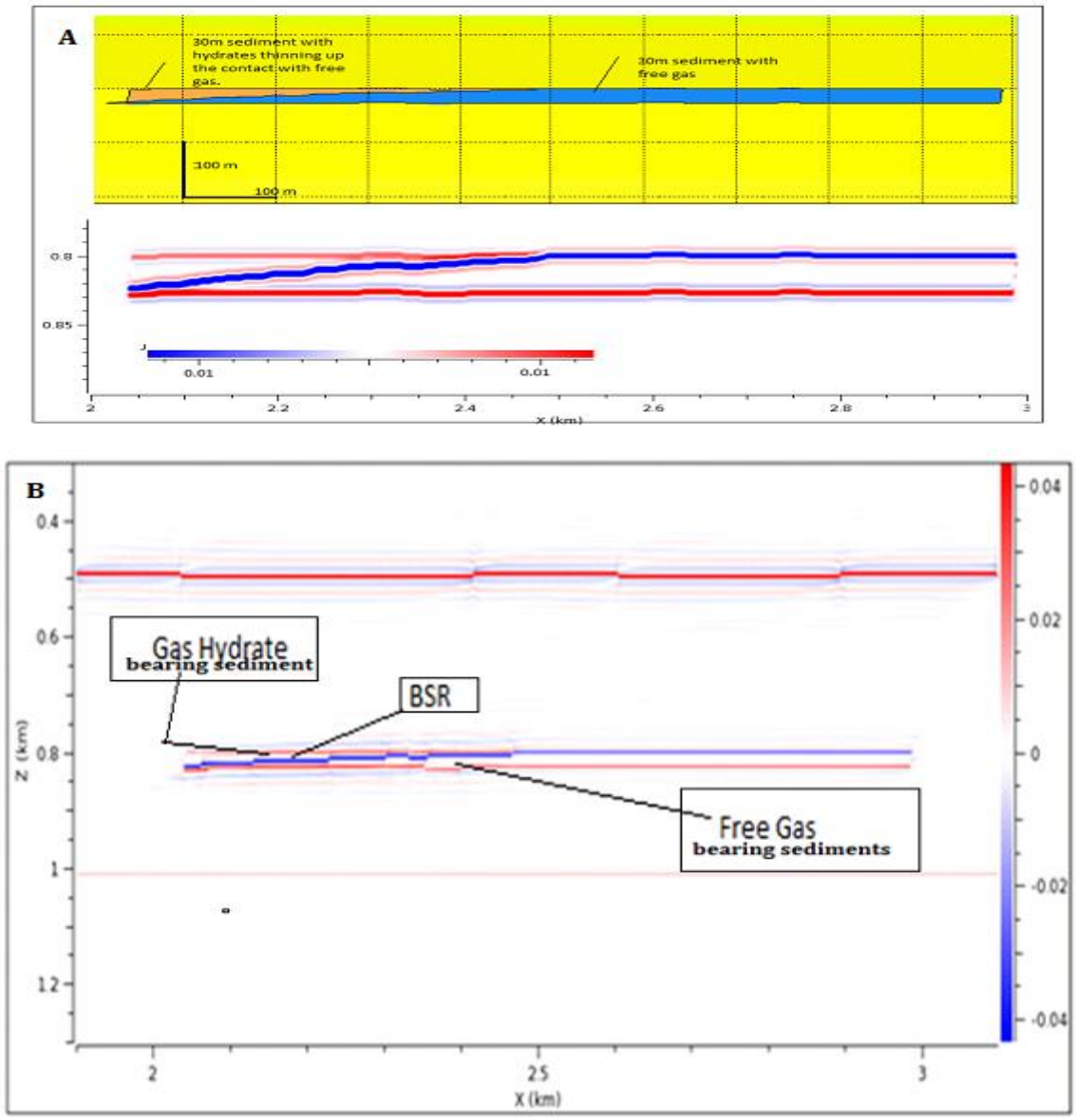

Figure 5.2 *shows **A**, geological model 7 and synthetic seismic result PSDM a proper BSR reflection and **B**, synthetic seismic result of PSDM of model 7 with the background.*

5.2.2 Model 9A, 9B and 9C is a 30m thick intercalation of porous sediment and less porous sediment.

To understand the gas hydrate system, four possible models of gas hydrate and free gas bearing sediments are compared with real data from the Hydratech high resolution seismic data.

The models are made, as the porous sediment is favorable for the accumulation of free gas. It thereby possibly forms gas hydrate in the porous sediment. The less porous sediments are assumed sediments without gas (i.e. negligible amount of gas to form gas hydrates to form) in model 9A. The formation of gas hydrate depends on many factors :gas and water migration pathways, the presence of seal and cape rock, sea bottom temperature, geothermal gradient, availability of gas and water, gas chemistry, pore-water salinity etc (Tan, 2012). The failure of one of the factors might result in the absences of gas hydrates in the sediments in the HSZ.

The bulk equilibrium for gas hydrate stability is not applied equally for fine grained and course grained sediments In fine-grained sediments, the hydrate phase may be destabilized thermodynamically, and perhaps inhibited from nucleating until the normal temperature is significantly cooler than the bulk equilibrium value probably by as much as 0.5 to 3°C. A Shift in the BSR upwards by tens of meters, relative to estimates based in the bulk stability equilibrium curves. This will raise the depth of the first hydrate appearances by a similar amount. This estimation is based on published experimental data (Henry et al, the issue).The bottom of the gas hydrate stability zone for intercalated layers might be at different depth.

In Model 9A the sediments without gas can possibly have less P-velocity 1750m/s and density from the nearby hydrate bearing sediment 1850m/s (model 9A2); they can also possibly have equal P-velocity and density or more than the hydrates p-velocity and density.

The effect of the surface activities in clay and the fine pore space is in deep sea sediment is not fully understood.(Hyndman et al.,1992). The important point in model 9A that is shown in Figure 4.21A is that the sediments without gas cross both the free gas and hydrate bearing regions and is intercalated with the hydrate bearing sediments above BGHS and with gas bearing sediments below BGHS.

Model 9B shows the occurrences of BSR as under a homogenous region of hydrate bearing at a contact in different concentrations of free gas bearing layers.

Less gas reduces the velocity of sediment significantly. If this gas can form hydrates in the HSZ, it can result to give an impedance contrast between the interface, in this case model 9B has made this illustrated in Figure 4.21C. To understand the gas hydrate sytem is a major challenge including gas sources, gas migration pathway , reservoier emplacement and seal (collett et al., 2009).

In Model 9C the occurrence of gas hydrate bearing sediments at different concentration in consecutive layers and different concentration of gas bearing layers has been made, it is illustrated in Figure 4.21B. This has been made with the velocity of gas bearing sediment variation from 1350m/s to 1550m/s at lower concentration. The velocity at the hydrate bearing sediment also varies from 1850 m/s to1780m/s as the higher hydrate p-velocity are assumed for high concentration of free gas. The results of the three models 9A, 9B and 9C at sampling in km (0.001, 001) in x and z direction at normal angle with 40Hz are similar.

The presence of BSR may show the presence of gas hydrate but the absences of BSR do not imply absence of gas hydrate (Rajuput et al., 2012). The strength of BSR reflection is governed by the amout of free gas below it (Andreassen et al., 2000a, Andreassen et al., 2000 b, Andreassen et al., 2003 ,chand and minshull 2003).

Model 9A, model 9B and model 9C give the same reflection proper reflection of undulating at lower frequency 40Hz at normal and sampling in km (0.005, 0.0025). They also gives the same result it is generated as a sampling in km (0.01,0.005) (Figure 5.3). At higher frequency, 80 Hz at normal and sampling in km (0.005, 0.0025) it also gives the same result as in a sampling in km (0.001,0.001) and (0.01,005) these three models give the same reflection at the BGHSZ termination of enhanced reflection and it is illustrated in Figure 5.4.

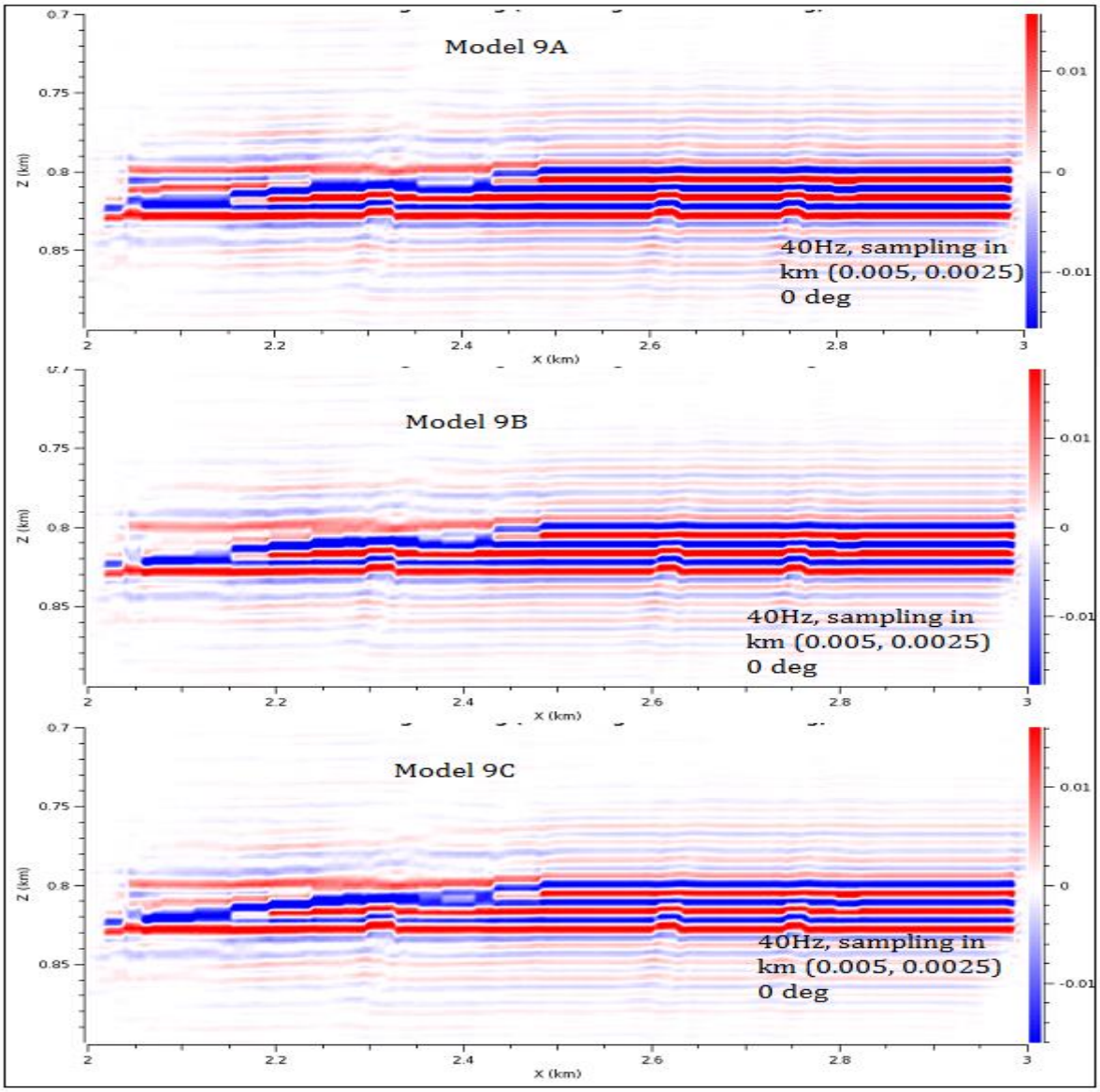

Figure 5.4 *shows the synthetic seismic result of model 9A, model 9B and model 9C undulating proper reflection BSR at three of the models show the same reflection.*

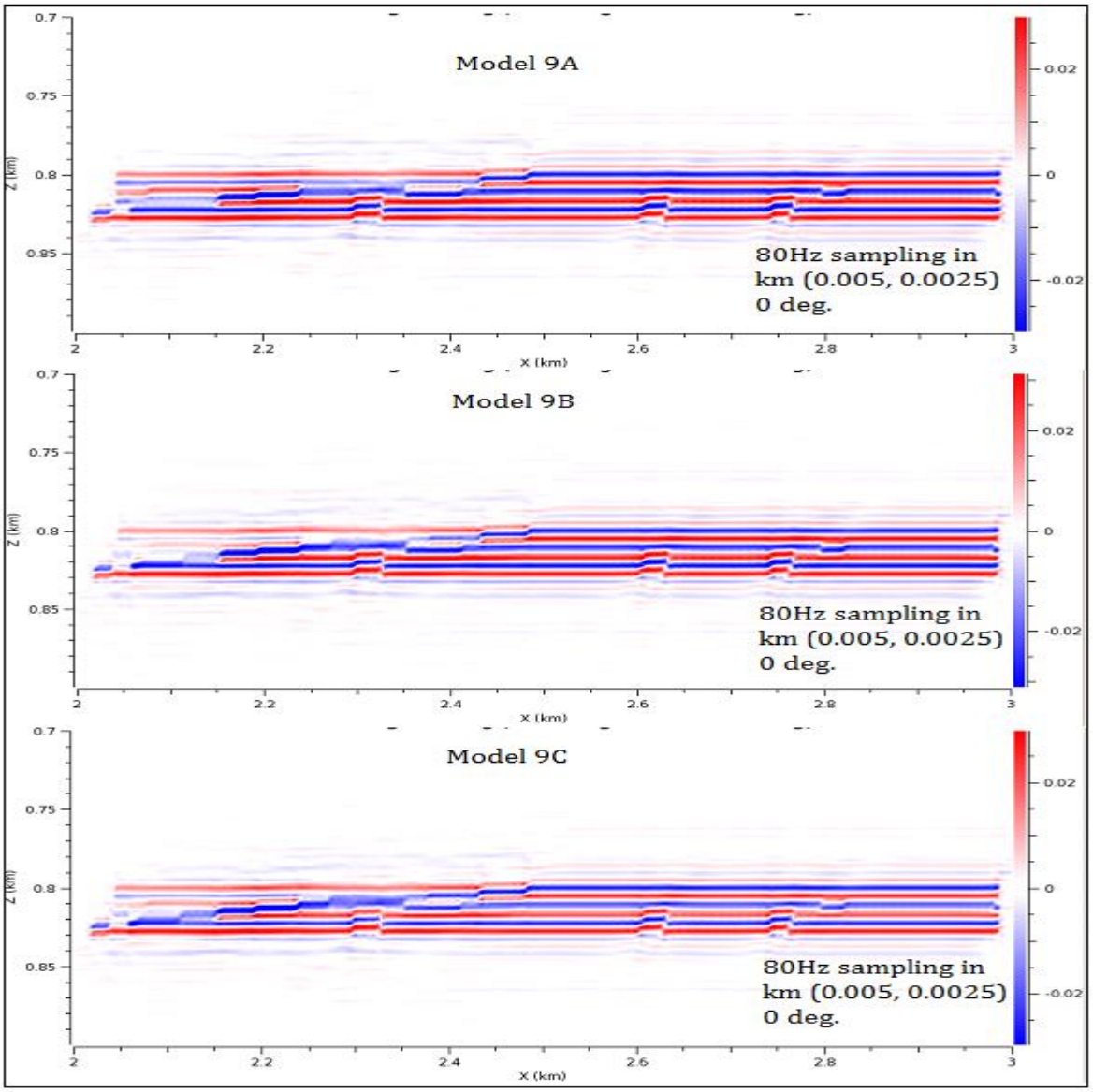

Figure 5.5 *shows the synthetic seismic result of model 9A, model 9B and model 9C shows termination of enhanced reflection at BGHSZ, three of the models show the same reflection*.

5.2.3 BSR on the mid Norwegian continental shelf

BSR on the mid Norwegian margin occurs in the southern part of the Vøring plateau (Bünz et al, 2003). The geological occurrences of BSR are shown only in the countouritic sediments and not with in interbedded glacial debris flow or fine grained sediment (Brent, 2004). This can be the capillarity of the rock to host hydrate. (Clennel, Hovland, Booth, Henry& Winters 1999).

The BSR was characterized by termination of enhanced reflection that coincide with theoretical GHSZ (Mienert, Posewang and Lukas 2001). In Some parts, the BSR proper cuts the strata. Bugge, (1983) first reported BSR in southern Vøring, He related the BSR with the black outer ridge (Shipley et al 1979). The Attempt to recover gas hydrate failed because of technical limitation (Mienert and Bryn, 1997) Figure 5.5 and 5.6 are the seismic sections from mid Norwegian margin.

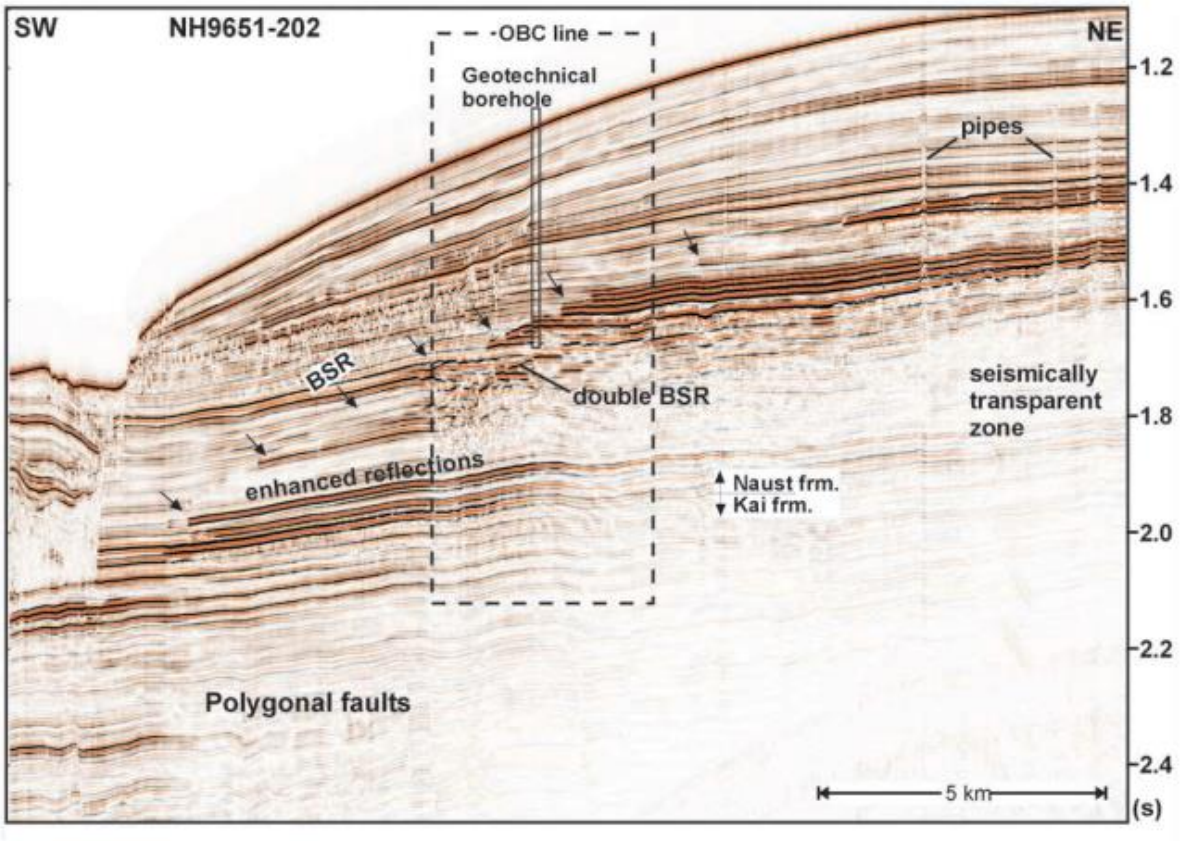

Figure 5.6 *shows the seismic section which includes terminated enhanced reflections at the BGHSZ in the mid Norwegian margin. Seismic data recorded by using 80-90 Hz dominant frequency and result CDP 12.5m from Buenz and Mienert (2004).*

The Hydratech high-resolution 3D seismic data collected by a cruise led by Ifremer, to the mid Norwegian margin in 2002 (Nouzé et al., 2004). The 3D seismic dataset covers an area of (3.5kmx7.5km) 28 km^2 it was located at a water depths 1050m - 1150m. The size of the bin is~6m of the dataset and the Dominant frequency (~80 Hz) provides an appreciable horizontal and vertical resolution compared to conventional industry 3D seismic data. (Hustoft et al., 2007).The acquisition consist of two seismic streamer with 25m separation each with 24 trace and 150m length and two air gun (mini GI) towed 12.5m apart (Thomas et al., 2004).

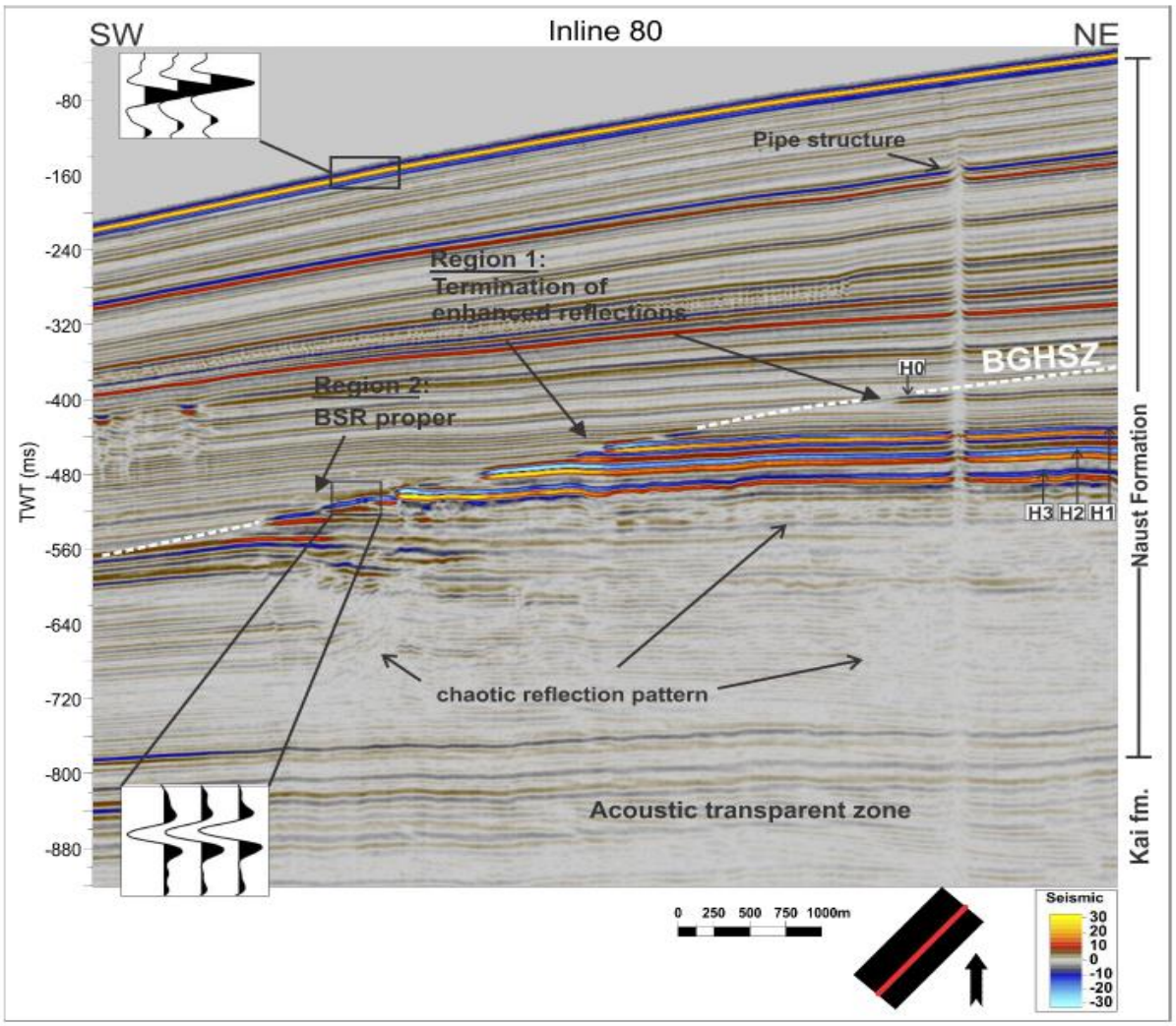

Figure 5.7 *shows the seismic section includes proper BSR and termination of enhanced reflection at BGHSZ. Data from Hydratech 3D recorded using 80 Hz dominant frequency and 6m wide bin from (Bjørnøy, 2015).*

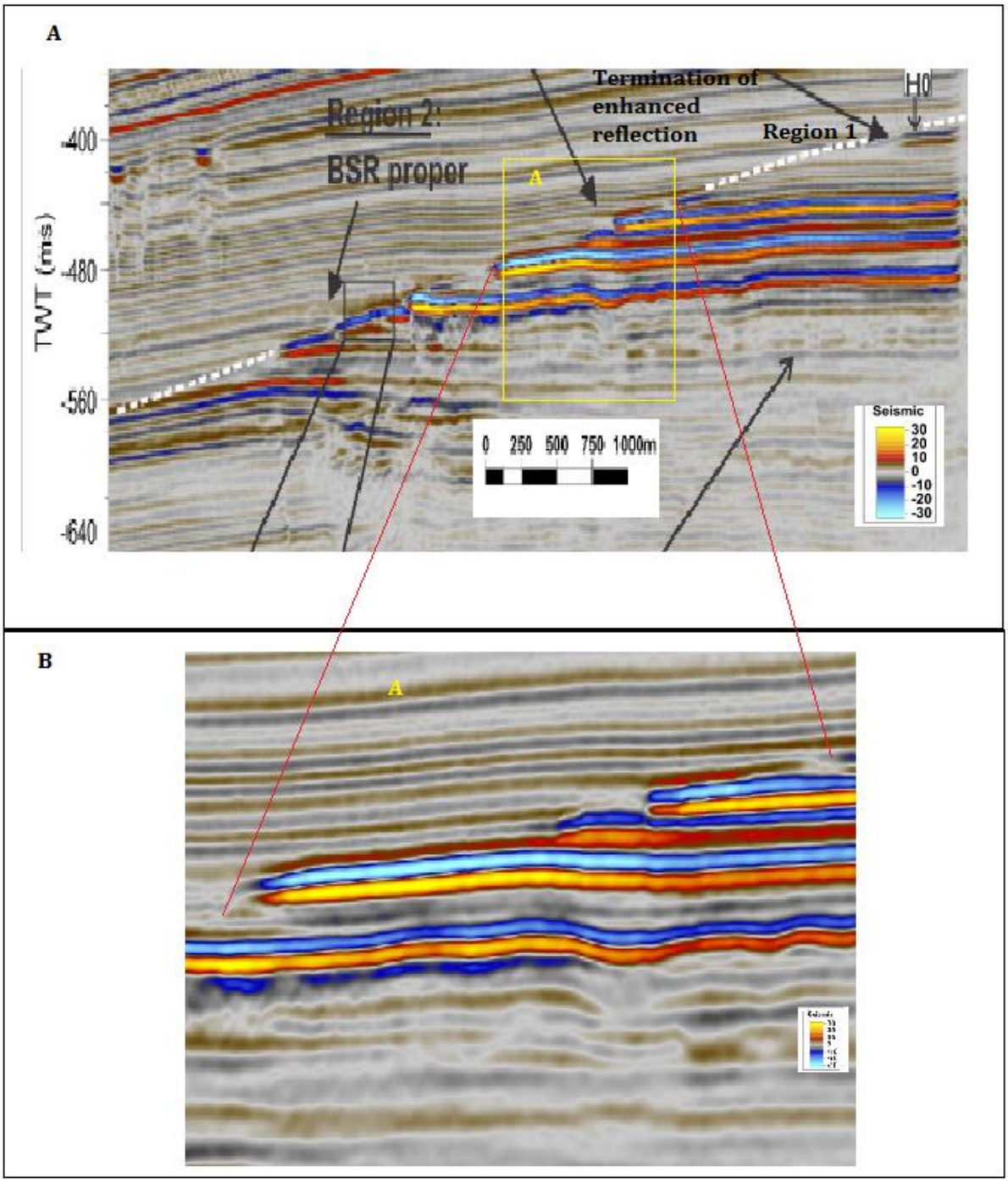

Figure 5.8 *A, shows two seismic sections A, section taken from the Hydratech 3D data and B, magnified size of section a yellow box marked A.*

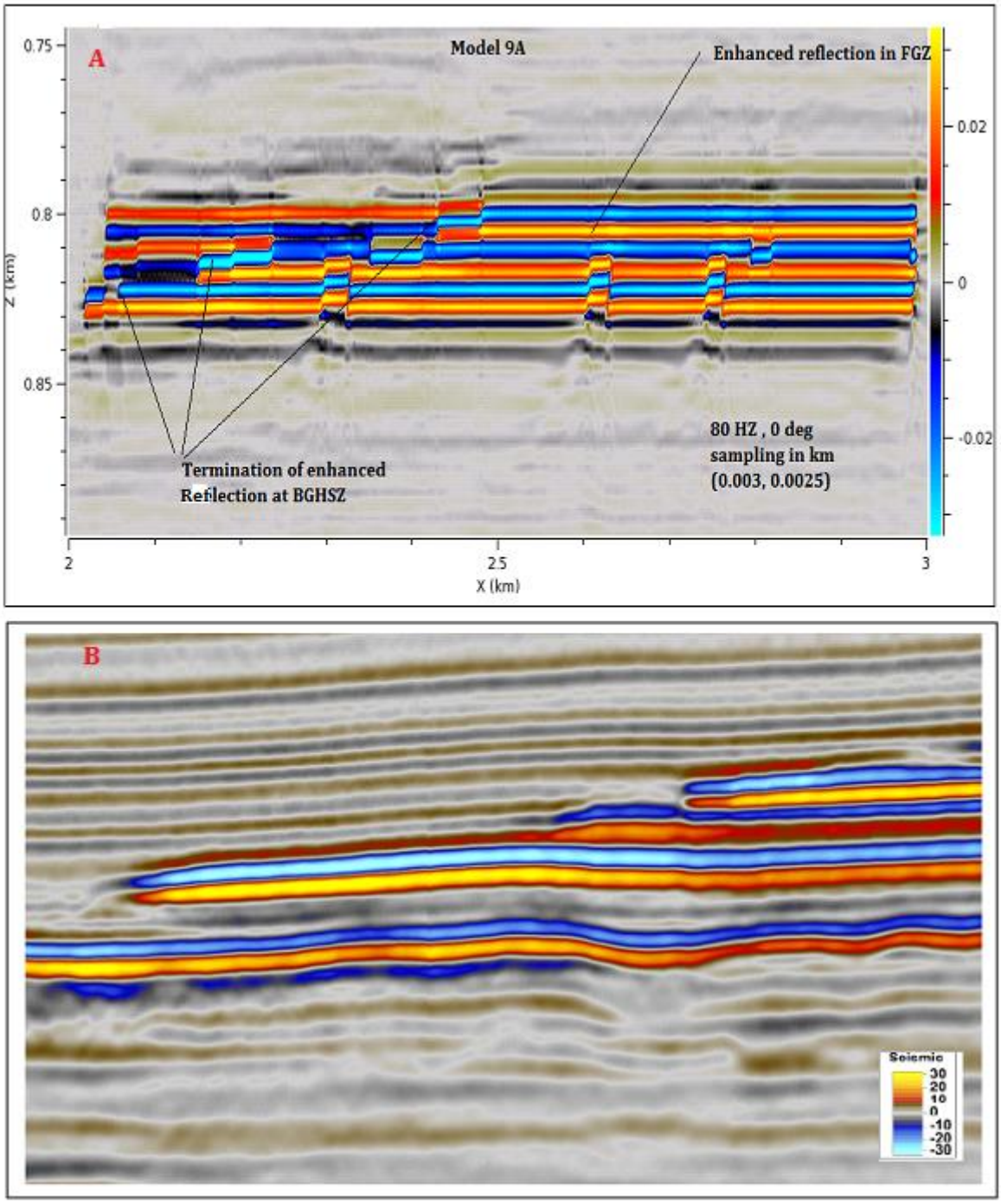

Figure 5.9 *shows synthetic and real seismic sections A, The synthetic seismic PSDM result Model 9A and B, a magnified section taken from figure 5.8 The Hydratech seismic section.*

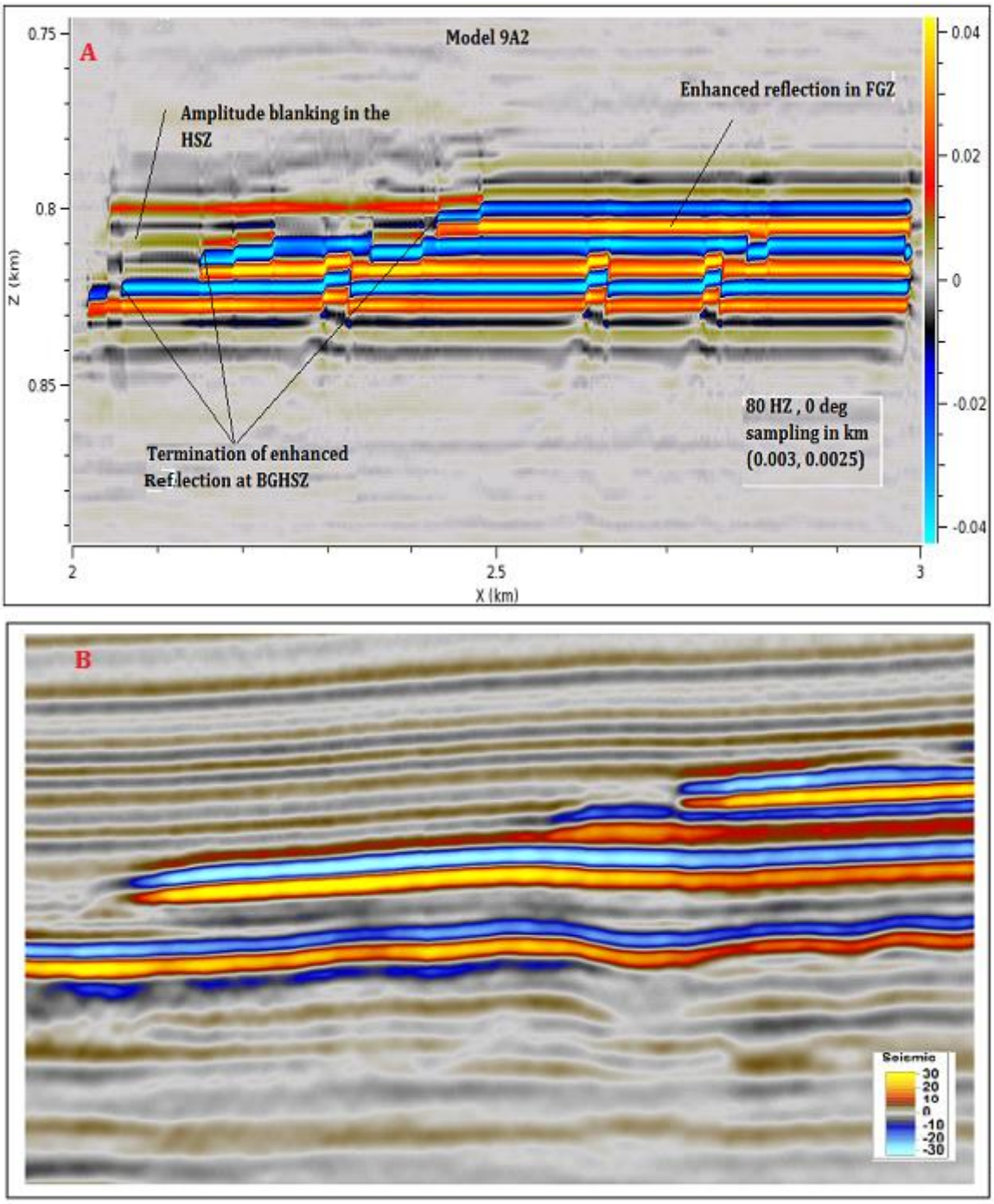

Figure 5.10 *shows synthetic and real seismic sections A, the synthetic seismic PSDM result model 9A2 and B, a magnified section taken from figure 5.8 the Hydratech seismic section.*

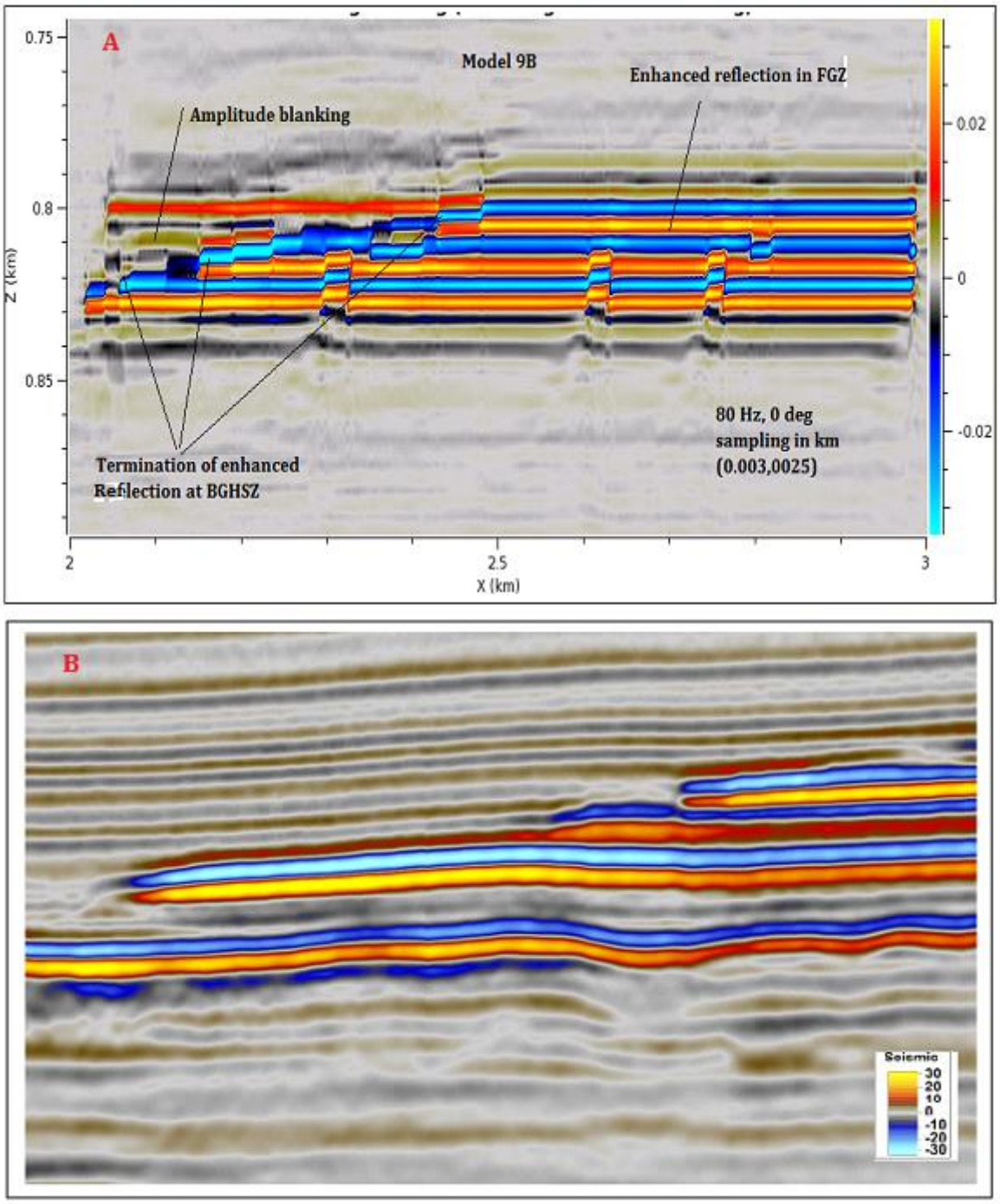

Figure 5.11 *shows synthetic and real seismic sections A, the synthetic seismic PSDM result model 9B and B, a magnified section taken from figure 5.8 the Hydratech 3D seismic section.*

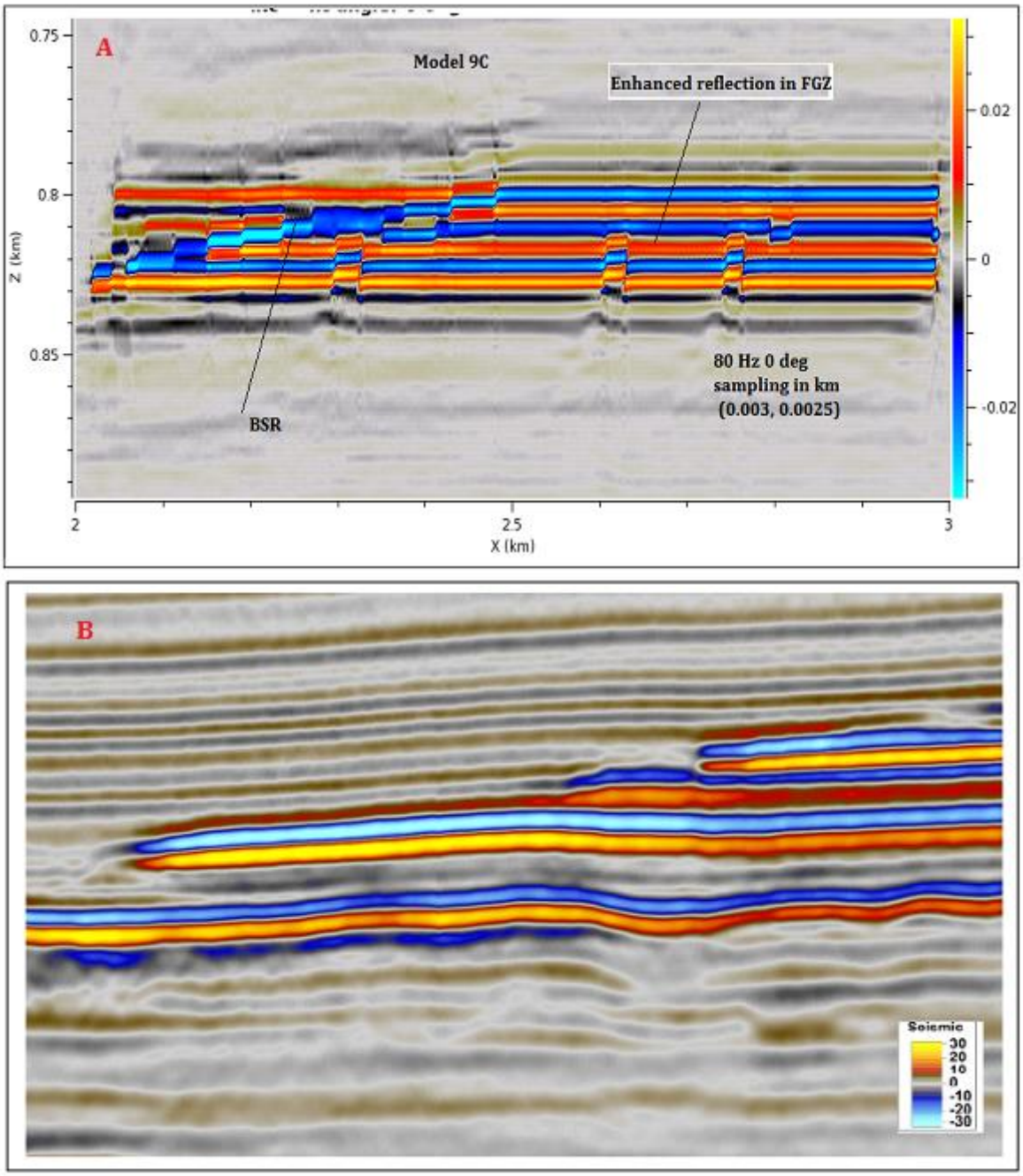

Figure 5.12 *shows synthetic and real seismic sections A, the synthetic seismic PSDM result model 9C and B, a magnified section taken from figure 5.8 the Hydratech 3D seismic section.*

Seismic modeling can be helpful to test for an interpretation model for 2D and 3D seismic data, or to model the response of the expected geology as an aid to plan a seismic reflection survey (Makris et al., 1999). The seismic image from the Hydratech 3D data (Bjørnøy, 2015) as shown in Figure 5.8 is compared with the synthetic seismic model 9. The synthetic seismic reflection PSDM generated at 80 Hz as well the Hydratech data are recorded at a dominant frequency of 80 Hz. The sampling in km for the synthetic seismic was 0.003,0.0025. The bin width for the Hydratech 3D was 6m. The seismic section from the Hydratech data was compared to four different occurences of hydrate bearing and gas bearing sediments in model 9. These are illustrated in Figure 5.9-5.12. The input seismic wavelet is chosen as close as possible as the original seismic acquisition.

The seismic section gives better matches with one of the models which included sediments without gas in both the HSZ and FGZ shown in Figure 5.10. The amplitude blancking in the HSZ and the termination of enhanced reflection at BGHSZ matches with model 9A2. Whereas the strength of the enhanced reflection amplitude on the synthetic image is higher than that of the Hydratech data. This is because the P-velocity selected for the gas free sediment was as high as 1850 m/s and this velocity is similar to the velocity values given to the near by hydrate bearing sediments. The similarity in p-wave velocity between the gas free sediments and the near by hydrate bearing sediments in turn causes amplitude blanking in the HSZ. However, the amplitude strength with model 9A that has the gas free sediments with P- velocity 1750m/s is more similar with the Hydratech datas amplitude strength as shown in Figure 5.9. The possible gas free sediment might have a value of 1750 m/s . It might result in amplitude blanking with nearby hydrate bearing sediment that might have values of between 1780-1800 m/s P-velocity and it might result in the same amplitude strength in the FGZ with a value of 1350 m/s of free gas P-velocity. .

6 Conclusion

1. One of the reasons, for the occurrence of BSR as a termination of enhanced reflection at BGHSZ might be due to the presence of sediments layers without gas. The layers without gas extend in to the HSZ and areas under BGHSZ on the free gas zone. The acoustic properties (P-wave velocity and density) of the gas free sediments are likely to be similar to the hydrate bearing sediments.
2. The proper reflection of BSR might be due to the tuning of thin layers of intercalated free gas bearing sediments and sediments without gas.
3. The observed enhanced reflection on the real seismic data (Hydratech 3D seismic data) may have resulted from the acoustic impedance contrast between gas bearing sediments and sediments free of gas.
4. The presence of amplitude blanking over the BGHSZ with termination of enhanced reflection below the BGHSZ might not necessarily be due to the presence of homogenous gas hydrate in HSZ.
5. The presence of gas free sediments with P-velocity higher or lesser than that of the hydrate would have produced slightly strong reflection in the HSZ.
6. A discontinuous dipping BSR has occurred truncating horizontal sediment layers in both the synthetic and Hydratech 3D seismic data. The discontinuity is likely generated due to the presence of intercalation of gas free and hydrate bearing layers above the BSR and gas free and gas bearing sediments below the BSR. The termination of enhanced reflections occur at the tuning thickness in the dipping BSR cross cutting horizontal lying strata of gas bearing sediments and sediments without gas.
7. Upward termination of enhanced reflection occurs at horizontal BSR and Anticlinal BSR cross cutting dipping strata of gas bearing sediment and sediment without gas.

References

Aki, K & Richards, P.G 1980.Quantitative seismology; :W.H. Freeman & Co. pp. 123.

Andreassen, K. (2009) Marine Geophysics-Lecture Notes for Geo-3123. University of Tromsø, 2013.

Andreassen, Karin, Hart Patrick E. , Mary Mackay, 1997, Amplitude versus Offset modeling of the bottom simulating reflection associated with submarine gas hydrates

Bünz, S & J.Mienert (2004) Acoustic imaging of gas hydrates and free gas at the storegga Slide. Journal of Geophysical research: Solid earth (1978-2012).

Bünz, S, J. Mienert, M. Vanneste, and K.Andreassen (2005) Gas hydrates at the Storegga Slide, Constraints from an analysis of Multicomponent, wide-angle seismic data. Geophysics, Vol. 70, No.5; p. B19-B34.

Bünz, S., J. Mienert & C.Berndt (2003) Geological controls on the storegga gas hydrate system of the mid Norwegian continental margin. Earth and planetary sciences Letters, 209,291-307.

Burger. H, Sheehan, .A and Jones.C, (2006) Introduction to applied Geophysics, Exploring the shallow subsurface.

Chopra et al., 2006, Seismic resolution and thin bed reflectivity inversion, CSEG Recorder 19.

Gawith, D.E & Gutteridge P.A 1996. Seismic Validation of reservoir simulation using a shared earth model. Petroleum geoscience, 2, 97-103.

Goldberg,D Wikens,R.H.& Moos, D. 1987 Seismic modeling of diagenetic effects in Cenozoic marine sediments at Deep Sea Drilling Project sites 612 and 613, DSDP initial report on Leg 95,23.

Helmberger, D.V. 1974, Understanding Seismograms by Constructing Numerical Models, Engineering and Sceience, 38, 26-29.

Hodgets,D. & Howell, J.A. 2000. Synthetics seismic modelling of large scale geological cross-section from the Book cliffs, Utah, USA, Petroleum Geosciences 6; -221-229

Hyndman, R.D & G.D. Spence (1992) A seismic study of methane hydrate marine bottom simulating reflectors, Journal of Geophysical Researchs,97, 6683-6698.

Janita.L.Nordhal,2015 modeling of seismic amplitude anomalies associated with co_2 underground storage, Uit Master's thesis.

Judd, A.G. & M.Hovland.2007. Seabed fluid flow: The impact of geology, biology and the marine environment. Cambridge: Cambridge university press.475.

Kirsti Bjørnøy, 2015, The nature of the gas-hydrate/free gas transition zone at the base of the hydrate-stability zone from high- resolution 3D seismic data, Uit. Master's thesis.

Kvenvolden, K.A & L.A. Barnard (1983) Gas hydrates of the black outer ridge site 533, deep-sea Drilling project Leg76: Intial reports of the deep-sea drilling project.76, 353-365.

Kvenvolden, K.A. (1993[a]) Gas hydrates- Geological perspective and global change .Review of Geophysics, 31,173-187.

Le. A, Huuse. M, Redfern. J, Gawtorphe. R, & Irving D, (2014) seismic characteristic of bottom stimulation reflection and plumbing system of the Cameroon at the margin. Marine and petroleum geology. (http://dx.doi.org/10.1016/j.marpetgeo.2014.12.006)

Lecomte, I, (2008). Resolution and illumination analyses in PSDM, A ray-based approach. The Leading Edge, 27, 650-663.

Linyun Tan,(2012) Control of reservoir and cap rock on gas hydrate formation; Search and Discovery Article no.40911.

M. Ben clennel[12], Martin Hovland[3], Jame S. Booth[4], Pierre Henry[5] and William J. winters, (1999) Formation of natural gas hydrate in marine sediment. Journal of geophysical research vol 104, No, B10, 22, 985-23,300.

Makris,J,Egloff, F.& Rihm,R.1999.WARRP(Wide Aperture Reflection and Refraction Profiling).The principle of successful data acquisition where conventional seismic fails SEG 1999 .

Mavko,G., Mukerji,T & Dvorkin, J. (1998). The rock physics hand book: tool for seismic analysis in porous media, Cambridge University Press.

Norsar 2011, SeisRox 2.2 manual, 2011

OBartel, T., Krastel, S., and Spiess, V,2007. Correlation of high resolution seismic data with ODP Leg 208 borehole measurements. In Kroon, D., Zachos, J.C., and Richter,C.(Eds), Proc. ODP, Sci. Results, 208 College Station, TX (Ocean Drilling Program), 1-27.

Rafaelsen.B, 2002 Seismic resolution (and frequency filtering), University of Tromsø).

Rajput.S Müller,T., Clennel. M, Rao. P.P & Thaku. N.K(2012) Constraint seismic reflection and mode of conversion at bottom simulation reflectors associated with gas hydrate, Journal of Petroleum sciences and Engineering . Vol, 88-89, page 48-60

Roar Heggland, 2002, Seismic evidence of vertical fluid migration through faults, application of chimney and fault detection. Statoil ASA, N-4035 Norway.

Sava,D: and B.Hardage,(2009), Rock physics model for gas hydrate systems associated with unconsolidated marine sediments.

Sheriff, R. E& Geldart, L.P. (1995). Exploration Seismology, Press Syndicate of the University of Cambridge.

Sloan,E.D, (1998) Physical and chemical properties of gas hydrates and application to world margin stability and climate change. Geological society, London, special publications 137, 31-50.

Stoll and Bryan, 1997

Vanneste, M., S. Guidard & J. Mienert (2005b). Arctic gas hydrate provinces along the western Svaldbard magin. Terra Nova, 17, 510-516.

Vanneste,M., M. De Batist,A. Golmshtok, A. Kremelv, and W.Versteeg, (2001), Multi – frequency seismic study of gas hydrate-bearing sediments in Lake Baikal,Siberia; Marine geology, 172, 1-21

Veeken,P.,(2007), Seismic stratigraphy basin analysis and Reservoir characterization. Handbook of geophysical exploration.

Appendix

Norsar 2D modelling procedure

1. File opened in and modelling selection, select project model then modelling section

Create project. Insert the required parameters under project. Area, Azimuth number of inline and cross line, etc. (figure below shows some of the procedures).

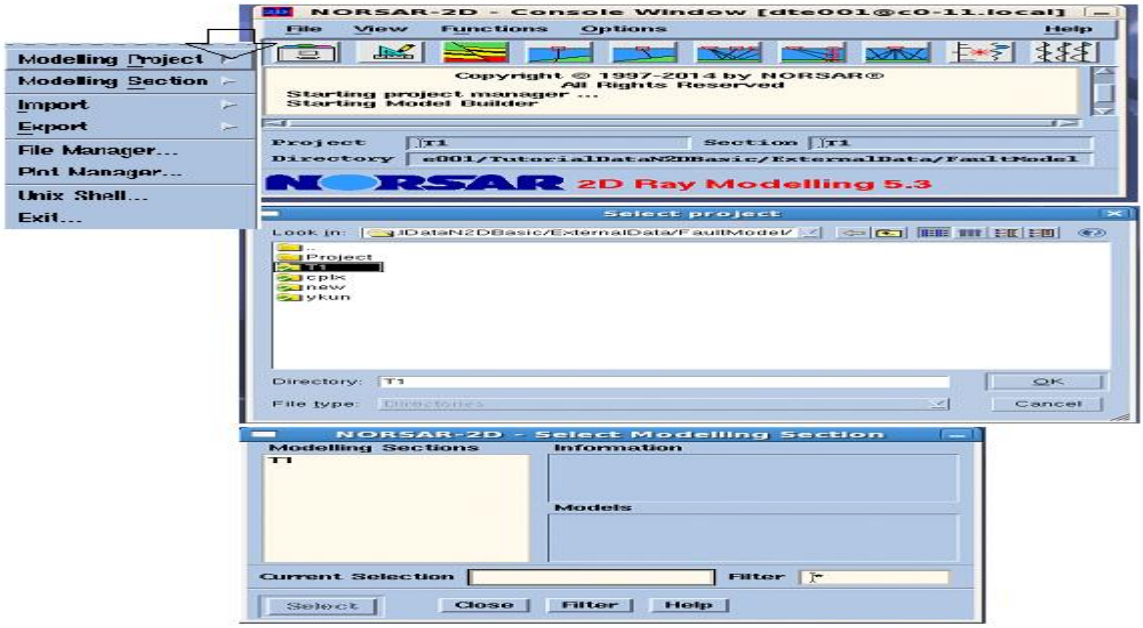

2. To create a model in Model builder open model builder from console window (CW) Set model dimension, in x and z or y and z this done under model geometry in the model

builder window. (figure below shows some of the procedures).

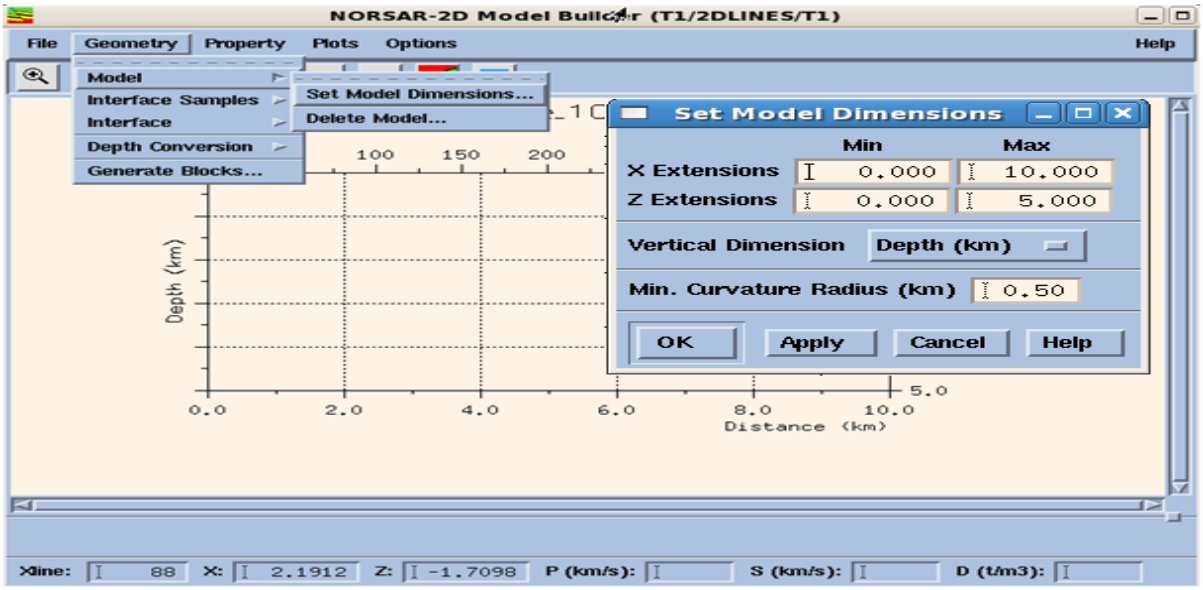

3 To insert the horizons it can be done from model geometry or from the model builder window create an interfaces. By clicking at the right depth a set pointes create a horizon. It may not be smooth, but smoothing can be done under model geometry by select smooth horizons. This step can be done several times you need the required horizons. An option of extending and shortening of interface is under the model builder window.

4. When all the horizons or interfaces is created blocks can be generated, Note that interfaces must make a closed lope and it is called blocks block geometry. We can save the model geometry under file menu by clicking store geometry and give a name. Inserting properties was done after we prepare block geometries.

5 Under the model builder, we finds the property menu, we set the required property first and then we continue to insert property by following the property menu. In the constant function by clicking by mouth 1 first on the area then on the required property menu mouth 2. Several times all over the cross section, then the same steps can be done for P- velocity, S – velocity and density. Analytic function can be used for gradually changing properties. (figures below shows some of the procedures).

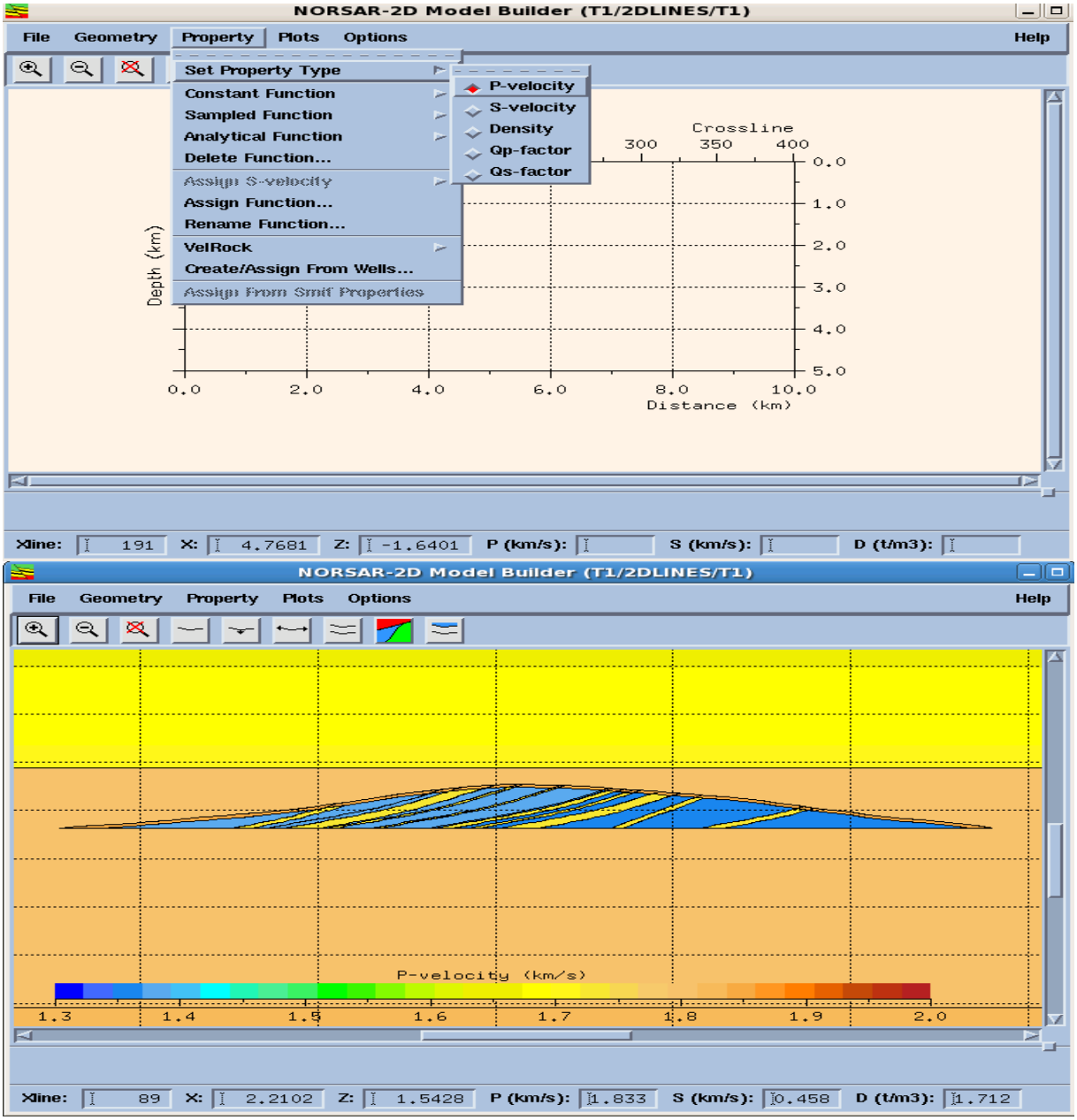
NORSAR-2D Model Builder (T1/2DLINES/T1)
File
Geometry
Property
Plots
Options
Help
Set Property Type
Constant Function
Sampled Function
Analytical Function
Delete Function...
Assign S-velocity
Assign Function...
Rename Function...
VelRock
Create/Assign From Wells...
Assign From Smlf Properties
P-velocity
S-velocity
Density
Qp-factor
Qs-factor
Crossline
300
350
400
Depth (km)
0.0
1.0
2.0
3.0
4.0
5.0
0.0
2.0
4.0
6.0
8.0
10.0
Distance (km)
Xline: 191
X: 4.7681
Z: -1.6401
P (km/s):
S (km/s):
D (t/m3):
NORSAR-2D Model Builder (T1/2DLINES/T1)
File
Geometry
Property
Plots
Options
Help
P-velocity (km/s)
1.3
1.4
1.5
1.6
1.7
1.8
1.9
2.0
Xline: 89
X: 2.2102
Z: 1.5428
P (km/s): 1.833
S (km/s): 0.458
D (t/m3): 1.712

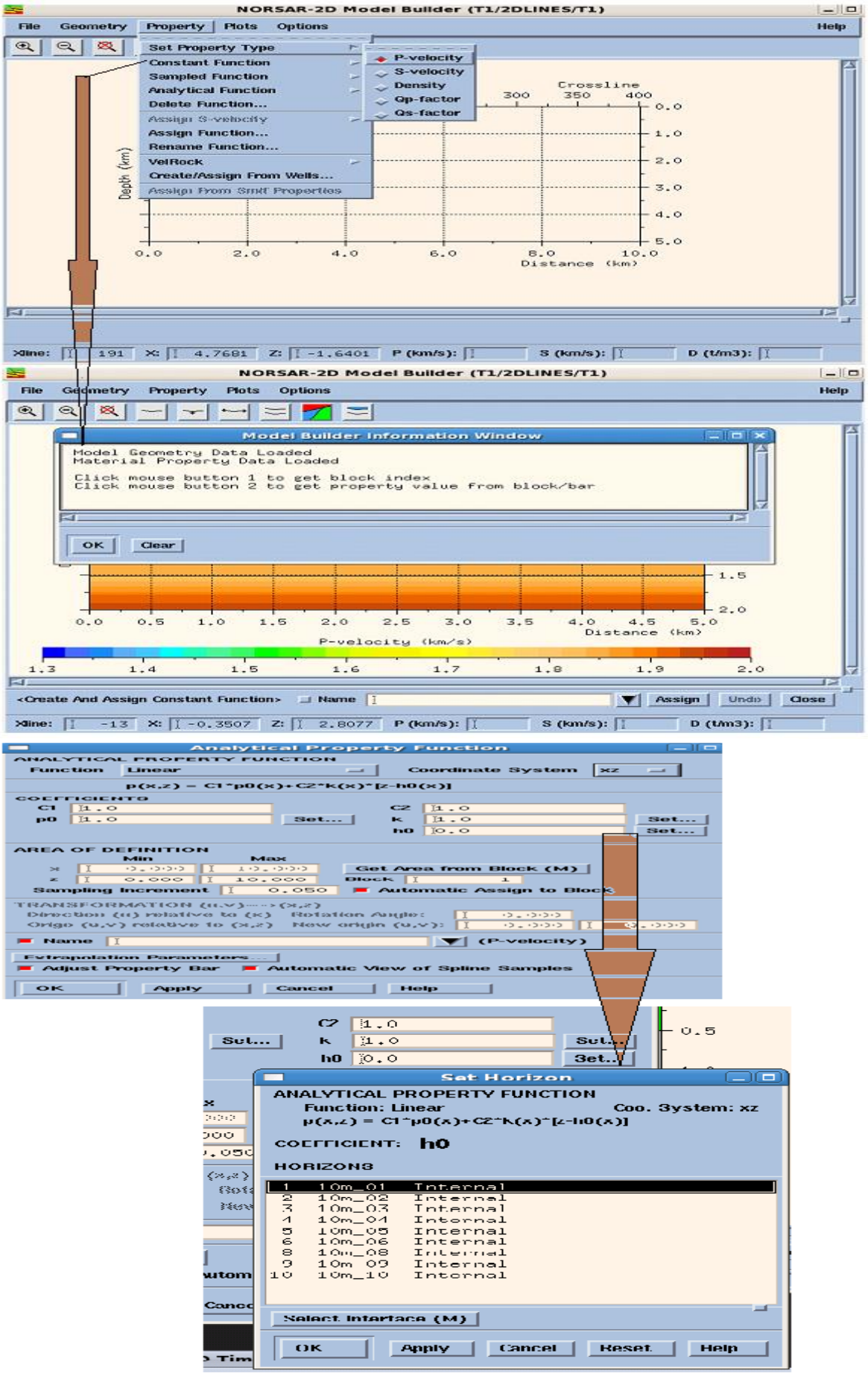
NORSAR-2D Model Builder (T1/2DLINES/T1)
File
Geometry
Property
Plots
Options
Help
Set Property Type
Constant Function
Sampled Function
Analytical Function
Delete Function...
Assign S-velocity
Assign Function...
Rename Function...
VelRock
Create/Assign From Wells...
Assign From SmkT Properties
P-velocity
S-velocity
Density
Qp-factor
Qs-factor
Crossline
300
350
400
Depth (km)
0.0
1.0
2.0
3.0
4.0
5.0
0.0
2.0
4.0
6.0
8.0
10.0
Distance (km)
Xline: 191 X: 4.7681 Z: -1.6401 P (km/s): S (km/s): D (t/m3):
NORSAR-2D Model Builder (T1/2DLINES/T1)
File
Geometry
Property
Plots
Options
Help
Model Builder Information Window
Model Geometry Data Loaded
Material Property Data Loaded
Click mouse button 1 to get block index
Click mouse button 2 to get property value from block/bar
OK
Clear
1.5
2.0
0.0
0.5
1.0
1.5
2.0
2.5
3.0
3.5
4.0
4.5
5.0
Distance (km)
P-velocity (km/s)
1.3
1.4
1.5
1.6
1.7
1.8
1.9
2.0
<Create And Assign Constant Function>
Name
Assign
Undo
Close
Xline: -13 X: -0.3507 Z: 2.8077 P (km/s): S (km/s): D (t/m3):
Analytical Property Function
ANALYTICAL PROPERTY FUNCTION
Function
Linear
Coordinate System
xz
p(x,z) = C1*p0(x)+C2*k(x)*[z-h0(x)]
COEFFICIENTS
C1
1.0
p0
1.0
Set...
C2
1.0
k
1.0
h0
0.0
Set...
AREA OF DEFINITION
Min
Max
Get Area from Block (M)
Block
1
Sampling Increment
0.050
Automatic Assign to Block
TRANSFORMATION (u,v)----->(x,z)
Direction (u) relative to (x)
Rotation Angle:
Origo (u,v) relative to (x,z)
New origin (u,v):
Name
(P-velocity)
Extrapolation Parameters...
Adjust Property Bar
Automatic View of Spline Samples
OK
Apply
Cancel
Help
C2
1.0
k
1.0
h0
0.0
Set...
0.5
Set Horizon
ANALYTICAL PROPERTY FUNCTION
Function: Linear
Coo. System: xz
p(x,z) = C1*p0(x)+C2*k(x)*[z-h0(x)]
COEFFICIENT: h0
HORIZONS
1 10m_01 Internal
2 10m_02 Internal
3 10m_03 Internal
4 10m_04 Internal
5 10m_05 Internal
6 10m_06 Internal
8 10m_08 Internal
9 10m_09 Internal
10 10m_10 Internal
Select Interface (M)
OK
Apply
Cancel
Reset
Help

6. SIMF genereted in Norsar 2D. exported from 2D Norsar under the file menu in to Norsar 3D. And it loaded in Norsar 3D. (figures below shows some of the procedures.)

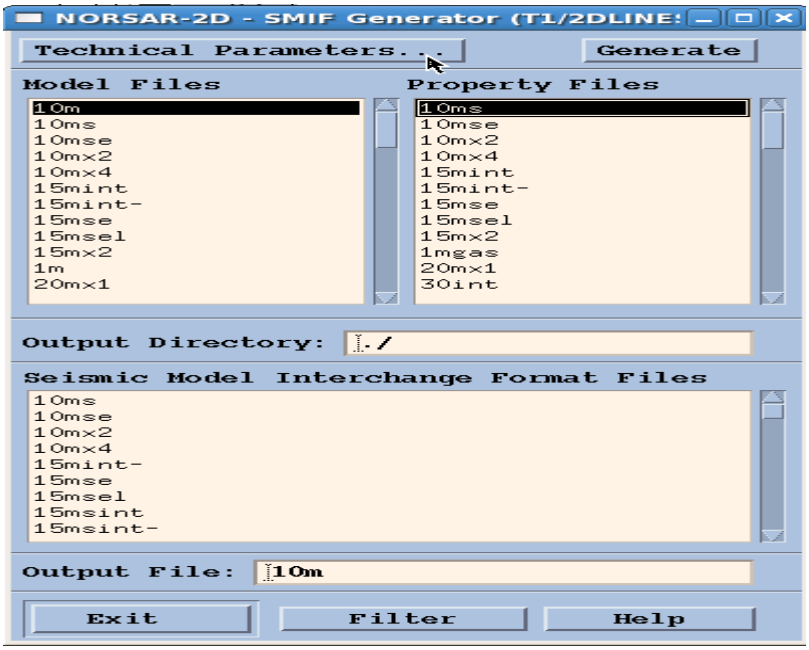

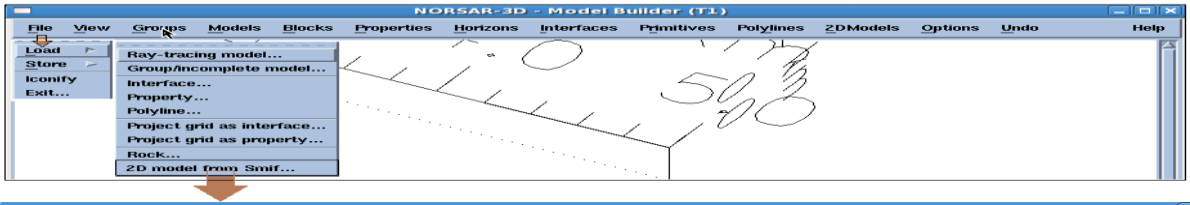

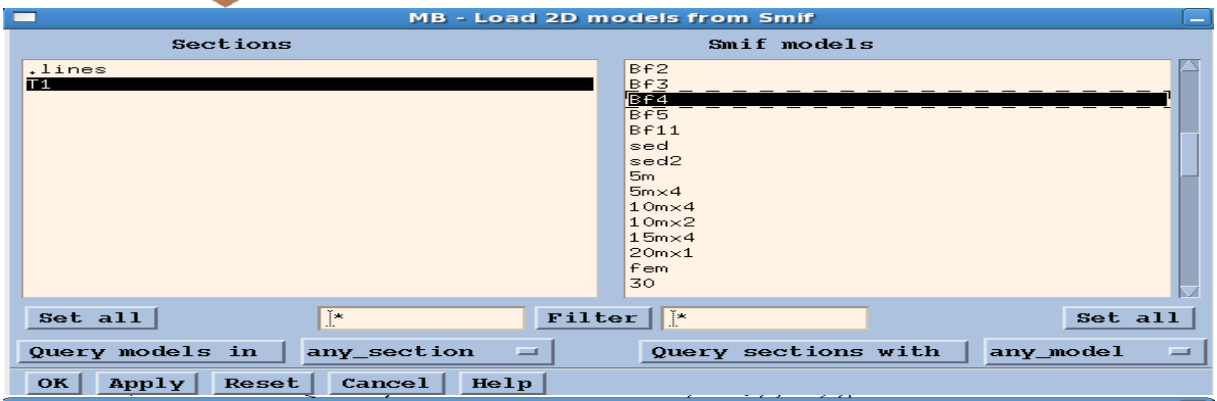

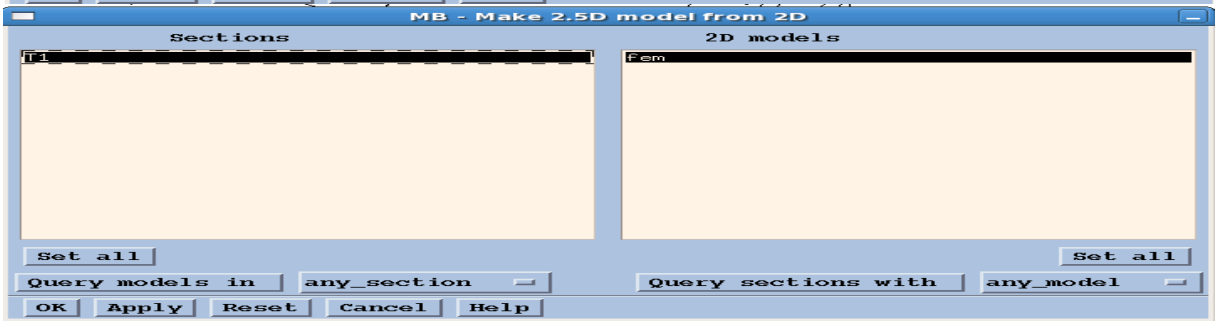

7. File saved under file menu in 3D Norsar store as Kirchhoff, Target horizon model,file ready for simulation in seisrox.

The work flow in seisrox

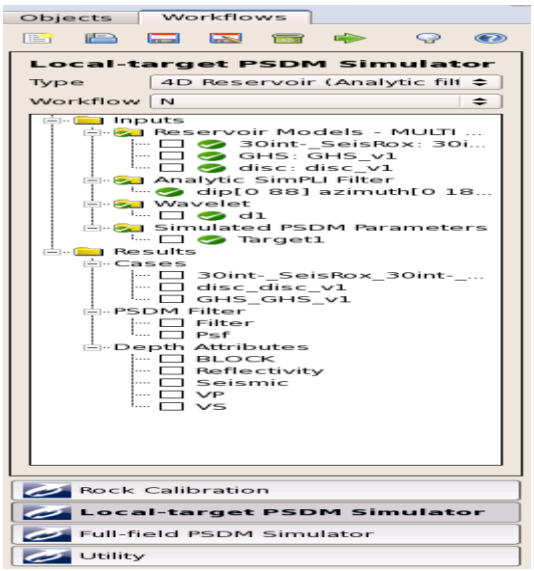

The target parameter can be inserted under the Target folder, the figure below.

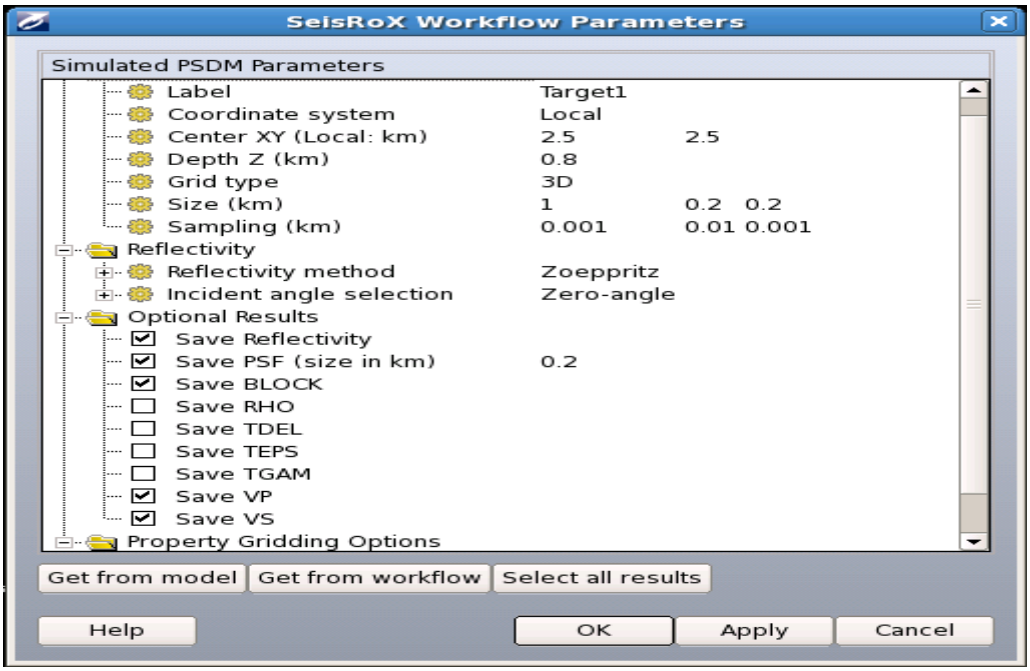

Over view of all models developed for this study with background model

Model 1

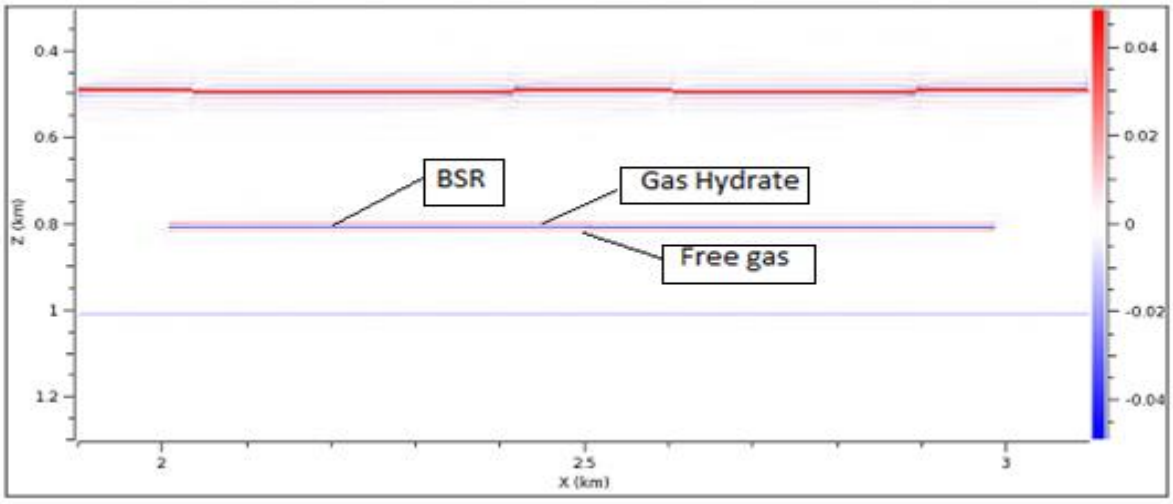

Figure 1 show seismic response of model 1 Horizontal BSR at a depth of 800m, 5m thick gas hydrate at the top of 5m thick free gas give strong reflecton at the horizontal contat which is reversed polarity(blue) in contrast to the sea floor in red.

Model 2

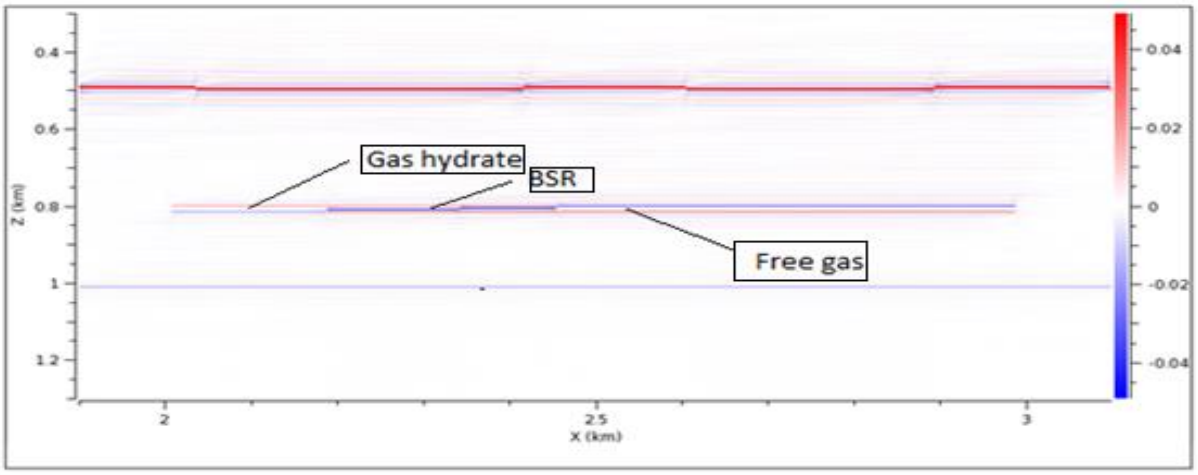

Figure 2 showing seismic response of model 2 near Horizonatl BSR , 5m gashydrate and 5m free gass at near horiziontal contact hydrate thickness increase to the left from center and free gas thickness increase to the right. It gives anomals storng reflection at the contact with thicker gas and terminate as the thickness of free gas reduces.

Model 3

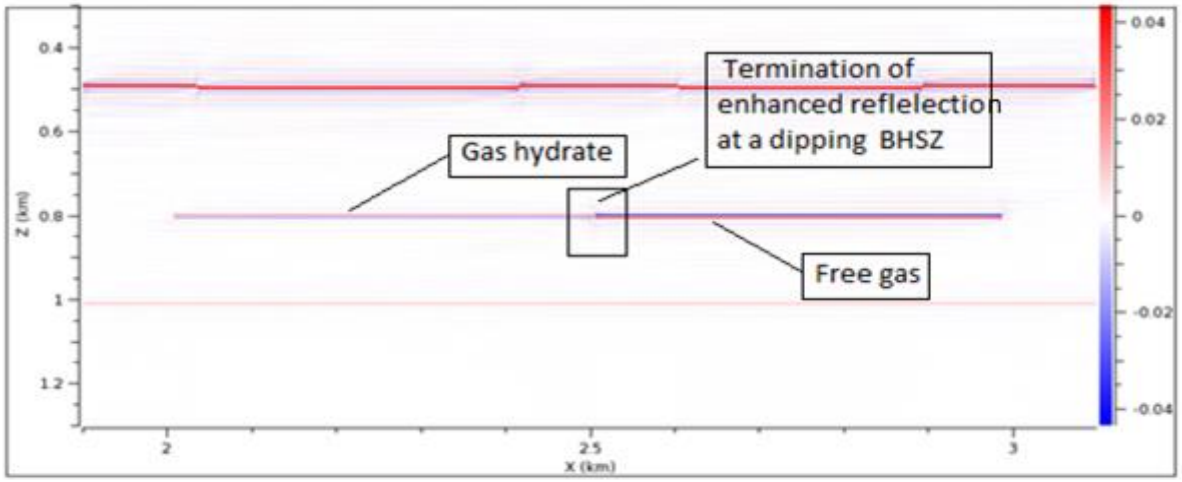

Figure.3 show steeply dipping BSR of 5m layers gas hydrate and free gas, 5m thick gas hydrate and 5 free gas with steeply dipping contact approximately 10-12m contact it shows termination of enhanced reflection which is seen by the free gas side.

Model 4

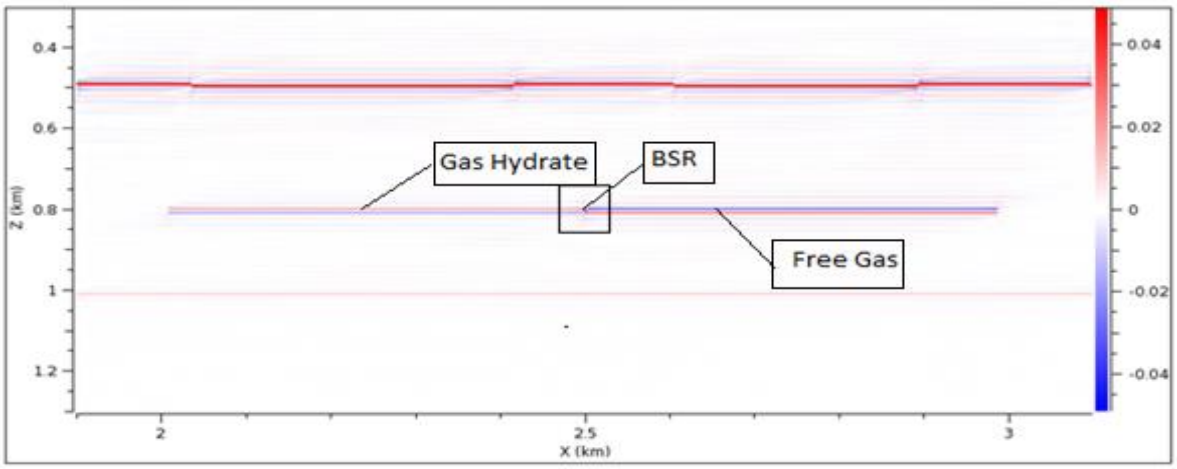

Figure 4 show steeply dipping BSR of 10m layers gas hydrate and free gas, the contact between gas hydrate and free gas approximetd about 12-15m it shows anomalus reflection as a BSR too small to identify with big window as thin point.

Model 5 .

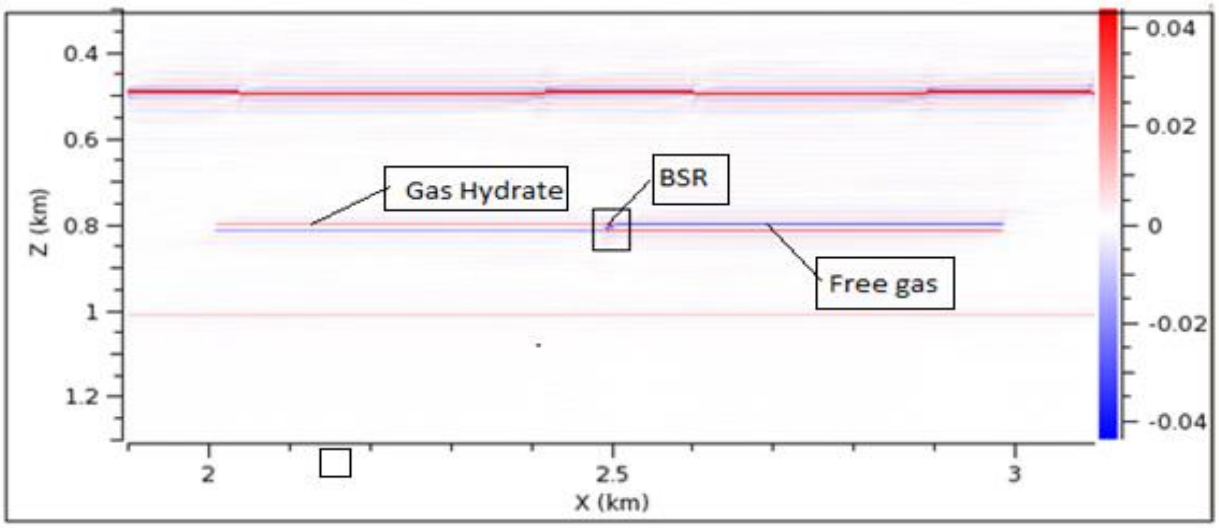

Figure 5 show steeply dipping BSR of 15m layers gas hydrate and free gas, as thickness increase and the length of the contact between gas hydrate and gas increases the BSR shows a better-identified proper reflection.

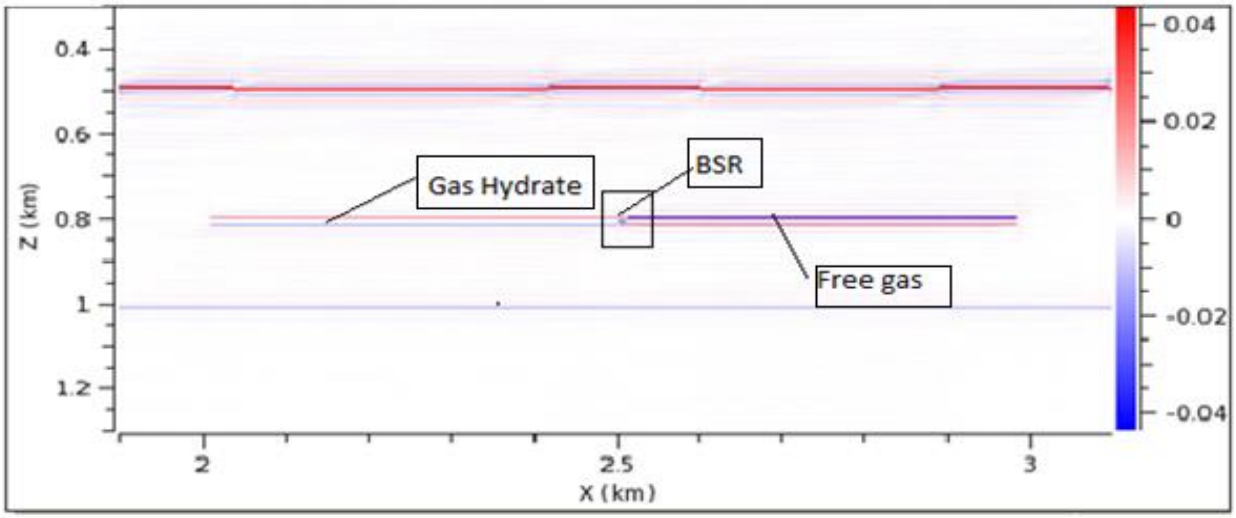

Figure 6 show steeply dipping BSR of 15m layers gas hydrate and free gas intercalated with 5m thin sediment free of gas, the contact between gas hydrate and free gas indicates the termination of enhanced reflection.

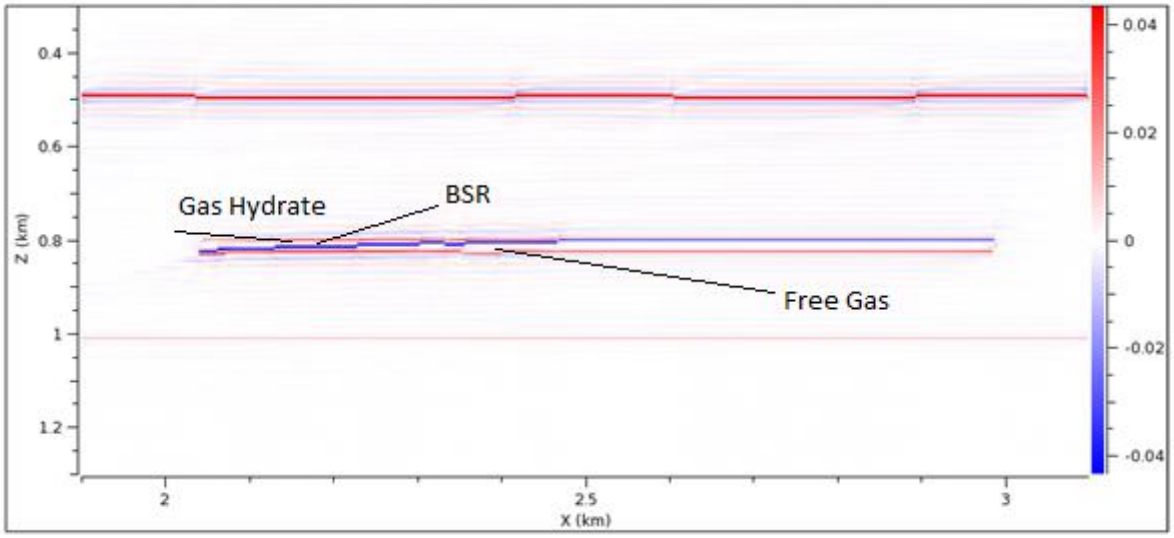

Figure 7 shows 30m gas hydrate and gas at near horizontal contact. The contact between hydrate and free gas shows strong proper reflections.

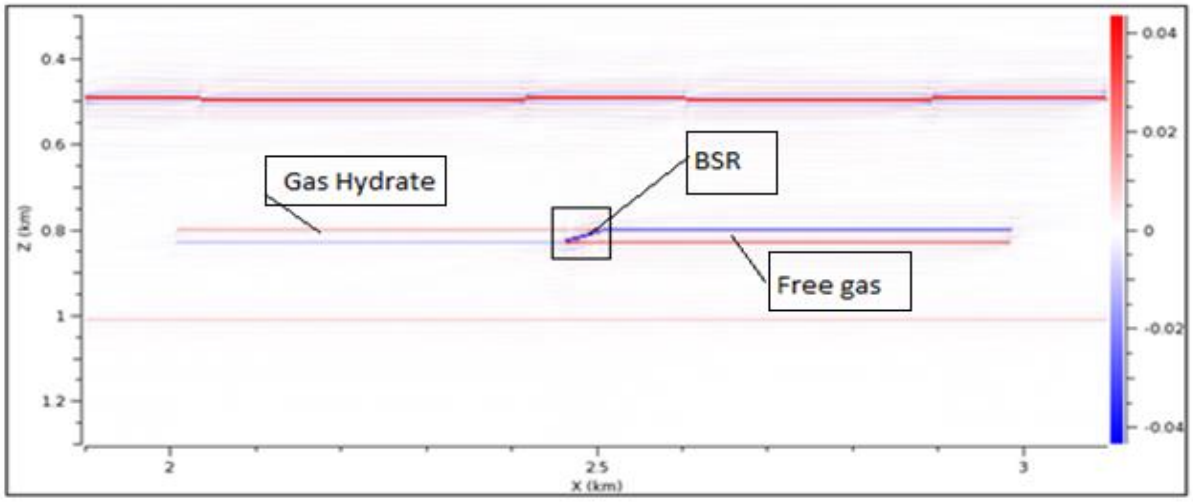

Figure 8 showing steeply dipping contact of hydrate and gas of 30m, as the thickness increases between the gas hydrate and free gas BSR gives strong proper reflection.

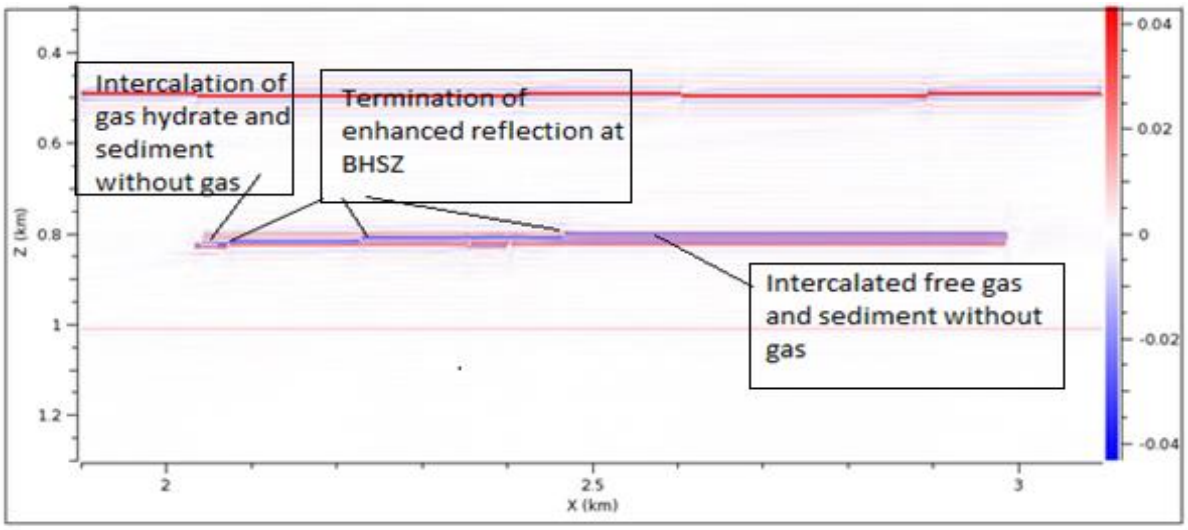

Figure 9 showing intercalation of 5m sediment layer with hydrate and free gas layer. The less porous sediment are assumed with out gas which are between the free gas and between hydrates. The BSR indicate by the termination of enhanced reflection at BHSZ.

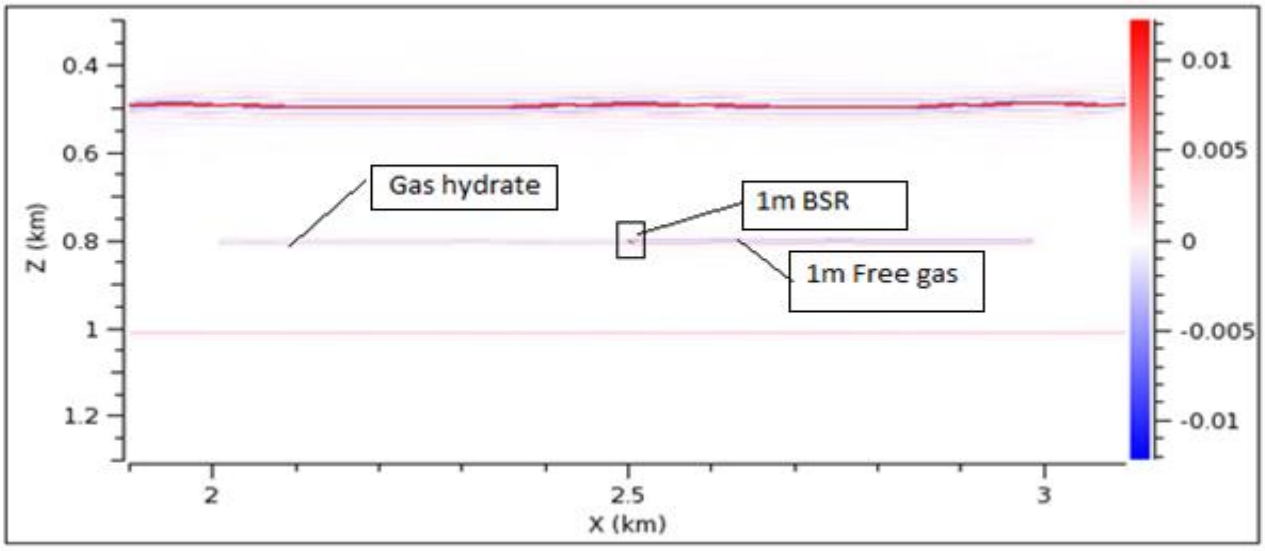

Figure10 showing dipping contact between hydrate and gas 1m thick sampling(km) at (x,z) (0.001, 001). BSR doesn't give reflection the free gases gas in contact with host sedimet gives dim reflections.

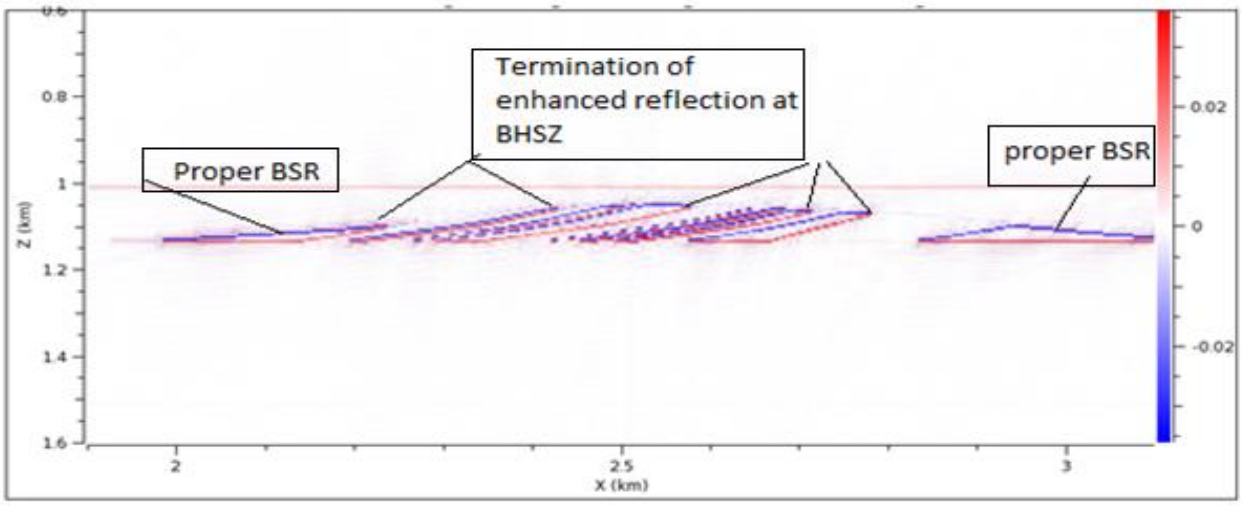

Figure 11 shows Anticlinal shape BSR with slightly dipping beds of thicker gas free sediment and free gas intercalated, Case hydrate not formed at top of sediment with out gas. Shows termination of enhanced reflection(blue) at BSR with contact of hydrate and free gas and very less or no reflection at top of less porous sediment.

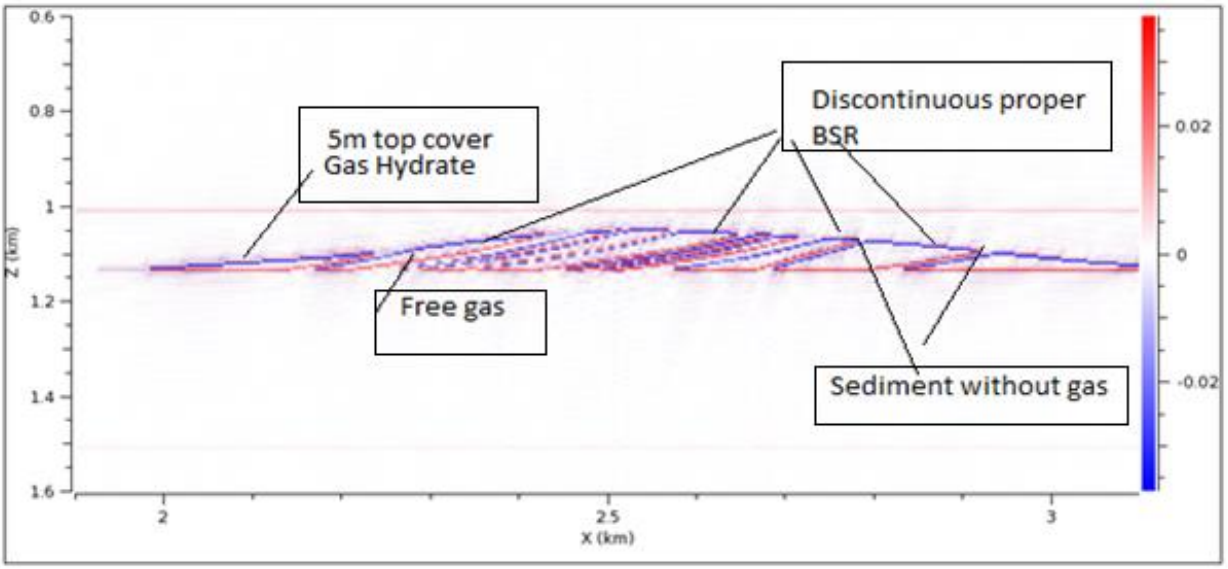

Figure 12 shows. Anticlinal shape BSR with slightly dipping beds of thin sediment without gas (less porous) and sediment with gas covered by gas hydrate. The reflection terminate at the contact of the free gas, lesspouros sediment and hydrate.